Research and realization of assistant off-line programming system for thermal spraying

Chaoyue Chen

SPIM

Thèse de Doctorat

école doctorale sciences pour l'ingénieur et microtechniques
UNIVERSITÉ DE TECHNOLOGIE BELFORT-MONTBÉLIARD

Research and realization of assistant off-line programming system for thermal spraying

Chaoyue CHEN

N° d'ordre :303 **Année : 2016**

Université de technologie de Belfort-Montbéliard
Ecole doctorale Sciences physiques pour l'Ingénieur et Microtechniques

THESE

Présentée pour obtenir le grade de

Docteur de l'Université de Technologie de Belfort-Montbéliard en Sciences pour l'Ingénieur

Research and realization of assistant off-line programming system for thermal spraying

Soutenue publiquement le 16 décembre 2016

Chaoyue CHEN

Rapporteurs

Madame Christine PRELLE, Professeur des Universités, Université de Technologie de Compiègne

Monsieur Vincent GUIPONT, Chercheur, HDR, MINES ParisTech

Examinateurs

Monsieur. Thierry BARRIERE, Professeur des Universités, FEMTO-ST

Monsieur. Philippe CHARLES, Product Manager, ABB France

Monsieur. Sihao DENG, Maître de Conférences-HDR, Université de Technologie de Belfort-Montbéliard

Monsieur. Hanlin LIAO, Professeur des Universités, Université de Technologie de Belfort-Montbéliard

Acknowledgement

As this thesis is mainly done in the laboratory of IRTES - LERMPS, and supported by China Scholarship Council (CSC) in the framework of UT-INSA (2013), my thanks first go to all the collaborating parties which made this work possible at all. So, I want to thank the CSC to give me the chance to study abroad and broaden my vision, and as well as Mrs. Langlade CECILE, the director of laboratory LERMPS, to give me the opportunity to continue my study in the laboratory LERMPS.

Firstly, my gratitude goes to the members of defence jury for their efforts in examining the work of thesis. In particular, I'm very thankful for Mrs. Christine PRELLE and Mr. Vincent GUIPONT to take their time to be the reviewers and help me improve the thesis. Besides, I feel honoured to have Mr. Thierry BARRIERE and Philippe CHARLES to be present as the jury members of the thesis defence session.

Secondly, I would express my greatest gratitude to my thesis supervisors Dr. Sihao DENG and Prof. Hanlin LIAO, who have been extremely supportive along this journey of scientific research. It is their patience and guidance that lead me to the fields of thermal spray and robotics, with which I was not familiar at the beginning of my thesis. The vast knowledge in the fields of materials science and automation and clear thinking owed by Dr. Sihao DENG and Prof. Hanlin LIAO can always give me surprising inspiration during the PhD period. I would also thank Dr. Sihao DENG to give me the chance to be a temporary teacher, which helps me practice my French and enhance my understanding in programming skills. Except for the academic life, I also want to appreciate Dr. Sihao DENG and his wife Mrs. Yunfang GUI, Prof. Hanlin LIAO and his wife Mrs Hui WANG to help me adapt to the life in France and give me the consideration and endless concerns that let me feel at home.

Thirdly, my thanks go to the colleagues in our laboratory who gave me countless help during my doctoral research and daily life in France. They are: Jean-Baptiste DEVILLERS, Emilie AUBIGNAT, Xinkun SUO, Taikai LIU, Baicheng ZHANG, Min YU, Xiaohua FENG, Jiangwei LIU, Duo YI, Amal Masmoudi, Nan KANG, Chunjie HUANG, Zexin YU, Xingcheng YAN, et al. Especially, I want to thank my good friends Shuo YIN, Yangzhou MA, Zhao ZHANG and Yingchun XIE for the academic cooperation and the scientific discussion, which broadens my vision and give me the inspiration.

Most importantly, I would like to thank my girlfriend Hui SHANG. Her support, encouragement, consideration and unwavering love help me achieve the PhD diploma.

Finally, I owe to my parents and my family at the moment, who have been the ones standing firmly behind my back. As always, during my study in France, they have been giving me wise advice and are always helping me to be a better person. My endless thoughts go to my grandmother who unfortunately passed away during my study in France.

Abstract

The offline programming technology provides the possibility to generate complex robot trajectories in thermal spray process. In the laboratory of LERMPS, an add-in software called “Thermal Spray Toolkit” (T.S.T.) has been developed to assist the offline programming in the field of thermal spray. However, efforts are still expected to improve the functionality of this software. The aim of this study is to improve the application of offline programming technology in the thermal spray process. According to the procedure of the offline programming in thermal spray, the work of this thesis consists of three parts.

Firstly, efforts have been dedicated to improve the module “PathKit” in T.S.T., which aim to improve the functionality of trajectory generation. The algorithm of trajectory generation for the curved substrate surface was improved to maintain a constant scan step. A novel Archimedean spiral trajectory was developed for damage component recovery application by cold spray. The experiment of an Al5056 coating depositing on a manually manufactured workpiece with a crater defect was carried out to validate the effects of spiral trajectory with adapted nozzle speed.

Secondly, numerical models were developed to simulate the coating thickness distribution in 2D and 3D, and then integrated in the RobotStudio™ as an individual module named “ProfileKit”. In the “ProfileKit 2D”, it is able to evaluate the effects of operating parameters on coating profile and optimize the parameters. In the “ProfileKit 3D”, coating thickness distribution can be simulated based on the nozzle trajectory and robot kinematics data. The functionalities were validated by the trapezoid cold sprayed coating.

At last, kinematic analysis was used to provide the optimization methods for a better robot performance in thermal spraying. In order to better evaluate the robot performance, an overall parameter (OP) that is the weighted mean of standard deviation of joint speed, was introduced to measure the complexity of a robot trajectory. Afterwards, the optimal nozzle mounting method as well as the optimal workpiece placement were investigated by the kinematic analysis and the overall parameter. The result shows that the kinematic optimization can effectively improve the robot performance to maintain the predefined speed.

Key words: Thermal spray, offline programming, robot trajectory, robot kinematics, cold spray, coating thickness, damage repair

Résumé

La technologie de programmation hors-ligne permet de façon générale la génération de trajectoires complexes. Dans le laboratoire IRTES - LERMPS, spécialisé dans les activités de la projection thermique, une extension logicielle appelée « Thermal Spray Toolkit » (T.S.T.) a été développée pour assister la programmation hors-ligne dans ce domaine spécifique. Cependant, des efforts sont encore attendus pour améliorer sa fonctionnalité. C'est pourquoi, l'objectif de cette thèse vise à améliorer l'application de la programmation hors-ligne en projection thermique. En accord avec la démarche de recherche engagée, les travaux de cette thèse se composent de trois parties.

Premièrement, les efforts sont dévoués à l'amélioration du module « PathKit » dans le module T.S.T, afin d'optimiser la fonctionnalité de la génération de trajectoires. L'algorithme pour la génération de trajectoires sur un substrat courbe a été étudié de manière à assurer le pas de balayage constant. Une nouvelle trajectoire appelée « Spirale d'Archimède » a été développée pour réparer les défauts formés en projection à froid. La réparation sur une pièce d'aluminium avec un défaut a été réalisé pour valider ce type de trajectoire en spirale d'Archimède.

Deuxièmement, des modélisations ont été développées pour simuler l'épaisseur du dépôt en 2D puis en 3D. Puis, ces modèles sont intégrés dans le logiciel RobotStudio™ comme un module individuel dit « ProfileKit ». Dans le « ProfileKit 2D », le module peut évaluer les effets des paramètres opératoires sur le profil du dépôt et puis optimiser les paramètres. Dans le « ProfileKit 3D », l'épaisseur du dépôt peut être simulée selon la trajectoire du robot et la cinématique du robot. Les fonctionnalités sont validées par un dépôt de forme trapézoïdale élaboré par la projection à froid avec des pas de balayage varié.

Troisièmement et dernièrement, l'analyse cinématique du robot a été étudiée pour optimiser sa performance pendant le processus de projection. Afin de mieux évaluer la performance du robot, le paramètre « overall parameter » (OP), qui correspond à la moyenne pondérée de l'écart-type de la vitesse articulaire, est introduit pour mesurer la complexité de la trajectoire du robot. Ensuite, l'optimisation du montage de la torche ainsi que l'optimisation de la disposition de la pièce sont étudiées par l'analyse cinématique du robot et du paramètre OP. Le résultat montre que l'optimisation cinématique peut améliorer efficacement la performance du robot pour maintenir la vitesse prédéfinie.

Mots clés : Projection thermique, programmation hors-ligne, trajectoire robot, cinématique robot, projection à froid, épaisseur du dépôt, réparation de défauts

Content

List of figures

Chapter 1 Introduction

Chapter 2 Trajectory generation by offline programming technology

Chapter 3 Effects of operating parameters on coating properties and coating thickness

Chapter 4 Kinematic optimization of robot trajectory

List of tables

Chapter 1 Introduction

Chapter 2 Trajectory generation by offline programming technology

Chapter 3 Effects of operating parameters on coating properties and coating thickness

Chapter 4 Kinematic optimization of robot trajectory

Chapter 1

Introduction

1.1 Thermal spray principle

Nowadays in the manufacturing industry, thermal spraying is becoming more and more important. With its abilities to provide corrosion protection, wear control, damage repair, fouling protection and temperature/oxidation protection, thermal spraying has drawn more and more attention [1]. As an important method of surface treatment, it has become an indispensable process in the manufacturing industry for durable products, such as automobiles, aircraft, aviation and shipping. Meanwhile, cold spray that is a newly-emerged coating deposition among various thermal spray technologies has been applied for efficient additive manufacturing and dimensional damage repair. The high precision and accuracy for coating profile control and an as-sprayed coating form leads to a higher demand for nozzle trajectory and its kinematic control. Thus, for the reasons above, an industrial robot was widely applied in the thermal spray process to improve the process precision and accuracy. In this section, the principle and basic information about thermal spray will be introduced.

1.1.1 Principle of thermal spray

Thermal spray is a process in which melted or heated material is deposited on the surface of a substrate for the purposes of providing various protection and additional functions to a component [1, 2]. It is able to deposit a coating with a wide range of thickness from 20 μm to several mm, which depends on the spraying technology and feedstock material. The thermal spraying process consists of heat and molten or semi-molten feedstock, in the form of a powder or thread, motivated by energy such as combustion or electricity. The molten or semi-molten particles will be accelerated and crashed onto the substrate surface, and then solidified to form a coating [1]. The thermal spray is available for materials including metal, ceramic, alloy, plastic, and composite. The energy source can be from the wire arc, flame, plasma, or air flow.

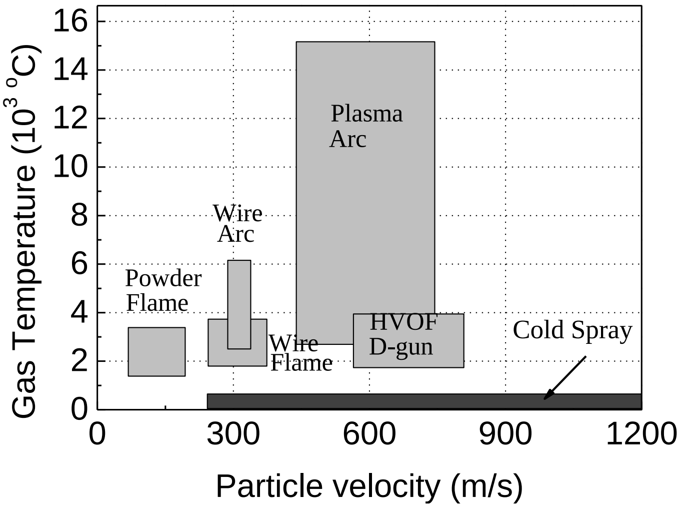

Figure 1.1 Comparison of different thermal spray technologies in terms of particle velocity and gas temperature.

According to the melting form and the energy source, a thermal spray can be divided into several sub-categories including plasma spraying, wire arc spraying, high velocity oxygen fuel spraying (HVOF) and cold spray. As shown in Figure 1.1, according to the particle velocity and the gas temperature, cold spray can be separated from other thermal spray technologies due to its low gas temperature and high particle velocity. The general principle of thermal spray (a) and cold spray (b) are shown in Figure 1.2, respectively. Table 1.1 shows the characteristics of different spray technologies, where the parameters are essential for the robot trajectory programming. In the following section, different thermal spray technologies will be briefly introduced.

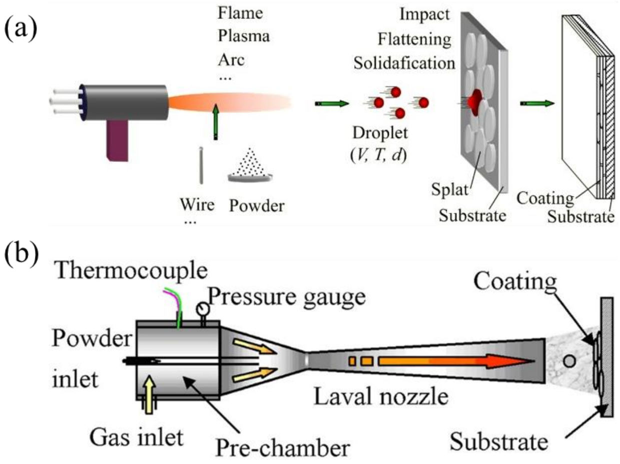

Figure 1.2 General principle of (a) conventional thermal spraying process, (b) cold spray process.

Table 1.1 General principle of thermal spraying process.

Process	Scanning Speed (mm/s)	Jet impacting Diameter (mm)	Spray Distance (mm)	Spray Distance Tolerance (mm)	Coating Thickness (mm)
Flame	500	10–20	100–200	10	0.1–1.5
HVOF	1000	10–40	100–250	20	0.2–3
Wire Arc	1250	8–20	80–150	10	0.05–1.5
Plasma APS	1000	30	150–350	20	0.05–1
Cold spray	10–100	4–8	10–30	10	0.01–10

1.1.2 Typical thermal spray technology

1.1.2.1 Plasma spray

Plasma spray [3, 4] is a thermal spray coating process used to produce a high quality coating by a combination of high temperature, high energy heat source, a relatively inert spraying medium, usually argon, and high particle velocities. Plasma is the term used to describe gas that has been raised to such a high temperature that it ionises and becomes electrically conductive. The utilisation of plasma spray coating technology allows the spraying of almost any metallic or ceramic onto a large range of materials with exceptional bond strength, while minimising distortion of the substrate.

Due to its versatility and excellent characteristics, the plasma spray coating process is selected by many technologists, which is able to offer the widest choice of coating materials. Its application includes wear and erosion resistance [5], high temperature protection, thermal barrier coatings (TBC) [6], erosion/abrasion resistance and so on. As a result, plasma spray has been widely used in the aerospace, automotive, medical devices, agriculture communication and so on.

1.1.2.2 High velocity oxygen fuel spraying (HVOF)

In the process of HVOF [7, 8], a mixture of fuel and oxygen is fed into a combustion chamber, where it is ignited and combusted continuously. The resultant hot gas at a pressure close to 1 MPa emanates through a converging-diverging nozzle and travels through a straight section. The fuels can be gases such as hydrogen, methane, propane, propylene, acetylene and natural gas or liquids such as kerosene. The jet velocity at the exit of the barrel is usually over 1000 m s^{-1} and thus exceeds the velocity of sound. Powder material is fed into the jet at the feed ports and the powder particles are heated and accelerated toward the substrate, where they impinge at high velocity to form a coating. The process has been most successful for depositing cermet materials such as WC–Co and other corrosion-resistant alloys such as stainless steels and nickel-based alloys.

1.1.2.3 Cold spray

Cold spray as a promising technology for damaged components recovery [9, 10] has been drawing more and more attention from both industrial and scientific communities with its unique characteristic—‘cold’. As a relatively new surface coating technology, there has been a rapid development for cold spray in the past two decades since its invention in the 1980s [5]. Differing from traditional thermal spray processes where molten or semi-molten particles deposit at a low velocity, the low temperature and high velocity of cold sprayed particles upon impact can avoid the occurrence of particle oxidation as well as local thermal residual stresses [6, 7]. Moreover, dominated by mechanical interlocking or metallurgical bonding, cold spray is able to provide dense and thick deposition with high adhesion strength, low residual stresses and low porous structure [8-10]. Because of the features that are superior to other techniques, cold spray has been widely applied for the deposition of various non-porous protective coatings and also dimensional recovery of worn-out or corrosive components [11-13]. Among all the potential application fields, the additive manufacturing for repairing damaged components in the aerospace industry is probably the largest beneficiary of repair by cold spray [14-16].

1.2 Application of industrial robot

Generally, a robot is a mechanical or virtual artificial agent that is guided by a programme or electronic circuitry. With the capacity of imitating certain human functions such as manipulation and moving objects, a robot is expected to serve as a substitute for human effort in certain tasks. This realisation is autonomously achieved based on the perception of the environment of the robot [11]. Since the first digital and programmable robot named Unimate invented by George Devol in 1954 for lifting pieces of hot metals from a die casting machine, robots have been widely spread and used in fields like manufacturing, assembly and packing, transport, earth and space exploration, surgery, mass production and laboratory research. Their advantages such as better performance, lower labour cost and higher repeatability have promoted their application in the fields mentioned above. They are also able to replace humans in those repetitive and dangerous tasks that humans prefer not to do, or are unable to do because of the size limitations or even those extreme environments such as outer space or the deep ocean [12, 13]. As a result, the definition of a robot has been divided into several categories, such as the mobile robots, industrial robots, collaborative robots, autonomy and ethical robots, military robots and so on.

Within all the classification, the industrial robots are widely adopted in the field of industrial manufacturing and processing. According to the IOS8373 definition, an industrial robot is an automatically controlled, reprogrammable, multipurpose manipulator with three or more axes. Typical applications of robots include welding, painting, assembly, pick and place, product inspection and testing, are all accomplished with high endurance, speed, and precision. Due to their advantages like repeatability, programmability and flexibility, industrial robots have liberated humans from unnecessary efforts and repetitive operations, brought increasing productivity and better human resource distribution. Meanwhile, due to the fact that the motion of industrial robots is planned and generated by programming language, it is flexible and can modify robot motion and its operating parameters while maintaining high precision. Another important factor is that industrial robots can protect human operators from potential harm from the working environment, such as noise, high temperature and toxic gases. For example, as for the application of welding, a robot can perform the welding motion more constantly and smoothly, providing a better welding quality. Moreover, protective measures such as goggles, protective clothing and ventilation, prepared for humans, are not necessary for robots. As a result, as long as the working routine is well programmed and prepared, robots can largely improve productivity. Due to the advantages that industrial robots have, robots been applied in various fields. Three typical application examples are provided as below in this section.

1.2.1 Thermal spray robot

In a thermal spray process, a spray nozzle is mounted on the sixth axis of the robot to deposit coating on the substrate surface. Due to the extreme working environment of a thermal spray, high temperature, noise, dust and noxious gas are potentially harmful to an operator during a thermal spray process. Thus, the application of an industrial robot becomes a perfect solution to protect the operator. Meanwhile, a qualified coating requires stable thermal spray operating parameters such as spray angle, standoff distance, and nozzle traverse speed. A robot-assisted thermal spray can provide the precision and stability that manual operating cannot offer, which makes an industrial robot a perfect assistant in the thermal spray process. Thus, the work in this thesis is based on the application of industrial robots in the thermal spray process.

1.2.2 Multi-axis robot system

Generally, a robot consists of two parts, including the manipulator and its controller system. A typical 6-axis robot is shown in Figure 1.3, which is an ABB IRB 2400 robot. The robot manipulator includes the main body, arm and wrist. The servomotor and reducer equipped at the wrist enables the movement and stability of robot motion. An end effector, also known as end-of-arm-tooling (EOT), can be installed at the 6th axis to achieve certain tasks. Common examples of end effectors include welding devices, spray guns, grinding and deburring devices, grippers and so on. End effectors can be highly complex according to different applications, which have further requirements for robot motion. Meanwhile, various sensors can be utilised to aid the robot system in locating, handling, and positioning products. For example, in the thermal spray process (plasma, HVOF, flame), the laser beam that follows the thermal spray spot could be used to in-situ remelt the coating by laser [14]. The laser followed by thermal spray spot can be used as a method of substrate pre-treatment [15].

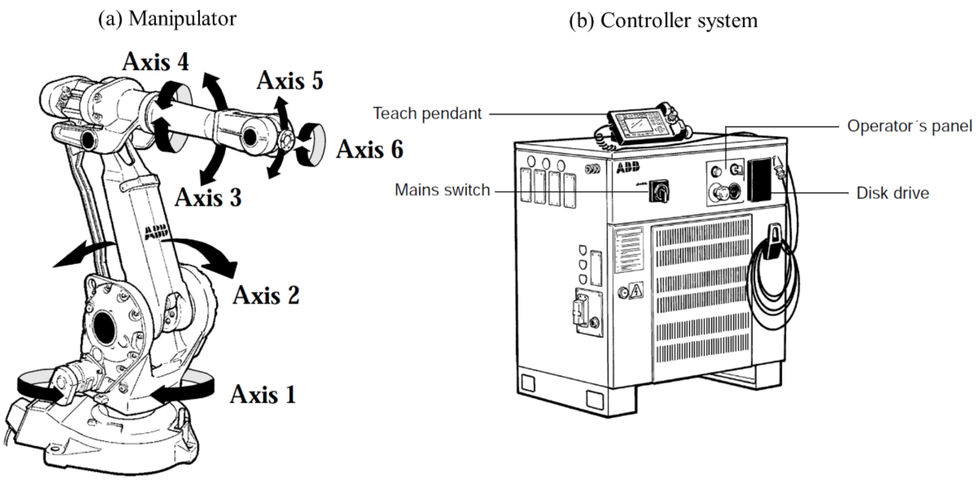

Figure 1.3 ABB IRB 2400 consisting of (a) manipulator with 6 axes and (b) controller system.

As an example of an ABB IRB2400 robot, the controller contains the electronics required to control the manipulator, external axes and peripheral equipment. The portable teach pendant, as shown in Figure 1.3 (b), is used to display robot status, to control and programme robot motion. Using the joystick on the teach pendant, the robot can be manually jogged (moved). The user determines the speed of robot movement by controlling the deflections of the joystick. Robot motion programmes prepared on the PC can be synchronised to the robot controller system via the disk drive shown in Figure 1.3 (b). The robot is equipped with an operating system called BaseWare OS, which controls every aspect of the robot, like motion control, development and the execution of application programmes communication.

1.2.3 Thermal spray operating parameter

As mentioned above, industrial robots have been widely applied in thermal spray processes due to their stability and precision of manipulation and motion, which leads to the fact that the coating quality is directly affected by robot kinematics. Thus, it is of great importance to study the influence of robot operating parameters on thermal sprayed coating quality. The thermal spraying process consists of a series of operating parameters, which also affects the thermal spraying process directly. These parameters have a significant influence on the deposition efficiency, temperature distribution on the substrate, morphology and structure of the coating, which are related to the coating quality [16-18]. Concerning robot kinematics and coating quality, the process can be controlled directly by the robot. As a result, the coating quality of the thermal spray can be directly controlled and influenced by robot kinematics, which can control the thermal spray operating parameters as well. Research into the relationship between coating quality, robot kinematics and thermal spray operating parameters is essential for the thermal spraying process. As shown in Figure 1.4 below, the operating parameters also called the kinematic parameters are listed below:

- Robot trajectory
- Relative speed between nozzle and substrate
- Spray distance
- Spray angle
- Scanning step

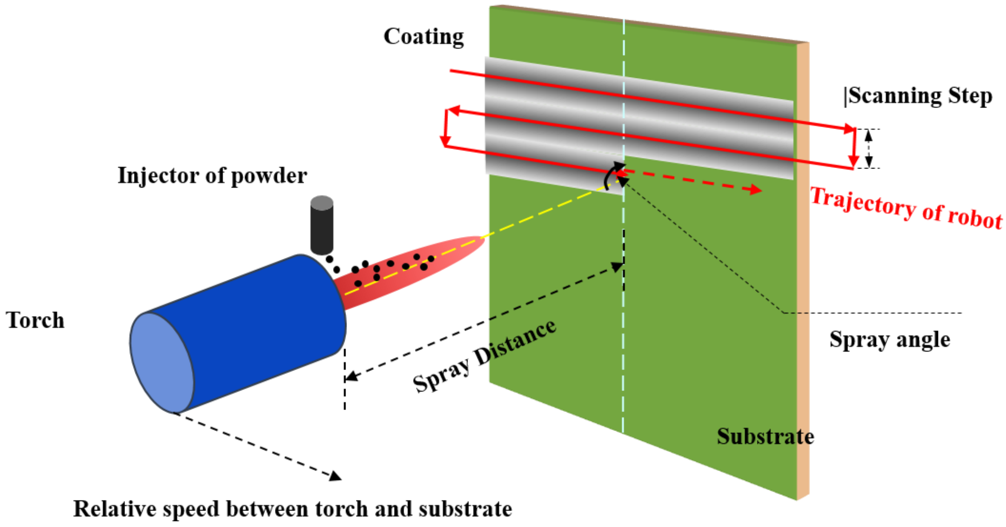

Figure 1.4 Operating parameters in the thermal spraying process.

1.2.3.1 Nozzle traverse speed

The nozzle traverse speed is the moving speed of the robot in relation to the substrate. With certain mass flow through the feedstock injector, it is a parameter that has the most influence on the mass distribution and coating thickness. If the nozzle moves faster, there will be fewer particles deposited at the substrate surface and the corresponding coating thickness will be decreased. Meanwhile, the slower the nozzle moves, the longer the heating source will stay on the same spot on the substrate surface, which leads to the deterioration of the coating quality caused by local over-heating and residual stress.

Generally, in order to make the coating thickness uniform, it is very important and necessary to maintain the relative nozzle speed constant. Normally, the effective moving speed of a robot during operation cannot be maintained at the predefined value due to the factor of inertia. For this purpose, the operator should eliminate the influence of the inertia of the nozzle setup and associated equipment on the robot speed. In order to obtain a uniform coating profile, studies have been performed to improve the stability of robot performance by kinematic optimisation [19, 20].

1.2.3.2 Spray angle

Generally, in the thermal spraying process, the nozzle is kept vertical to the substrate surface, which is considered to have a maximum deposition efficiency. The inclined spray angle will increase the particle loss and decrease the deposition efficiency due to the particle rebound at the substrate. In the same time, the porosity of the coating will increase if the spray angle decreases from 90° [21, 22]. So maintaining the nozzle vertical to the substrate will increase the coating quality, which is easier to achieve for the plane surface. For the workpieces that have complex geometry, the direction of each target point in the trajectory on the substrate is should be well defined for keeping the nozzle vertical to the substrate during the entire spray process. As a result, a relatively more complex programming method with CAD (computer-aided design) file is necessary.

But for the workpiece with a complex shape, one of the robot axes will reach its rotation limit at a certain point on the workpiece. There are also circumstances in which the robot has to compromise the spray angle to obtain a smoother scanning speed and coating quality. The spray angle between 90° and 45° is considered acceptable, by striking a balance between deposition efficiency and the coating quality. Therefore, many approaches have been developed to simulate the coating thickness, which is mainly to find the relation between the spray angle and the coating thickness [23-25].

1.2.3.3 Standoff distance

The spray distance is the gap between the nozzle and the substrate surface, which will decide particle states while reaching the surface and the impacting intensity of particle on substrate. The value of spray distance will also affect the coating thickness and deposition efficiency [20].

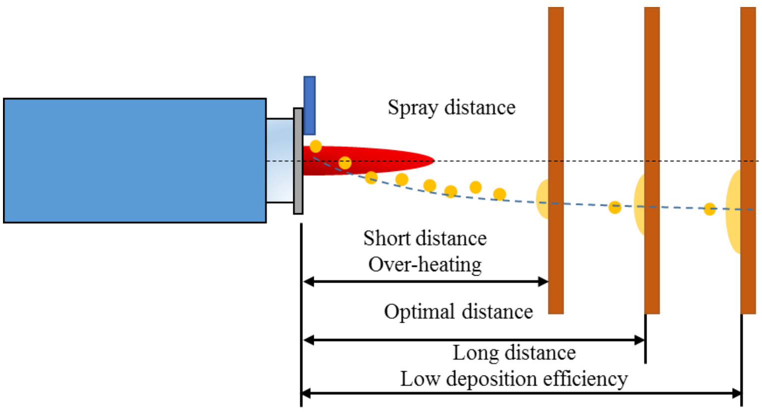

Figure 1.5 Influence of spray distance.

As shown in Figure 1.5, the spray distance will directly influence the flight duration of particles from the nozzle to the substrate [26]. If the distance is too short, the particles injected in the nozzle will stay in the state of a solid and cannot be accelerated to a sufficient speed. However, when the distance is too long, the molten particles could have solidified before reaching the substrate, which will decrease the deposition efficiency. As a result, when an appropriate value of spray distance is defined, it should be constant during the operating process.

1.2.3.4 Scanning step

For a coating deposited by a multi-path trajectory, its coating profile can be considered as the superposition of the profile by each individual nozzle path. So the interval between two successive scanning paths is the key factor for the uniformity of coating and the coating thickness, as presented in Figure 1.6. The optimal value of the scanning step can result in a uniform coating. If the scan step is too small, the coating surface roughness will become rather low; however, the residual stress will increase significantly for the reason of local overheating. For the APS (atmosphere plasma spray), the optimal scan step is between 5 and 15 mm.

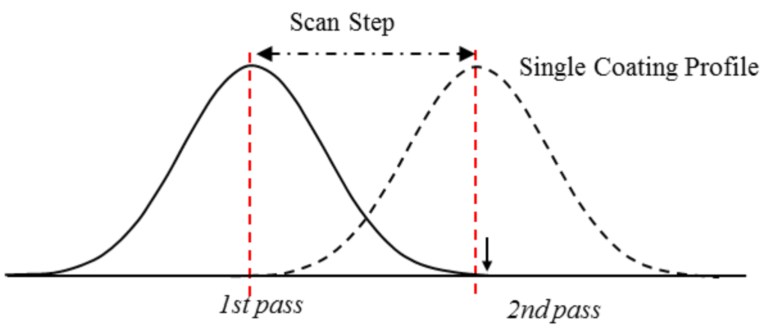

Figure 1.6 Structure of coating surface.

1.2.3.5 Over-length

The parameter called over-length is a part of the trajectory that exceeds the boundary of the workpiece, as shown in Figure 1.7. In order to change the scanning direction between two successive passes, the robot has to overcome the inertia from itself and the weight of nozzle. So over-length is the length of the area for the robot to accelerate and decelerate between two successive passes, which will help the robot move at the predefined speed on the substrate to spray. However, no coating will be deposited while the nozzle is outside the area of the substrate. An appropriate value of over-length is needed to avoid an unnecessary waste of materials, which leaves enough space to reach the predefined speed.

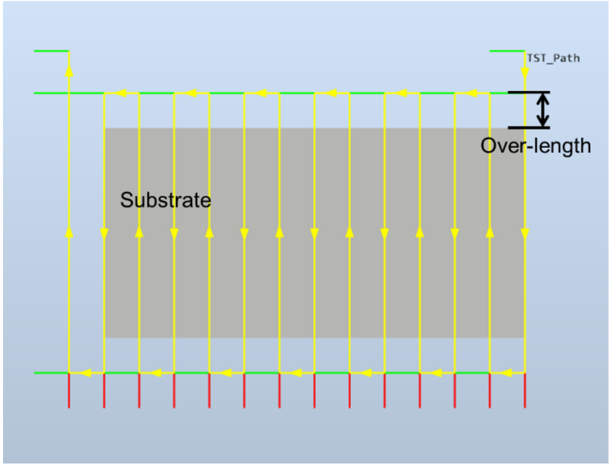

Figure 1.7 Round-trip trajectory with an over-length.

1.2.4 Robot kinematic parameter

1.2.4.1 Degree of freedom

Generally, the number of axes for a simple manipulator such as a CNC machine is between 2 and 3, and between 3 and 6 for the programmable robots [27]. Theoretically, for a simple manipulator it requires two axes to reach a point in a plane, and three axes to reach a point in space. Meanwhile, for the programmable robots, in order to fully control the orientation of the end-effector, three more axes (yaw, pitch and roll) are required. In other words, to move a rigid body to a position with a predefined orientation, three components of translation and three components of rotation are required to be defined [28]. Generally, the degree of freedom is the same as the number of axes. As a result, the degree of freedom is usually six for a typical industrial robot.

1.2.4.2 Working envelope

In robotics, a working envelope is defined as the maximum overall area within which the robot arm can move. For a robot, the working envelope is its range of movement, usually measured from the base of the robot (base coordinate system). As shown in Figure 1.8, it is the shape that is created when a manipulator reaches forward, backward, up, and down. These distances are determined by the robot properties such as length/diameter of each joint component, rotation range of each joint, and design of the axes. Each axis contributes its own range of motion. A very important factor is that the trajectory and robot motion should be planned within the limits of the working envelope [27].

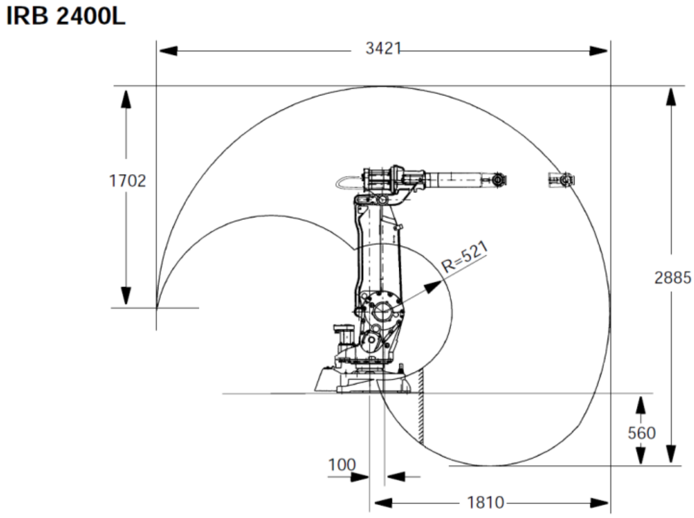

Figure 1.8 Working envelope of ABB IRB 2400L robot.

1.2.4.3 Payload

The payload or carrying capacity is based on the size of robot and power of actuator. It stands for the weight of work pieces on the assembly line, or the operation tools. For the security reasons, the payload of a robot is measured under the largest operation speed. Nowadays, an industry with higher and higher power support can bring a bigger and bigger payload, which is very useful for applications like lifting, manipulation, welding on large surface. Also, for the application of transfer robot, the payload can vary from 900 Kg to 3000 Kg. For example, the payload of robot IRT 501-90R from ABB Company is 2950 Kg.

In the laboratory of LERMPS, three ABB robots are equipped for different thermal spray processes. For example, an ABB IRB 4400 M98 robot that has a maximum load capacity of 60 Kg [29] is equipped for plasma spray processes, which can handle the spray system including nozzle, cable and powder feed system. As for the cold spray system, an ABB IRB 2400 robot with maximum load capacity of 10 Kg [30] is used, which can satisfy the less complicated spray system mounted on the robot.

1.2.4.4 Speed

Robot speed is the capacity of how fast a robot can move the TCP (tool centre point) within the working envelope, which is a very important characteristic for evaluating the robot performance. Similar to the robot payload, robot speed also depends on the size, power and other specifics of the robot. It also depends on the kinematic performance of each axis during operation [31].

Normally, there is a limit for the robot speed and the rotation speed of each axis. While the distance for acceleration or deceleration is not enough, the robot could not reach the predefined speed. Meanwhile, the speed of the robot largely depends on the performance and the motion of each axis. A constant or smooth motion of the robot is very important for many applications including, painting, welding, etc. A robot speed that deviates from the predefined value cannot ensure the product quality. As a result, it is very important to ensure a constant robot speed concerning robot kinematics.

Actually, in the thermal spray process, different nozzle traverse speeds are applied according to the desired coating thickness and the specific thermal spray technology. For example, in cold spray, the nozzle traverse speed is chosen as 40 mm/s [32] to 200 mm/s [33, 34] to achieve a full coating deposition. Sometimes, a nozzle traverse speed [35, 36] as high as 500 mm/s is used to obtain the single particle deposition on substrate, which is usually for the study of bonding mechanism and particle deformation behaviour. However, due to the high-energy input by the heat source in the thermal spray process, the nozzle traverse speed can be significantly different. In an atmosphere plasma spray (APS) process, the nozzle traverse speed is usually set as 500 to 1500 mm/s [37, 38], which is similar in a suspension plasma spray (SPS) [37] process.

1.2.4.5 Joint motion

For each axis during the robot movement, its motion can be separated into three parts: joint position, speed and acceleration. For the joint position, it represents the value of axis rotation at a given time, with a unit of degree. As a result, the joint positions of each axis decide the TCP position and orientation in the working envelope. At the same time, a smooth changing joint position within its rotation limit is favourable for a better motion performance. A sudden change of joint position will take more energy for a servomotor of an axis to complete a defined robot motion, and also result in more fluctuation of TCP speed. As for the joint speed, it is the angular speed of an axis, which is defined by the derivative of the joint position with respect to time. It has a unit of degree per second (°/s).

Table 1.2 Technical specifications of robot ABB IRB 2400/16.

Item	Value
Unidirectional pose repeatability (mm)	0.06
Linear path accuracy (mm)	0.45–1.0
Linear path repeatability (mm)	0.14–0.25
Axis motion resolution (°)	0.01

As another variable to evaluate the axis performance, the joint speed represents how fast an axis is rotating, whose limit is based on the servomotor performance. A sudden change of joint speed of an axis will bring rapid change of joint position with the risk of reaching its limit. A constant or gradually changing value of the joint speed is suitable for the robot motion. In other words, joint acceleration can be used to evaluate the robot motion. Generally, the joint acceleration is to evaluate how joint speed varies, with a unit of °/s2. The larger the joint acceleration, the greater the power the servomotor has to provide. A joint acceleration that is low or constantly maintained can reduce the mechanical wear. As a result, for a single axis, three limits exist and restrict each other. In order to improve the robot performance and maintain the TCP speed, it is important to make sure that all the joint positions are within limits; moreover, the joint speed of all axes are constant or changing smoothly.

Table 1.3 Axis motion specification of robot ABB IRB 2400/16.

	Range of Movement, °	Maximum axis speed, °/s
Axis 1	+180 to -180	150
Axis 2	+110 to -100	150
Axis 3	+65 to -60	150
Axis 4	+200 to -200	360
Axis 5	+120 to -120	360
Axis 6	+400 to -400	450

1.3 Robot programming

Based on the application in the thermal spraying process, industrial robots are required to perform the complicated movements with high precision. The trajectory generation should be based on different operating parameters, as well as the workpiece geometry. Thus, an efficient and proper programming method is necessary for trajectory generation and post-analysis. Depending on the type and complexity of a robot, various programming methods have been developed for the generation of robot trajectory. Nowadays, in the field of robot programming, most operations are achieved on-line, such as on-line testing and measurements. Most of the robotic programming uses the teaching method, which is appropriate and efficient for some simple tasks. However, as for the movements with more requirements in precision, trajectory complexity and its optimisation, the method called the off-line programming method is adopted more and more. In this section, these methods of trajectory generation for robots will be presented.

1.3.1 On-line programming method

The on-line programming method is also called programming by teaching. Currently, it is the most used programming method in industry. In general, the tool and its assembly are first installed on end-effector of robot (wrist). The operator uses a handheld control and programming unit called the teach pendant, which allows manually jogging of the robot and moves the TCP to the desired position, and then stock these points (including positions and orientation of robot) in a series of movement instructions. Thus, after all the target points and robot movement instructions are stored, the trajectory is accomplished and ready to test.

This method of programming has the advantage of low-learning costs and is easy-to-use. Once the abilities of controlling a robot and storing the instructions and positions are acquired, the operator is thought to be qualified for this work. However, due to the fact that this method requires many manual operations and robot movements, the programming process will be tedious and time-consuming. On the other hand, the production has to be interrupted for the robot programming. However, this will not be a problem for the robots with unchanged and repetitive tasks. But for the tasks that demand not only high complexity and precision but also the requirements of modification, the on-line programming method is not appropriate because the complexity and time for programming will largely increase. For example, in Figure 1.9 (a), the trajectory on a workpiece with a plane surface can be generated by finding the vertex of the workpiece and defining the over-length value, and the orientation of different target points can be defined at the same value. As for the example in Figure 1.9 (b), not only the vertex, but also the target points along the horizontal scan on the surface with a constant interval are required to describe the trajectory. In addition, the normal vector of each target on the surface should be obtained in order to define its orientation and ensure that the spray angle is 90°. Thus, in this instance, the on-line programming method is no longer able to satisfy the trajectory generation. Furthermore, the precision of the robot trajectory and its performance will mostly depend on the operator's skill and experience, which is obviously out of tolerance. The second programming method called the off-line programming method will be presented in the next part, which is developed for the generation trajectory on a complex workpiece, as the example in Figure 1.9 (b).

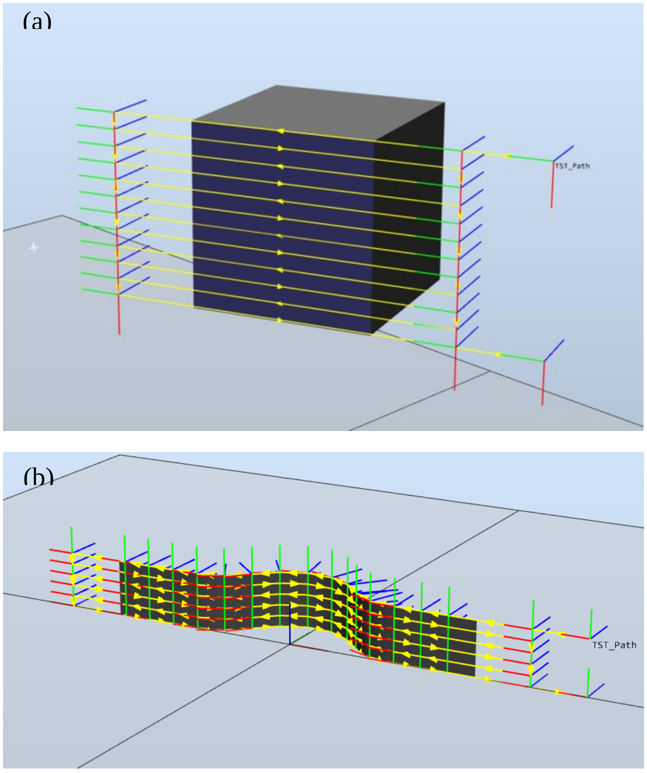

Figure 1.9 Two examples of generated trajectory: (a) planar surface, (b) curved surface.

1.3.2 Off-line programming method

Most robots perform movement by storing a series of positions in memory manually, and moving to them at a pre-defined speed in the programme sequence. The robot programme can be composed directly on a computer terminal by editing the instruction language of the robot in a text file. For a complex robot movement, large amount of target points is required to define the trajectory, such as a trajectory to cover a curved surface (Figure 1.9 (b)). Some points on the first scanning can be defined in the work cell and then the trajectory can be achieved by adding the extruded points generated in other software such as MatLab, based on the Cartesian coordinates (x, y, z). However, this simple method does not meet all the requirements for complex trajectory generation. Finally, there is an advanced technology called off-line programming that provides a complete solution for industrial robots, from trajectory generation, parameter selection to procedure simulation and trajectory optimisation. The robot trajectory can be generated by using the geometrical data of the workpiece to guarantee the trajectory precision [39-41].

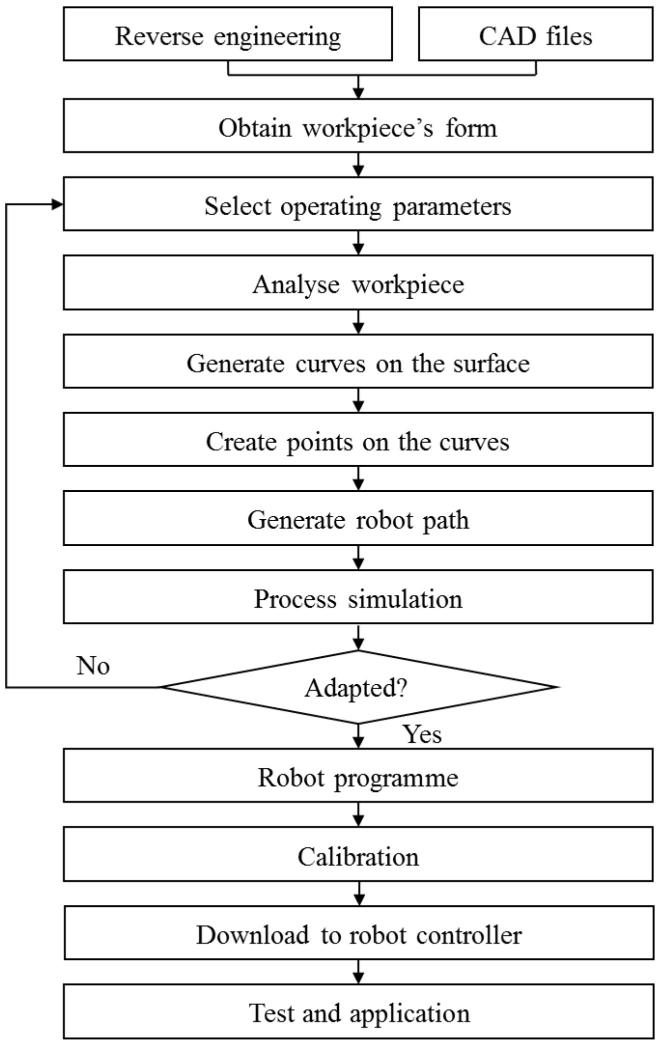

Figure 1.10 Procedure of an off-line trajectory

Figure 1.10 shows the diagram of this method for a thermal spray. Meanwhile, with the help of CAD/CAM (computer aided design/computer aided manufacturing) software, robot off-line programming method has the potential to provide a visualisation of the workshop [42, 43]. Also, the robot programme can be generated and simulated with this visualisation system. The robot motion data can be easily accessed with the visualised software based on the off-line programming method, such as robot speed, joint position of each axis and so on. As a result, with these data and corresponding algorithms, post-processing such as collision detection and kinematic analysis of the robot during the movement can be achieved. The trajectory optimisation based on the robot motion data and the kinematic analysis also becomes possible.

Programming by graphic requires the CAD geometry of the workpiece can be used to create robot trajectories. Therefore, the first step is to acquire 3D geometric model. If there is no original CAD model available, it must create a simple model that can describe an operation object in CAD software such as: Catia (Dassault Systèmes), SolidWorks (Dassault Systèmes), Pro/Engineer (Parametric Technology Corporation), etc. If the workpiece is too complicated to be recreated by CAD software, the acquisition of a geometric model called reverse engineering should be considered. The geometric information of the workpiece can be obtained by the coordinated measuring machine or laser scanner system. The 3D model can then be rebuilt from these measured points [44]. This method is particularly effective for complex workpieces without CAD files. In section 2, the detail of generating a trajectory with off-line programming method in the thermal spraying process will be presented.

1.3.3 RobotStudio™

Due to the various advantages of off-line programming, an off-line programming software called RobotStudio™ is used for the studies in this thesis. It is a commercial software developed by ABB that enables modelling, off-line programming and simulation of robot systems using a standard Windows based PC. RobotStudio™ provides the tools to increase the profitability of a robot system by performing tasks such as training, programming, and optimisation without disturbing production. RobotStudio™ works with an off-line controller, which is a virtual IRC5 controller running locally at the PC. This off-line controller is also referred to as the virtual controller (VC). RobotStudio™ also works with the real physical IRC5 controller, which is simply referred to the real controller. Thus, users can benefit from numerous advantages including: risk reduction, quicker start-up, shorter change-over and increased productivity. Figure 1.11 shows a case of cooperation between multi robots provided by RobotStudio™.

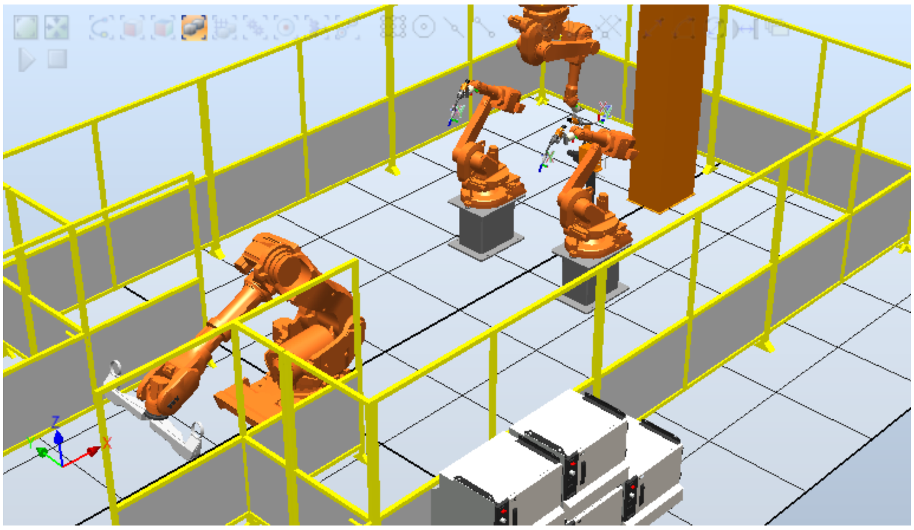

Figure 1.11 An example of robot cooperation in the software RobotStudio™.

In order to develop a robot application model as the example in Figure 1.11, the first step is to create a station with a specific robot system. Thus, a corresponding virtual controller (VC) is also created for the following robot movement simulation and modelling. A tool can be imported from the equipment library and mounted on the robot manipulator, which allows the robot to perform specific tasks. After that, a tool coordinate system (Figure 1.12) should be defined, known as the tool centre point, to specify the tool's centre point position and its orientation. In fact, several other coordinate systems are provided in RobotStudio™ for different definitions. The world coordinate system defines a reference to the floor, which is the starting point for the other coordinate systems. Using this coordinate system, it is possible to relate the mechanical unit position to a fixed point in the workshop. The world coordinate system is also very useful when two mechanical units work together or when using a mechanical unit carrier. The base coordinate system is attached to the base mounting surface of the mechanical unit. The user coordinate system specifies the position of a fixture or workpiece manipulator. The object coordinate system specifies how a workpiece is positioned in a fixture or workpiece manipulator.

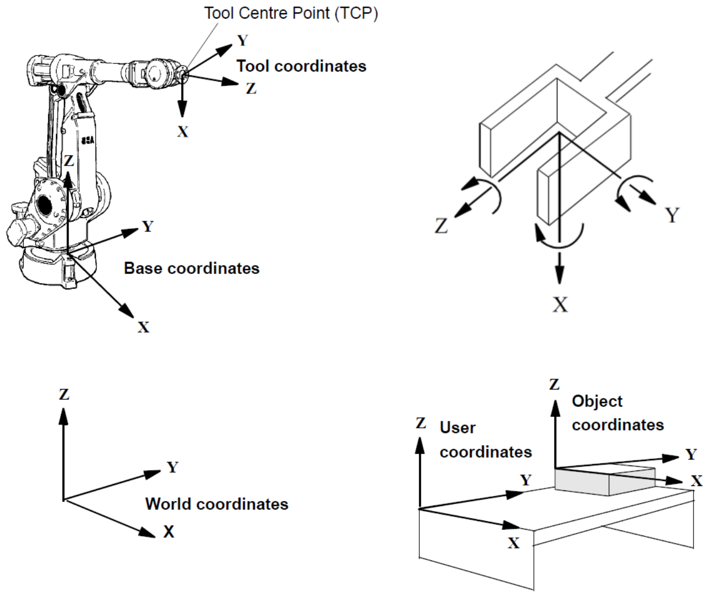

Figure 1.12 Coordinate systems used in RobotStudio™.

The coordinate systems can be programmed by specifying numeric values or jogging the mechanical unit through a number of positions (the tool does not have to be removed). Each position is specified in object coordinates with respect to the tool's position and orientation. This means that even if a tool is replaced, the original programme can still be used, unchanged, by making a new definition of the tool. If a fixture or workpiece is moved, only the user or object coordinate system has to be redefined.

The workpiece can be created by importing CAD files, whose formats vary from STL, IGES, STEP and ASCII, to ACIS. Thus, with the help of CAD files, it is easier and more accurate to obtain and define a target point position, which will result in a trajectory with higher precision. As for the workpiece with simple geometry, a 3D model can be generated directly with the function of Boolean operation, surface and curve extrusion.

After the workpiece is placed in the operation position, the target points that compose a trajectory should be created on the workpiece. In RobotStudio™, a target can be created by two methods. In the first method, a target can be created by teaching, which means its position and orientation are defined by the ones of the current TCP. Users can jog the virtual robot to the desired position with an orientation in order to create a target. In the second method, users can directly define the position and orientation of a target. RobotStudio allows users to snap a point directly on the workpiece and obtain its position. As for the orientation, the z-axis of each target is normal to the surface by default. For certain demands, users can rotate the target to re-orientate.

RobotStudio™ also provides a function to automatically generate a trajectory from a curve, which is frequently used in the process of welding and cutting. However, users can select the desired targets to form a trajectory. After the generation of the trajectory, with the virtual robotic system provided by RobotStudio™, it is able to execute a robot movement based on the generated trajectory. The motion data could be recorded by an analysis module, which includes the TCP speed, joint movement of all six axes. It provides the possibility to analyse the robot kinematics during operation. RobotStudio™ also permits the collision detection and the signal of collision in order to avoid the risk of collision during operation.

1.4 Necessity of assistant system for thermal spray application

Based on the off-line programming provided by RobotStudio™ and other software, the robot trajectory is able to be generated according to the CAD model of the workpiece. In RobotStudio™, the trajectory can be directly created on a curve or an edge of the workpiece for the application of welding. However, as for the thermal spray process, the trajectory of the end-effector that is a nozzle should cover the entire surface of the substrate rather than the edge in the welding process. The trajectory for the thermal spray process consists of the paths separated by the constant scan step. Meanwhile, for the purpose of high coating quality, several operating parameters must be constant. For example, the nozzle should be perpendicular to the substrate surface, and the distance between the nozzle and substrate should be constant as well. A few exemplary trajectories for the thermal spray process are shown in Figure 1.14, where the trajectory is generated on a curved substrate surface with a constant scan step and spray angle. It is time-consuming to create target points composing the trajectory manually in the software, and lacks precision as well. As a result, the automatic function of trajectory generation in RobotStudio™ cannot meet the standard and manual generation of the trajectory that consists of many target points, which takes much time and lacks precision as well.

With the specific requirements in the thermal spray process, it is necessary to develop software based on the off-line programming platform to assist the generation of nozzle trajectory. The software should have the capacity to generate the trajectory on the substrate with different kinds of geometries automatically. The generated trajectory should also meet the specific requirements in the thermal spray process.

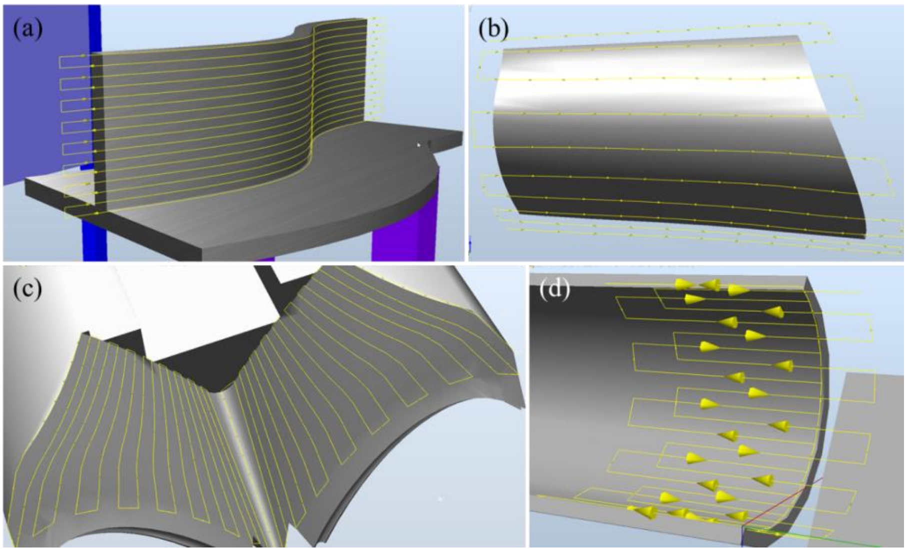

Figure 1.13 Nozzle trajectory generated for thermal spray process on the surface of different substrates.

1.5 Thermal Spray Toolkit (TST)

For the generation of trajectory in a thermal spray application, LERMPS (Laboratoire d'Etudes et de Recherches sur les Matériaux, les Procédés et les Surfaces) has developed an add-in software called Thermal Spray Toolkit (TST) based on the off-line programming platform RobotStudio™. Figure 1.14 shows the modules of TST in the thermal spraying process. In the first step, PathKit can create robot trajectory on a workpiece based on its geometry. ProfileKit then simulates the depositing of the coating and gives out a theoretical coating profile. During the spraying process, MonitorKit monitors the speed and trajectory of the robot by communicating with the operating robot. After spraying, ProfileKit can provide surface characters to evaluate the quality of coating. Therefore, it can provide the kinematic analysis to improve and optimise the robot trajectory and spray strategy. In the next part, the main functions of TST will be presented briefly.

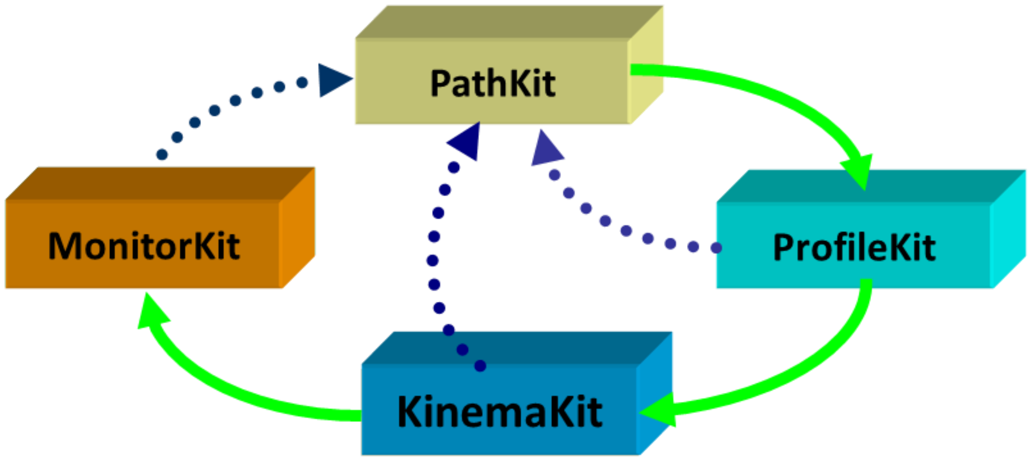

Figure 1.14 Modules in Thermal Spray Toolkit (TST).

1.5.1 PathKit

The PathKit presents a method using orthogonal planes to cut the surface to be coated, and generating a series of scanning curves. The normal vector is calculated to define the orientation of the nozzle on every point of the curves. The PathKit uses this method to generate robot trajectories in the off-line programming software RobotStudio™ for thermal spray [45, 46]. This software offers a function to perform object Boolean operations (such as union, intersection and cut) on different parts. Based on the functions mentioned above, it is able to generate a trajectory quickly and automatically according to the shape of the workpiece that meets the required operating parameters [47]. Figure 1.15 shows the cutting method applied for a test sample. First of all, the surface for coating and the edge to start with are chosen (Figure 1.15 (a)). The individual nozzle path and its target points are created according to the scan step (Figure 1.15 (b)). The final trajectory is presented in Figure 1.15 (c) and (d). PathKit is developed to generate trajectories on the surface of workpieces with different kinds of geometric shapes, including the rectangular surface, circular surface, curved surface, rotation of a workpiece.

Although a powerful trajectory generation tool called PathKit was developed, problems still emerge while encountering complex workpieces with irregular geometry. It is difficult to choose the orientation of the auxiliary planes to cut the surface when the curvature of the surface is too large. In this case, keeping the thermal spraying operating parameters constant—especially the scan step—is impossible. A mesh with uniform distribution of nodes and curves of a smooth transition can compose a trajectory for the thermal spraying process. A new module in the add-in software TST, called the MeshKit, has been developed based on the mesh for the purpose of generating trajectory on irregular workpieces.

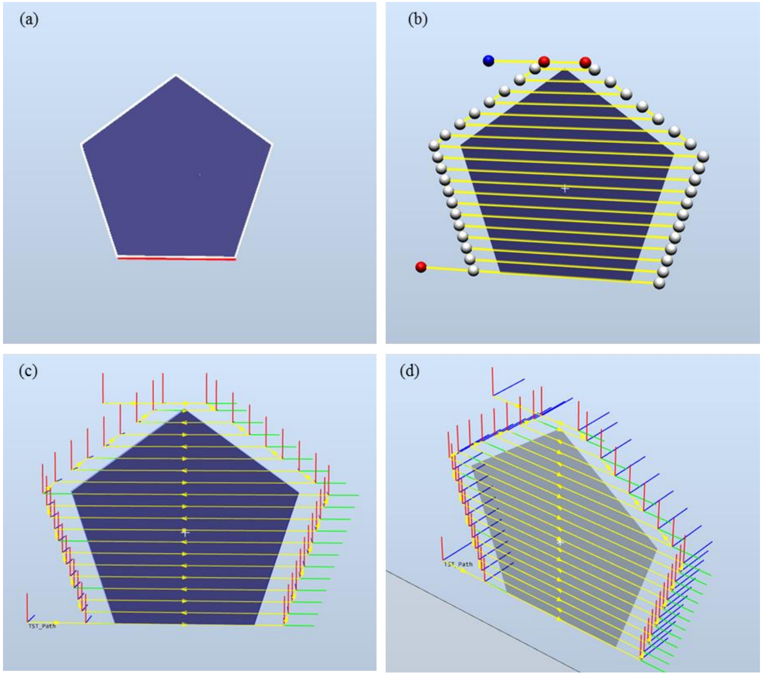

Figure 1.15 Procedure of generation trajectory in PathKit.

This add-in programme can import the mesh information created in the engineering simulation software ANSYS to the off-line programming software RobotStudio™. ANSYS provides a strategy using computer-based finite element calculation and engineering simulation, and the preprocess module of CutCell meshing is able to produce elements on complex 3D geometry. With the help of MeshKit, the mesh information generated by ANSYS can be transferred to RobotStudio™ to assist the trajectory generation.

In the first step, ANSYS is used to create mesh for the trajectory generation. ANSYS is a finite element modelling and analysis tool, which can be used to analyse complex problems in mechanical structures, thermal processes, computational fluid dynamics, electrical fields, etc. It provides graphics capability that can be used to display results of analysis on a high-resolution graphics workstation. The preprocessing of ANSYS analyses the geometry by a numerical technique called finite element analysis (FEA). FEA is a mathematical representation of a physical system, which contains a part/assembly (model), material properties, and applicable boundary conditions. The pre-processor function of ANSYS uses the CAD model to represent the physical model (Figure 1.16 (a)) and divide it by mesh. The size of the mesh element depends on the requirements of users and the shape of the workpiece.

According to the characteristics of the robot trajectory in the thermal spray, the scanning of the nozzle should be a set of parallel series on the surface to spray. So the hexahedral unit is the best choice while defining the mesh element type. The length of the hexahedral unit edge is in accordance with the step distance of the nozzle scanning, which is normally set as 5–10 mm. As shown in Figure 1.16 (b), the mesh can be generated by ANSYS. Then, the mesh grid information will be saved as a text file, which will be used in MeshKit for the trajectory generation. After the mesh information is transferred to RobotStudio™, it is stored in arrays for a recursive call in order to generate operational curves. Depending on the mesh information, a series of curves can be created according to the requirements of users. In general, the distance between two adjacent curves is equal to the scan step of the robot. They will automatically appear in the graphical view of RobotStudio™ for intuitive operation by users.

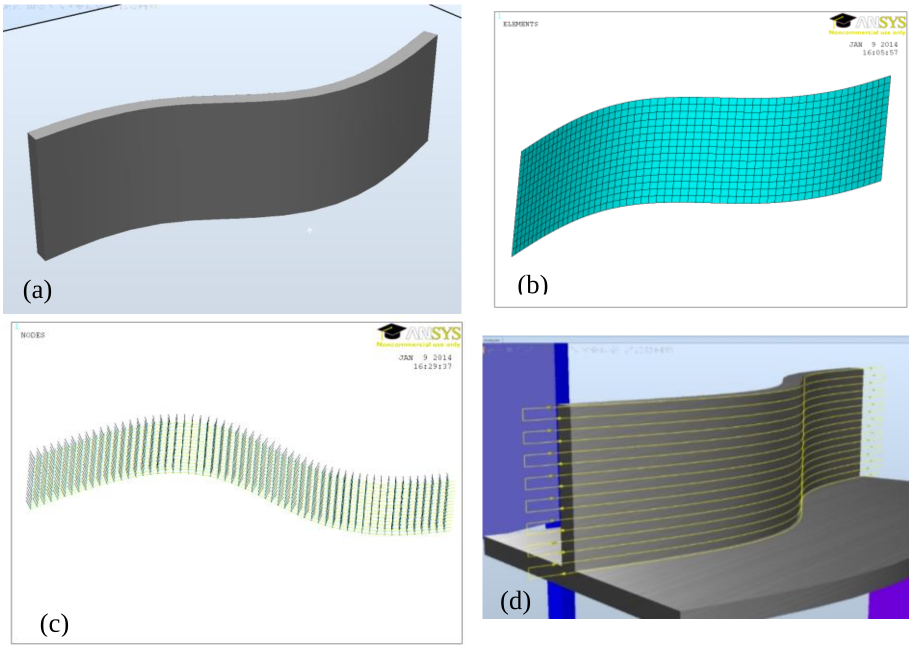

Figure 1.16 Procedure of trajectory generation in MeshKit.

Lastly, users will choose the other operating parameters in a user-interface in MeshKit and the trajectory will be generated and displayed in RobotStudio™. As mentioned above, the operating parameters include the spray speed, scanning step, spray angle and over-length. In this method, the scan step is the size of the mesh element. The spray angle is defined as 90°. So the orientation of each target point on the trajectory is normal to the surface, as shown in Figure 1.16 (c). The other operating parameters can be defined in the user interface. Figure 1.16 (d) presents the final trajectory generated for a thermal spray by MeshKit in RobotStudio™.

1.5.2 ProfileKit

Due to the features of high deposition efficiency, high adhesion strength, low oxidation and low residual stress, cold spray is considered as an effective technology of additive manufacturing (AM) or 3D printing [48-51]. However, most additive manufacturing or dimensional repairs done by cold spray are achieved by machinery on the cold sprayed block coating, which causes great amount of unavoidable material waste. Less attention is focused on the design of the as-sprayed coating shape or coating profile control with high accuracy. For the purpose of effective additive manufacturing by cold spray, it is of great importance to determine the dependence of operating parameters such as spray angle, nozzle traverse speed, scanning step and standoff distance on coating thickness distribution.

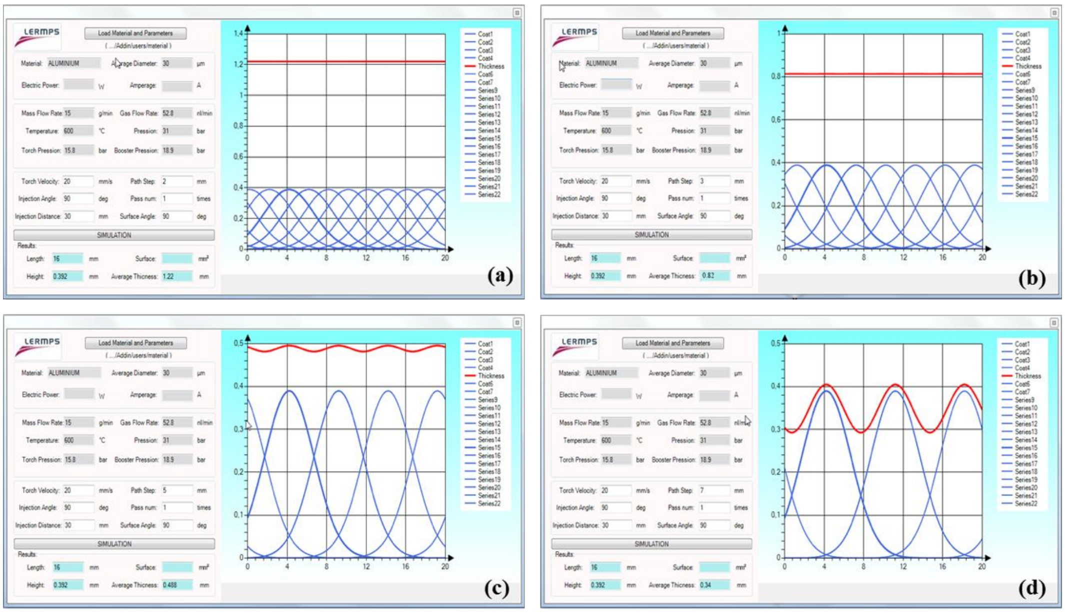

Figure 1.17 Coating thickness simulated by ProfileKit at different scanning steps: (a) 2 mm, (b) 3 mm, (c) 5 mm, (d) 7 mm.

For the purpose of coating thickness prediction and trajectory optimisation, a coating thickness model was developed. Based on the numerical model, Deng [45] and Cai [20] developed a module called ProfileKit based on TST. Based on current research, the single coating profile is simulated with a symmetric Gaussian distribution curve in the ProfileKit, and combining the curve with the optimised robot kinematic parameters offered by (TST). Thus, the suitable coating thickness can be obtained within the required tolerances. A concept called 'flatness' is added to illustrate the homogeneity of coated thickness, and the relevant simulated coating thickness and flatness result, which were calculated by TST, have been presented and displayed on the graphic interface of TST. As shown in Figure 1.17, the user interface of ProfileKit is given. The user can alternate the operating parameters in the panel on the left side and the corresponding coating profile will show on the right side. According to the work by Cai, coating profiles at different scanning steps are shown in Figure 1.17 (a-d). The flatness of the coating surface increases as the scanning step decreases.

1.5.3 MonitorKit

Although a robot is designed as a highly accurate manipulator, the weight of electric cables, the nozzle and other accessories can cause dynamic divergences between the expected and actual robot trajectory during the thermal spray process. Such deviation of the robot trajectory can lead to further effects on coating quality and coating thickness distribution. It is necessary to obtain the actual robot trajectory and its speed to compare it with the designed trajectory. Deng developed a MonitorKit module, which enables the possibility of monitoring the robot movement. For the purpose of obtaining the actual robot trajectory, it is necessary to get the motion parameters of the robot, including space position, tool orientation and robot posture, which are directly obtained from the robot controller. A standard PC with Ethernet card was used to communicate with the robot and extract the sampling data.

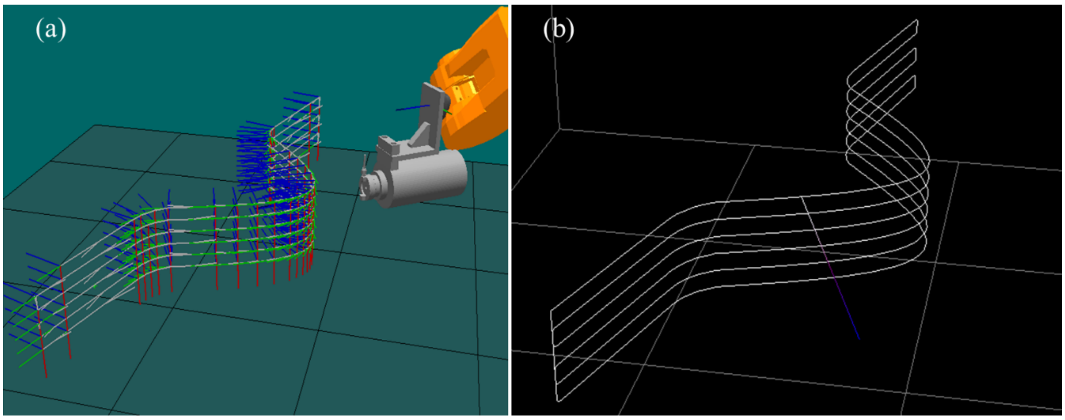

Figure 1.18 (a) Trajectory degenerated by RobotStudio™ and (b) actual trajectory captured by MonitorKit.

The robot speed is obtained by the DAQPad 6020E with a sampling rate of 1000 Hz. All data are stored in a text file. The TCP coordinate can be obtained easily from the controller, and the tool orientation is described by a quaternion array (q1, q2, q3, q4). According to analytic geometry, the tool orientation is transformed from quaternion to rotation matrix so that it can be indicated on screen correctly. Based on the TCP position and orientation, it is able to display the nozzle trajectory in a visual space; a set of API (application programming interface) in the computer graphic standard, OpenGL, (SGI Silicon Graphics, Inc.) was used for 3D graphics development.

Figure 1.18 (a) shows a trajectory generated by RobotStudio™. After synchronising the programme to the robot controller, the trajectory can be executed by the robot. By using the MonitorKit, the actual robot trajectory is captured and displayed in a 3D space. It is able to compare these two trajectories and evaluate the path accuracy, which can provide evidence for trajectory optimisation.

1.6 Conclusion

With the increasing demands for accuracy, repeatability and working intensity in industry, more and more industrial robots are introduced to replace manual operations. The procedure of robot applications in industry includes the trajectory planning, robot programming, process simulation, kinematic analysis/optimisation, coordinates calibration, programme synchronisation and execution tests. In these steps, the trajectory planning and kinematic optimisation are the key points to improve the robot performance and the productivity as well. As a result, the studies concerning the trajectory generation and the kinematic analysis of industry robot are becoming more and more important. In the meantime, due to the advantages of robots, more and more industrial robots have been introduced to the thermal spraying process. Considering the increasing requirement for robot performance and coating quality, the trajectory generation, kinematic analysis and trajectory optimisation are becoming hot topics in this field of industry. Therefore, in this chapter, the aspect of trajectory generation is introduced based on the robot's application in the thermal spraying process.

1.7 Objectives

The main goal of the present work focuses on the application of offline programming methods in the thermal spray process. As presented above, the application process of the off-line programming method includes trajectory generation, simulation of robot kinematics and further optimisation. As a result, the present work is divided into three parts according to the application process. The details of each part are presented as follows.

1. Firstly, the functionalities of PathKit in TST are further optimised by improving the user

interface. The algorithm of trajectory generation on a curved surface is optimised by ensuring a constant scanning step. Furthermore, a novel trajectory based on the Archimedean spiral pattern is developed for the application of damage repair by cold spray. The trajectory generation process as well as the trajectory optimisation method is introduced. A validation experiment is made by applying the Archimedean spiral trajectory to repair an aluminium block with an irregular defect.

2. Secondly, a numerical model is developed to simulate the coating profile in 2D and coating thickness distribution in 3D. In this model, the influence of operating parameters such as spray angle, scanning step and nozzle traverse speed are included. Experimental validation is made by comparing the cold sprayed coating with the resulting simulation results. Moreover, the numerical model is included in the TST as an individual module called ProfileKit. It is able to simulate the coating thickness based on the robot kinematics data by simulation of the virtual robot system in RobotStudio™.

3. Kinematic optimisation is introduced based on the robot's application in the thermal spraying process. An investigation on the robot kinematics is proposed to find the rules of motion in an application case. The results demonstrate the motion behaviour of each axis in the robot that identifies the motion problems in the trajectory. This approach optimises the robot trajectory in a limited working envelope. Therefore, different approaches of kinematic optimisation were introduced to improve the robot performance and coating quality, which took into account the torch setup, or workpiece placement on the worktable. As a powerful tool provided by the off-line programming software, the kinematic analysis is used to evaluate the robot performance, which includes the motion of each axis, the TCP speed, cycle time, etc.

References

1. L. Pawlowski, *The science and engineering of thermal spray coatings*. John Wiley & Sons. 2008.
2. P. Fauchais and M. Vardelle, Plasma spraying: present and future. *Pure Appl Chem*, 1994. **66**(6), p 1247-1258.
3. D. Apelian, M. Paliwal, R. Smith, and W. Schilling, Melting and solidification in plasma spray deposition—phenomenological review. *International metals reviews*, 2013.
4. N.P. Padture, M. Gell, and E.H. Jordan, Thermal barrier coatings for gas-turbine engine applications. *Science*, 2002. **296**(5566), p 280-284.
5. Y. Wang, J. Liu, N. Kang, G. Darut, T. Poirier, J. Stella, H. Liao, and M.-P. Planche, Cavitation erosion of plasma-sprayed CoMoCrSi coatings. *Tribol Int*, 2016. **102**, p 429-435.
6. T. Liu, S.-W. Yao, L.-S. Wang, G.-J. Yang, C.-X. Li, and C.-J. Li, Plasma-Sprayed Thermal Barrier Coatings with Enhanced Splat Bonding for CMAS and Corrosion Protection. *J Therm Spray Technol*, 2016. **25**(1), p 213-221.
7. T. Sidhu, S. Prakash, and R. Agrawal, State of the Art of HVOF Coating Investigations—A Review. *Mar Technol Soc J*, 2005. **39**(2), p 53-64.
8. M. Li and P.D. Christofides, Modeling and control of high-velocity oxygen-fuel (HVOF) thermal spray: A tutorial review. *J Therm Spray Technol*, 2009. **18**(5-6), p 753-768.
9. V. Champagne and D. Helfritch, Critical Assessment 11: Structural repairs by cold spray. *Mater Sci Technol*, 2015. **31**(6), p 627-634.
10. V.K. Champagne, The repair of magnesium rotorcraft components by cold spray. *Journal of Failure Analysis and Prevention*, 2008. **8**(2), p 164-175.
11. J. Lallemand and S. Zeghloul, *Robotique, Aspects fondamentaux, Modélisation mécanique, CAO robotique–Commande*. Enseignement de la physique. Paris, Masson. 1994.
12. M. Puttre, Space-age robots come down to earth. *Mech Eng*, 1995. **117**(1), p 88-89.
13. R.L. Wernli, Robotics undersea. *Mech. Eng*, 1982. **104**(8).
14. J. Suutala, J. Tuominen, and P. Vuoristo, Laser-assisted spraying and laser treatment of thermally sprayed coatings. *Surf Coat Technol*, 2006. **201**(5), p 1981-1987.
15. S. Costil, S. Lukat, P. Bertrand, C. Langlade, and C. Coddet, Surface treatment effects

on ceramic matrix composites: Case of a thermal sprayed alumina coating on SiC composites. *Surf Coat Technol*, 2010. **205**(4), p 1047-1054.

16. F.-I. Trifa, G. Montavon, and C. Coddet, On the relationships between the geometric processing parameters of APS and the Al 2 O 3–TiO 2 deposit shapes. *Surface and Coatings Technology*, 2005. **195**(1), p 54-69.
17. C.-J. Li and B. Sun, Effects of spray parameters on the microstructure and property of Al 2 O 3 coatings sprayed by a low power plasma torch with a novel hollow cathode. *Thin Solid Films*, 2004. **450**(2), p 282-289.
18. F.I. Trifa, *Modèle de dépôt pour la simulation , la conception et la réalisation de revêtements élaborés par projection thermique: pplication au cas de l'alumine-rutile (Al2O3-13%TiO2) projetée à la torche atmosphérique à plasma d'arc*, in *Graduate School of" Physics for Engineers and Microtechnology*. 2004, University of technology of Belfort-Montbéliard, France.
19. D. Fang, S. Deng, H. Liao, and C. Coddet, The effect of robot kinematics on the coating thickness uniformity. *J Therm Spray Technol*, 2010. **19**(4), p 796-804.
20. Z. Cai, S. Deng, H. Liao, C. Zeng, and G. Montavon, The Effect of Spray Distance and Scanning Step on the Coating Thickness Uniformity in Cold Spray Process. *J Therm Spray Technol*, 2014. **23**(3), p 354-362.
21. J. Ilavsky, A.J. Allen, G.G. Long, S. Krueger, C.C. Berndt, and H. Herman, Influence of Spray Angle on the Pore and Crack Microstructure of Plasma Sprayed Deposits. *J Am Ceram Soc*, 1997. **80**(3), p 733-742.
22. V. Sobolev and J. Guilemany, Flattening of droplets and formation of splats in thermal spraying: A review of recent work—Part 1. *J Therm Spray Technol*, 1999. **8**(1), p 87-101.
23. Z. Djurić and P. Grant, An inverse problem in modelling liquid metal spraying. *Appl Math Model*, 2003. **27**(5), p 379-396.
24. S. Duncan, P. Jones, and P. Wellstead, A frequency-domain approach to determining the path separation for spray coating. *Automation Science and Engineering, IEEE Transactions on*, 2005. **2**(3), p 233-239.
25. H.-K. Seok, K.H. Oh, H.Y. Ra, D.-H. Yeo, and H.-I. Lee, A three-dimensional model of the spray forming method. *Metallurgical and Materials Transactions B*, 1998. **29**(3), p 699-708.
26. S. Guessasma, G. Montavon, and C. Coddet, Modeling of the APS plasma spray process using artificial neural networks: basis, requirements and an example. *Computational*

Materials Science, 2004. **29**(3), p 315-333.

27. M.W. Spong, *Robot Dynamics And Control*. Wiley India Pvt. Limited. 2008.
28. E. Pennestri, M. Cavacece, and L. Vita. On the computation of degrees-of-freedom: a didactic perspective. *ASME 2005 International Design Engineering Technical Conferences and Computers and Information in Engineering Conference*. 2005, American Society of Mechanical Engineers. 2005. p 1733-1741
29. ABB, *Product Specification – IRB 4400*. Sweden. 2005.
30. ABB, *Product Specification – IRB 2400*. Sweden. 2004.
31. E. Dombre, *Analyse et modélisation des robots manipulateurs*. Hermès science publications. 2001.
32. X.-T. Luo, Y.-K. Wei, Y. Wang, and C.-J. Li, Microstructure and mechanical property of Ti and Ti6Al4V prepared by an in-situ shot peening assisted cold spraying. *Mater Design*, 2015. **85**, p 527-533.
33. S. Yin, X. Suo, J. Su, Z. Guo, H. Liao, and X. Wang, Effects of Substrate Hardness and Spray Angle on the Deposition Behavior of Cold-Sprayed Ti Particles. *J Therm Spray Technol*, 2014. **23**(1-2), p 76-83.
34. S. Yin, Y. Xie, X. Suo, H. Liao, and X. Wang, Interfacial bonding features of Ni coating on Al substrate with different surface pretreatments in cold spray. *Mater Lett*, 2015. **138**, p 143-147.
35. C. Chen, Y. Xie, S. Yin, M.-P. Planche, S. Deng, R. Lupoi, and H. Liao, Evaluation of the interfacial bonding between particles and substrate in angular cold spray. *Mater Lett*, 2016. **173**, p 76-79.
36. S. Yin, X. Wang, X. Suo, H. Liao, Z. Guo, W. Li, and C. Coddet, Deposition behavior of thermally softened copper particles in cold spraying. *Acta Mater*, 2013. **61**(14), p 5105-5118.
37. M. Aghasibeig, M. Mousavi, F. Ben Ettouill, C. Moreau, R. Wuthrich, and A. Dolatabadi, Electrocatalytically Active Nickel-Based Electrode Coatings Formed by Atmospheric and Suspension Plasma Spraying. *J Therm Spray Technol*, 2014. **23**(1), p 220-226.
38. S. Malmberg and J. Heberlein, Effect of plasma spray operating conditions on plasma jet characteristics and coating properties. *J Therm Spray Technol*, 1993. **2**(4), p 339-344.
39. S. Deng, *Robot offline programming and real-time monitoring of trajectories: development of an add-in program of robotstudio™ for the thermal spraying*, in

Graduate School of Physics for Engineers and Microtechnology. 2006, University of Technology of Belfort-Montbéliard, France.

40. Z. Bi and S.Y. Lang, A framework for CAD-and sensor-based robotic coating automation. *Industrial Informatics, IEEE Transactions on*, 2007. **3**(1), p 84-91.
41. S. Deng, Z. Cai, D. Fang, H. Liao, and G. Montavon, Application of robot offline programming in thermal spraying. *Surf Coat Technol*, 2012. **206**(19-20), p 3875-3882.
42. S. Mitsi, K.-D. Bouzakis, G. Mansour, D. Sagris, and G. Maliaris, Off-line programming of an industrial robot for manufacturing. *Int J Adv Manuf Technol*, 2005. **26**(3), p 262-267.
43. W.-Y. Li, S. Yin, X. Guo, H. Liao, X.-F. Wang, and C. Coddet, An Investigation on Temperature Distribution Within the Substrate and Nozzle Wall in Cold Spraying by Numerical and Experimental Methods. *J Therm Spray Technol*, 2012. **21**(1), p 41-48.
44. A. Frutos Martínez, *Numerical analysis of the temperature distribution and offline programming of industrial robot for thermal spraying*. 2009, University of Stuttgart, Germany.
45. S. Deng, H. Li, H. Liao, C. Coddet, and C. Zeng. New Functions of Thermal Spray Toolkit A Software Developed for Off-line and Rapid Robot Programming. *International Thermal Spray Conference*. 2006 (Seattle, USA). 2006. p 1437-1442.
46. S. Deng, H. Liao, C. Zeng, P. Charles, and C. Coddet. Robotic trajectory autogeneration in thermal spraying. *International Thermal Spray Conference* 2005 (Seattle, Washington, USA). 2005. p 481-485
47. D. Fang, S. Deng, H. Liao, and C. Coddet. The Improvements of Thermal Spray Toolkit, Extended Software for Robotic Off-Line Programming. *International Thermal Spray Conference* 2010 (Singapore). 2010. p 522-526.
48. J. Pattison, S. Celotto, R. Morgan, M. Bray, and W. O'Neill, Cold gas dynamic manufacturing: A non-thermal approach to freeform fabrication. *Int J Mach Tool Manu*, 2007. **47**(3–4), p 627-634.
49. A. Sova, S. Grigoriev, A. Okunkova, and I. Smurov, Potential of cold gas dynamic spray as additive manufacturing technology. *Int J Adv Manuf Tech*, 2013. **69**(9-12), p 2269-2278.
50. Y. Cormier, P. Dupuis, B. Jodoin, and A. Corbeil, Mechanical Properties of Cold Gas Dynamic-Sprayed Near-Net-Shaped Fin Arrays. *J Therm Spray Technol*, 2015. **24**(3), p 476-488.
51. A. Farjam, Y. Cormier, P. Dupuis, B. Jodoin, and A. Corbeil, Influence of Alumina

Addition to Aluminum Fins for Compact Heat Exchangers Produced by Cold Spray Additive Manufacturing. *J Therm Spray Technol*, 2015. **24**(7), p 1256-1268.

Chapter 2

Trajectory generation by off-line programming technology

2.1 Introduction of PathKit

As mentioned in the introduction, an add-in software called Thermal Spray Toolkit (TST) was developed under the off-line programming software RobotStudio™. It provides a complete solution for the thermal spray process from the generation of nozzle trajectory to the simulation of coating thickness. As an important factor in thermal spray process, nozzle trajectory has a large influence on coating quality and coating formation. Due to the specifics of the thermal spray process, the nozzle trajectory has to satisfy a few demands, such as the constant scanning path, the perpendicular spray angle and the constant standoff distance. With the help of off-line programming technology, the PathKit module in TST enables the trajectory generation for thermal spray applications. In this chapter, following the work by Deng, Fang and Cai, it continues to improve the functionality in PathKit. Meanwhile, a novel spiral trajectory is developed specifically for the application of damage component recovery in cold spray.

2.1.1 Functionality of PathKit

In the PathKit, a graphical user interface (UI) is presented to assist the operating parameter altering and trajectory generation. As shown in Figure 2.1, the graphical interface consists of the TST ribbon-tab (1), the graphics window for main operation and display (2), the tool window of a specific function in TST (3), and the output window for information display (4).

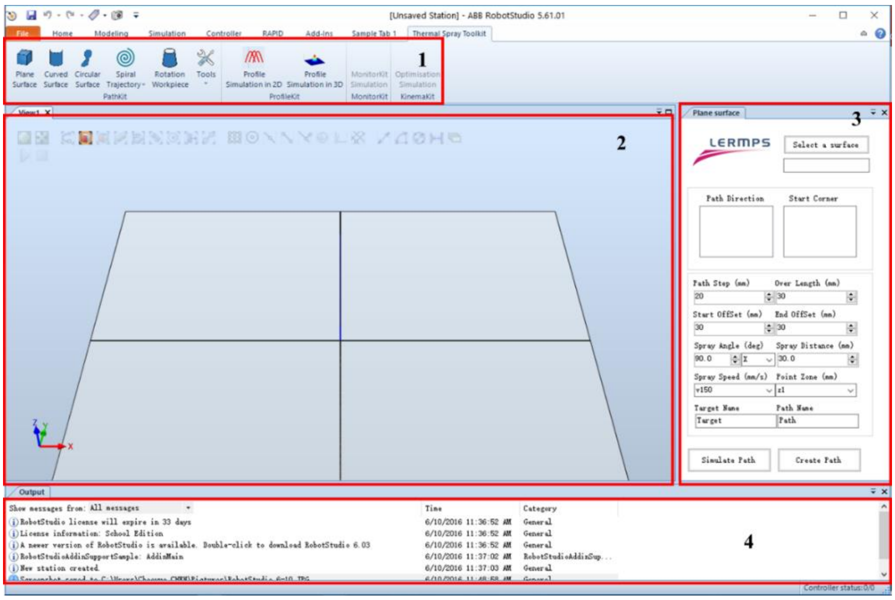

Figure 2.1 User interface of Thermal Spray Toolkit and PathKit embedded in RobotStudio™.

After the creation of a new station in RobotStudio, the TST will be activated automatically in RobotStudio™, which is embedded following the default ribbons such as Home, Modelling and Simulation as shown in Figure 2.1. Similar to regular utilisation of RobotStudio™, a robot system is prepared by specifying the robot type, importing the CAD files of substrate model and nozzle tool, and defining the parameters such as the tool centre point (TCP) before using PathKit. Afterwards, a specific module in PathKit will be chosen according to a specific substrate type and spray strategy. The tool window of the chosen module will appear after clicking in the ribbon tabs of TST. Users can generate the trajectory on a substrate surface by altering parameters in the module tool window, and the result will display in the main window. In PathKit, the modules developed are listed as below.

- Planar surface
- Curved surface
- Circular surface
- Spiral trajectory
- Rotation workpiece

The details of each module and application are introduced in the following sections.

2.1.2 Model topology – computer graphics

As mentioned in Chapter 1, the trajectory generation for thermal spray application in PathKit of TST is based on computer graphics. Target points composing the trajectory are obtained by a series of graphic processing methods. Thus, it is of great importance to investigate the model topology, which refers to the spatial relation between various entities of the model in computer graphics. The relationship of the conceptual topology elements used in RobotStudio™ is shown in Figure 2.2, which is based on the definition of the boundary representation of a 3D ACIS Modeler (ACIS). These elements are implemented in ACIS using the C++ classes Body, Shell, Face, Loop, Wire, Coedge, Edge and Vertex. Each of these classes is derived from the Entity class. The specific definition and inheritance relation of each class is described as follows. An example of the topology on a cube is given in Figure 2.3 for a better understanding of the relationship.

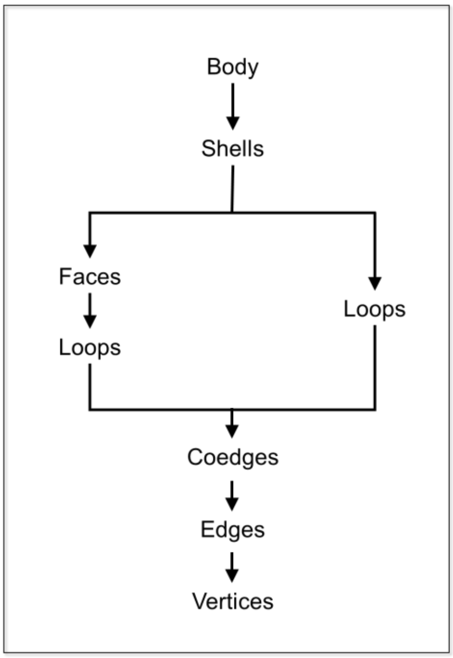

Figure 2.2 Model topology.

Bodies are the highest-level entities in ACIS models. Typically, a Body is a single solid or sheet component, such as an engine block, a plate, or a cross section. Several Bodies can be grouped in a part. Bodies consist of one or several shells. A Shell is a set of connected Faces and Wires. It is normally the outside of a solid Body, but it can also be the inside of a hollow Body. According to the scheme shown in Figure 2.2, both the concepts of Face and Wire can be accessed through a Shell.

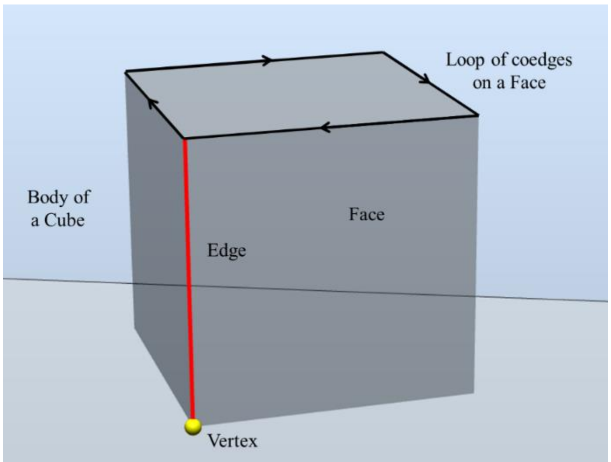

Figure 2.3 Topology of an exemplary cube.

A Face is a bounded portion of a single geometric surface. The boundary is represented by one or more Loops or Edges. Each Face is simply connected, implying that one can traverse from any point on the interior of the Face to any other point on the interior of the Face without crossing the boundary of the Face. A Loop represents a connected portion of the boundary of a Face. It consists of a set of Coedges linked in a doubly-linked chain, which may be circular or open-ended.

Meanwhile, a Wire is a connected collection of Edges that are not attached to Faces and do not enclose any volume. Wires may represent abstract items like profiles, construction lines and centre lines, or idealisations of rod or beam-like objects or internal passages. They are also commonly used to form wire frames to form solid-bounding Shells.

A Coedge records the occurrence of an edge in a loop of a face. A Coedge stores its relationships with adjacent edges and with superior owning entities. (In some contexts, the Coedge may be viewed as the use of an edge by a Face or Wire.) The data structures formed by these relationships (stored as pointers) and their interpretation depend upon the nature of the owning entity. A Coedge can be accessed through a Wire or a Loop in a Face, which is based on the model geometry.

As shown in Figure 2.3, an Edge is bounded by one or more vertices, referring to one Vertex at each end. Edges are closely related to Coedges, which allows the Edge to occur in more than one Face, thus making it possible to create solids. A Vertex is the corner of either a Face or a Wire. Vertex refers to a point in the object space and to the edges that it bounds.

2.1.3 Trajectory generation by PathKit

2.1.3.1 Trajectory for planar surface

Round-trip trajectory is mostly used in thermal spraying processes for the deposition on a planar substrate surface. The methodology used for trajectory generation was mentioned in Chapter 1, which is mainly achieved by the Boolean operating between the substrate surface and an orthogonal plate created for reference. During the process, the first step is to choose the surface to spray. In order to define the spray direction, the boundary and starting point are also needed. Next, the thermal spraying operating parameters should be defined. Then the trajectory can be generated automatically, as shown in Figure 2.4. The operating parameters were introduced in the previous chapter.

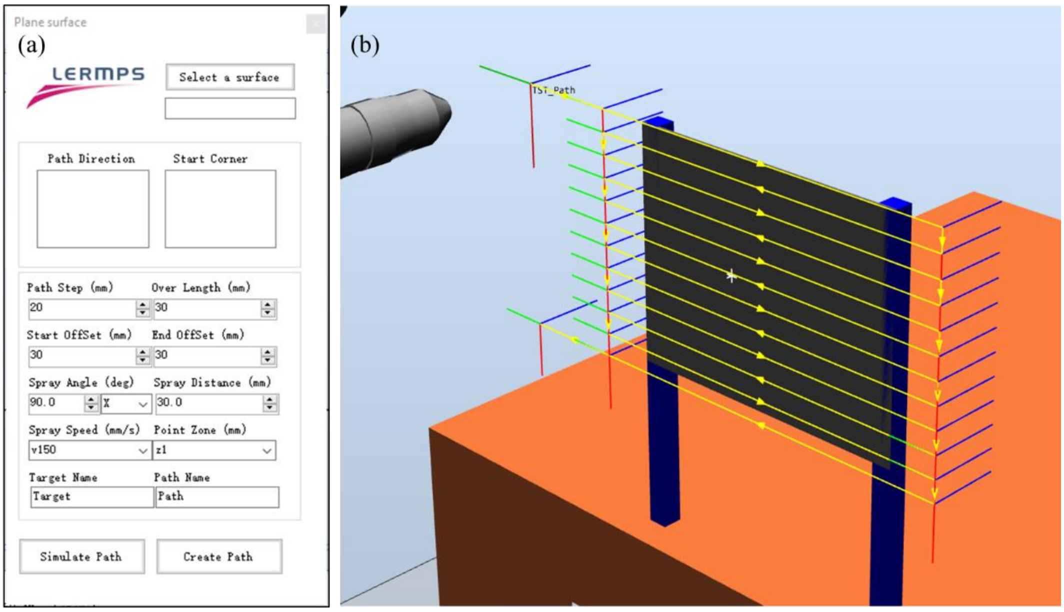

Figure 2.4 (a) UI of PathKit for planar surface, (b) round-trip trajectory generated for a plane surface workpiece.

In the meantime, the meander trajectory for defect repair and workpiece pre-heating is also developed. As shown in Figure 2.5, only a rectangular area in the middle needs to be deposited. For a traditional round-trip trajectory, the over-length is necessary to maintain the nozzle traverse speed within the substrate area as the predefined value. However, an obvious waste of feedstock material and system energy cannot be avoided in the over-length area. By eliminating the over-length with the meander trajectory, the deposit area can be restrained strictly within the area, which can significantly decrease the process duration, the consumption of spray system as well as the powder. Only the entrance and exit scanning will exist on the exterior area.

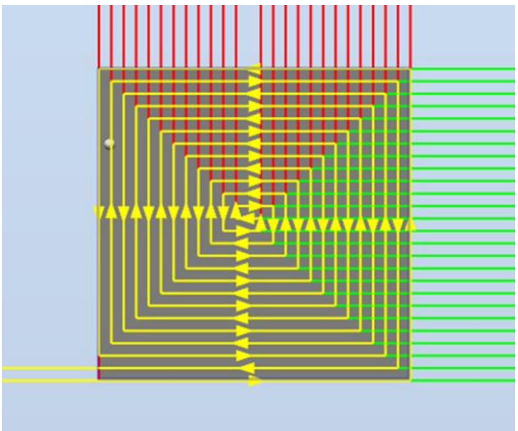

Figure 2.5 Meander trajectory generated for a rectangular surface.

2.1.3.2 Trajectory for curved surface

In the thermal spray process, the operating parameters such as spray angle and standoff distance should be kept constant to obtain an optimal coating quality. In the case of a curved substrate surface, it is rather difficult to ensure these terms by manual trajectory generation in off-line programming software. However, with the help of the graphical off-line programming software, the orientation of each target point can be calculated and obtained automatically according to the geometry and thermal spraying operating parameters (Figure 2.6).

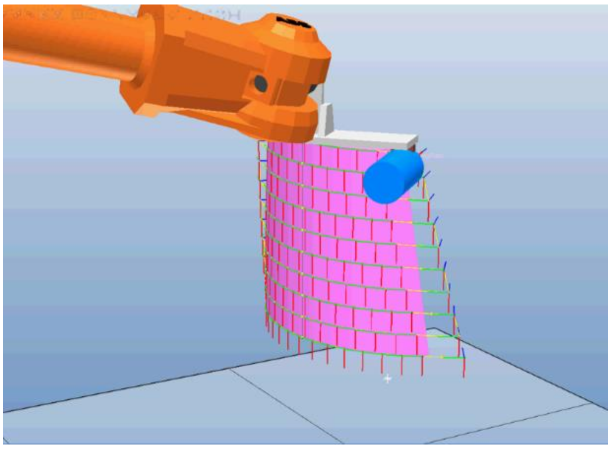

Figure 2.6 Trajectory generated for a curved surface.

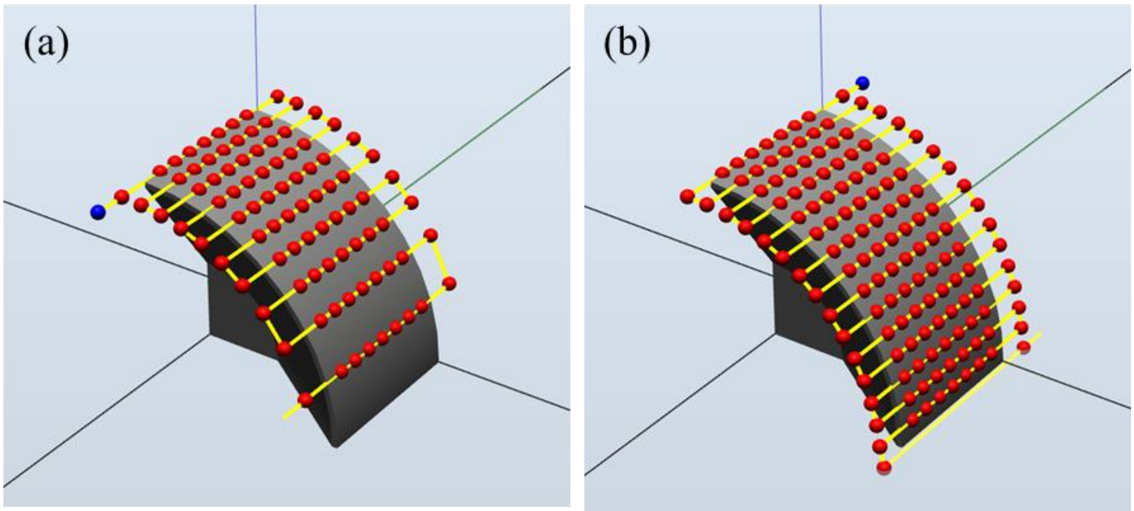

Figure 2.7 Optimised trajectory generation for curved surface: (a) original trajectory, (b) optimised trajectory.

In this thesis, in order to maintain a constant scan step, an improvement in the trajectory generation algorithm was made, as shown in Figure 2.7. In PathKit, similar to the planar surface, the target points generated on a curved surface are obtained by the Boolean operating between the surface to be deposited and an orthogonal surface. Thus, the target points on the substrate are on the intersection edge between these two surfaces. For each step, the orthogonal surface is moved by the distance of the scan step. However, in the case of a curved surface, the movement direction of the orthogonal surface should correspond to the substrate curvature. As shown in Figure 2.7 (a), while the moving offset of the orthogonal surface is constant during the operation, an inconstant scan step between each scan step can be observed due to the changing substrate curvature. However, it can be found in Figure 2.7 (b) that the constant scan step can be ensured while the moving orthogonal surface is based on the substrate curvature.

2.2 Generation of Archimedean spiral trajectory

Nowadays, with the rapid development of aeronautics and the astronautics industry and gradually limited resources, dimensional recovery of components is playing a more and more important role [1, 2]. Due to the unique ‘cold’ feature, the cold spray technology has been widely applied as a promising method for damaged components recovery as well as additive manufacturing. Differing from the traditional thermal spray, the low temperature and high velocity of cold sprayed particles upon impact can prevent the occurrence of particle oxidation as well as local thermal residual stresses [3, 4].

Most of the research has focused mainly on the improvement of the cold spray system and the mechanical properties of repaired coating, including bonding mechanism, bonding strength, and fatigue of coating [1, 5-7]. However, investigations on the nozzle trajectory and robot kinematics have barely been carried out so far. In fact, these factors are of great importance to the coating microstructure, coating thickness and coating surface quality [8, 9]. Hence, a proper strategy for nozzle trajectory and robot kinematics is very crucial to the recovery quality of damage components. Generally, the cold spray nozzle is controlled either manually in the low pressure portable system [1, 5] or automatically by the robot arm in the high pressure system with a simple round-trip trajectory. Either way, the as-sprayed coating formed on the damaged region hardly matches the original damaged defect shape because of the arbitrary nozzle trajectory and complex surface topography on the damaged part. More specifically, the coating is normally over-deposited for the purpose of covering the entire zone of the damaged part. In this case, the post-manufacturing of the as-sprayed coating must be carried out to obtain the desired shape and surface. In this process, a large amount of feedstock will be wasted, which significantly increases the cost for recovery. In order to improve the deposition precision and reduce the amount of post-machining work, it is necessary to develop an advanced trajectory in terms of robot kinematics, which can take the surface topography of the damage part into account.

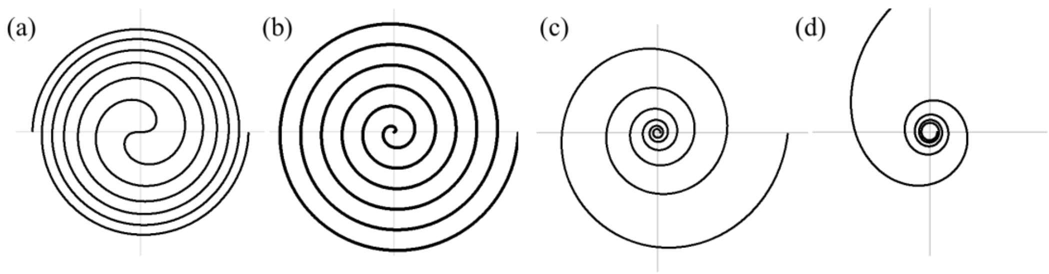

Figure 2.8 Schematic of different well-known patterns of spiral trajectory: (a) Fermat's spiral, (b) Archimedean spiral, (c) logarithmic spiral and (d) hyperbolic spiral.

Spiral trajectory is a kind of novel trajectory strategy, generated according to the damage area contour and thus capable of restricting the nozzle movement within the damaged area, in order to reduce the material waste due to the over-deposition. Figure 2.8 shows some well-known patterns of spiral trajectory. Among these trajectories, Fermat's spiral, hyperbolic spiral and logarithmic spiral normally result in inconstant thicknesses distribution and qualities at different parts of a coating due to the inconstant separation between adjacent turns. Mathematically, the Archimedean spiral is a set of discrete points formed through the point moving from a fixed original point at a constant linear speed and rotating around the original point at a constant angular speed simultaneously. Geometrically, a series of successive turns in the Archimedean spiral is composited the aforementioned points. Another important fact regarding the Archimedean spiral is that the distance between two successive turns is constant, which corresponds to the constant scan step in the spray process to ensure the smooth coating surface. As a result, an Archimedean spiral is an excellent robot trajectory for coating deposition due to its constant scan step and overall coverage of the deposition area.

Therefore, in this study, a novel trajectory strategy based on the Archimedean spiral pattern was proposed and used to repair the workpiece with crater defect via cold spray. With this novel trajectory, the coating can be strictly deposited within the defect area of the damaged workpiece. Experimental studies of cold sprayed Al5056 coating on a damaged Al2017A workpiece with a crater defect was also carried out to validate the feasibility of the proposed Archimedean spiral trajectory.

2.2.1 Trajectory generation

In order to evaluate the feasibility of the Archimedean spiral trajectory in the dimensional recovery of a damaged workpiece, a crater defect was created on an aluminum block by software CATIA (V6, Dassault Système, France), which is shown, respectively, in Figure 2.9a. A crater defect with a maximum depth of 4.3 mm and a volume of 9.8 mm^3 was created on the block, as shown in Figure 2.9a. The white lines on the crater area are the contour lines of height. In order to further understand the depth distribution in the crater defect on the substrate surface, the result is given in Figure 2.9b with the colour legend indicating the depth value. It can be seen that the depth increases from the crater edge to the centre. The cross-sectional view of the crater defect shown in Figure 2.9c gives a clearer view of the depth distribution in the crater defect. Moreover, form Figure 2.9c, it can also be seen that the depth reduces at an inclination angle of about 70° with a flat surface appearing at the central zone. Based on the aforementioned model information, a real crater defect having the similar geometry with the CAD model was manufactured on a 123 mm × 74 mm Al2017A block. The digital photo of the crater defect is provided in Figure 2.9d.

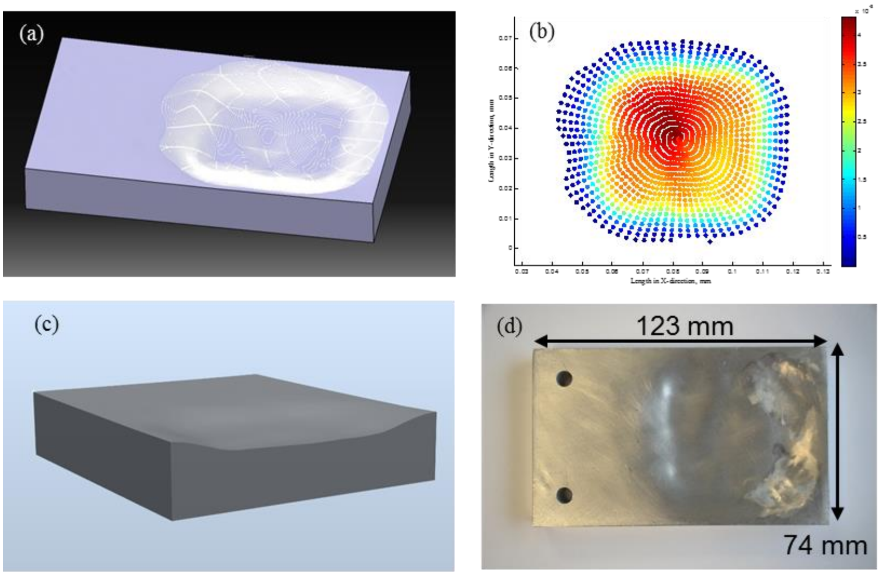

Figure 2.9 Defect #1: (a) CAD model of the damaged workpiece, (b) depth distribution in the crater defect of the damaged workpiece with the colour legend indicating the depth value, (c) cross-sectional view of the damaged workpiece and (d) digital photo of the damaged workpiece.

2.2.1.1 Archimedean spiral trajectory

Figure 2.10 shows the generation process of the Archimedean spiral trajectory on a workpiece with semi-spherical crater. The spiral trajectory was created from the edge to the centre according to the contour of the semi-sphere. In the first place, a series of reference points coloured in red with constant interval distance was created on the crater edge (Figure 2.10 (a)). Secondly, as shown in Figure 2.10 (b), the target points coloured in blue at the first turn were created by gradually moving each red point towards the centre. The distance between each pair of blue and red points increased linearly from zero to the value of the scan step. Thirdly, another series of reference points coloured in red was created by moving the original reference points at the crater edge towards the centre at a distance of the scan step to form a concentric shape (Figure 2.10 (c)). Then, by repeating the second procedure shown in Figure 2.10 (b), the target points on the second turn were created (Figure 2.10 (d)). Finally, by repeating the aforementioned procedures up to the centre, a complete Archimedean spiral pattern was created. Figure 2.10 (e) shows the target points of the Archimedean spiral pattern, in which the references points were removed. Thus, the entrance Archimedean spiral trajectory is created. By symmetrically mapping the entrance spiral trajectory at the central plane, the exit trajectory coloured in yellow was created. Figure 2.10 (f) shows complete target points on the Archimedean spiral trajectory.

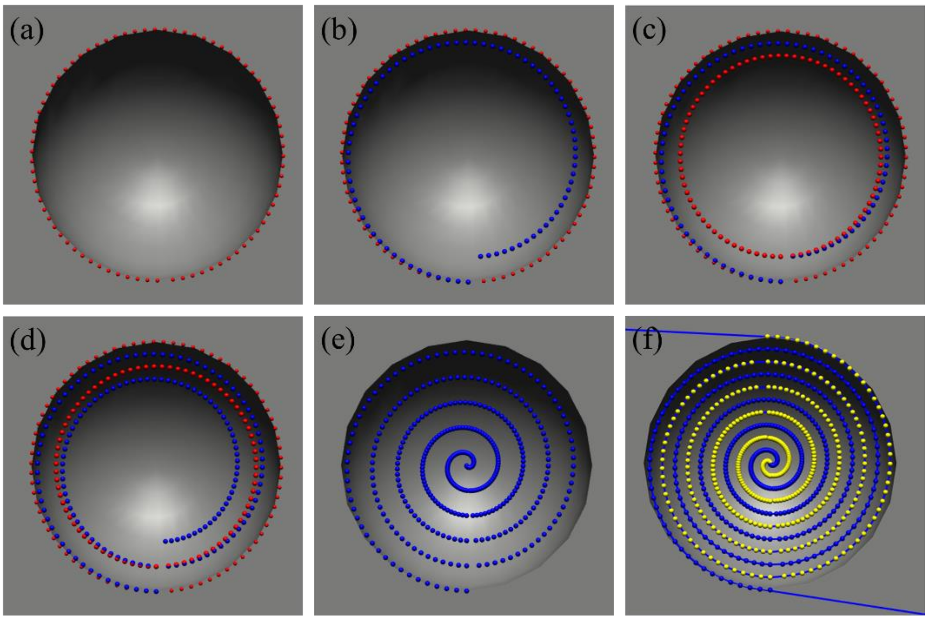

Figure 2.10 Generation process of the Archimedean spiral trajectory on a workpiece with semi-spherical crater.

2.2.1.2 Scaling method for irregular defect

In practical problems, a defect area normally has an irregular contour rather than a perfect semi-sphere. It is impossible to apply the standard Archimedean spiral trajectory to the irregular contour. Thus, a scaling method based on linear transformation theory was used to create successive contours applicable to the irregular defect. With this approach, the object can be enlarged or shrunk based on an original point by adjusting the scale factors in each direction. The positive or negative scale factors represent enlargement or shrinking of the object, respectively. As described by the linear transformation theory, the position and orientation of a transformed object can be obtained by multiplying the transformation matrix M_s to the object vector P_0 as described by Eq. 1. The general scaling transformation is performed according to the original point (0, 0, 0). Hence, the object should be moved to the original point before being scaled and returned to previous position after scaling. So, the linear transformation of displacement M_d should also be multiplied in order to scale the object according to the predefined original point (x_0, y_0, z_0) as presented in Eqs. 2 and 3, where the s_x, s_y, s_z are the scale factors in each direction. The original point (x_0, y_0, z_0) should be chosen as the centre point of the object in order to ensure the constant spacing between adjacent scaled contours. As a result, the scaled object is obtained by applying the Eq. 4.

$$P_0' = M_s \cdot P_0 \quad \text{Eq. 2.1}$$

$$M_s = M_d \cdot M_s \cdot M_d' \quad \text{Eq. 2.2}$$

$$M_s = \begin{bmatrix} 1 & 0 & 0 & x_0 \\ 0 & 1 & 0 & y_0 \\ 0 & 0 & 1 & z_0 \\ 0 & 0 & 0 & 1 \end{bmatrix} \cdot \begin{bmatrix} s_x & 0 & 0 & 0 \\ 0 & s_y & 0 & 0 \\ 0 & 0 & s_z & 0 \\ 0 & 0 & 0 & 1 \end{bmatrix} \cdot \begin{bmatrix} 1 & 0 & 0 & -x_0 \\ 0 & 1 & 0 & -y_0 \\ 0 & 0 & 1 & -z_0 \\ 0 & 0 & 0 & 1 \end{bmatrix} \quad \text{Eq. 2.3}$$

$$\begin{bmatrix} x' \\ y' \\ z' \\ 1 \end{bmatrix} = \begin{bmatrix} s_x & 0 & 0 & (1-s_x)\cdot x_0 \\ 0 & s_y & 0 & (1-s_y)\cdot y_0 \\ 0 & 0 & s_z & (1-s_z)\cdot z_0 \\ 0 & 0 & 0 & 1 \end{bmatrix} \cdot \begin{bmatrix} x \\ y \\ z \\ 1 \end{bmatrix} \quad \text{Eq. 2.4}$$

With Eq. 4, the scaled Archimedean spiral trajectory, which is applicable to the defect area in this work, was obtained and is shown in Figure 2.11. Figure 2.11 (a) provides reference points of the first three turns at different scale factors based on edge contour. By gradually adjusting the reference points towards the adjacent contour, a complete spiral trajectory was generated according to the edge contour of damaged area. Figure 2.11 (b) shows the final robot trajectory after scaling. As can be seen, the trajectory perfectly suits the crater contour. In this case, the whole defect area can be perfectly deposited with less coating outside the defect area.

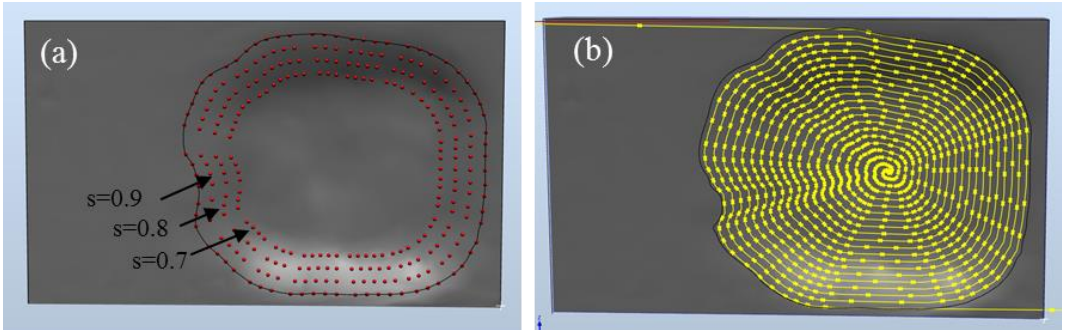

Figure 2.11 Schematic of scaling method: (a) the scaled contours obtained by different scale factors, (b) the spiral trajectory generated by scaling method.

2.2.2 Speed adaptation

The Archimedean spiral trajectory is able to perfectly cover the defect area as discussed in the last paragraph, but the inconstant depth distribution of the crater may also lead to the over-coating and low surface quality. In order to solve this problem, the nozzle traverse speed was adjusted according to the crater depth to control the deposition amount at different positions of the crater. First of all, the relation between nozzle traverse speed and thickness of cold sprayed Al5056 coating was experimentally studied. Experiments were conducted with different nozzle traverse speeds and other fixed working conditions. Only a single-track coating was produced on the aluminum substrate. The as-sprayed coating shows a Gaussian distribution profile, while the maximum thickness was used for the investigation. For each sample, three different locations were randomly selected for measurement to get an averaged value. Figure 2.12 shows the coating thickness as a function of nozzle traverse speed. As can be seen, the coating thickness decreased gradually as the nozzle traverse speed increases. When the nozzle traverse speed increased from 150 mm/s to 300 mm/s, the maximum coating thickness decreased rapidly from 289 μm to 145 μm. However, for a nozzle traverse speed below 150 mm/s, which is normally applied in coating deposition process by cold spray, the relation was nearly linear. In this work, the approximation of a linear correlation between nozzle speed and coating thickness was used to compensate the effect of crater depth. The minimal nozzle traverse speed was 50 mm/s, which has a maximum coating thickness of 800 μm. Thus, the correlation between nozzle speed and the crater depth was established, as given in Eq. 5.

$$v = v_{max} + (v_{min} - v_{max}) \cdot \frac{D}{D_{max}} \quad \text{Eq. 2.5}$$

Where v_{min} is the minimum nozzle speed, which appears in the deepest position, v_{max} is the maximum nozzle speed, D is the crater depth, D_{max} is the maximum depth. By adopting the linear relation between speed and depth, the distribution of nozzle traverse speed at each target point was obtained and is shown in Figure 2.12.

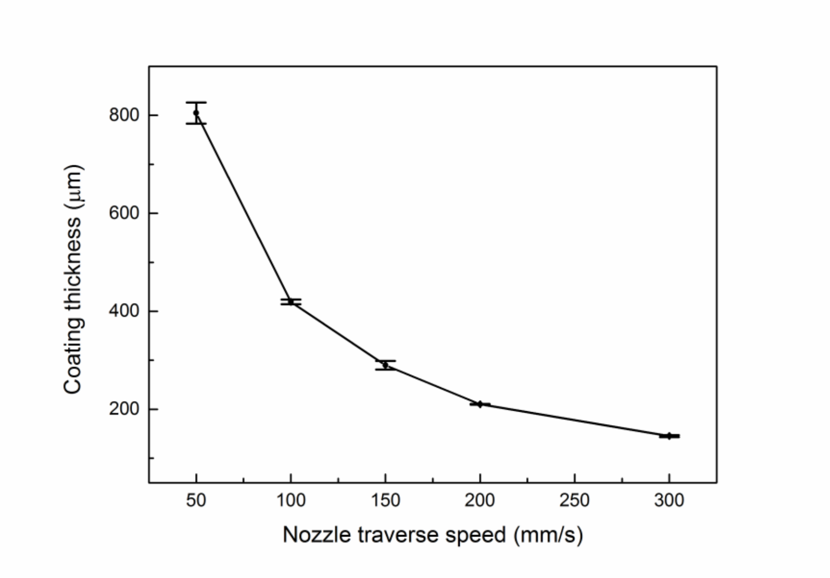

Figure 2.12 Coating thickness as a function of nozzle traverse speed.

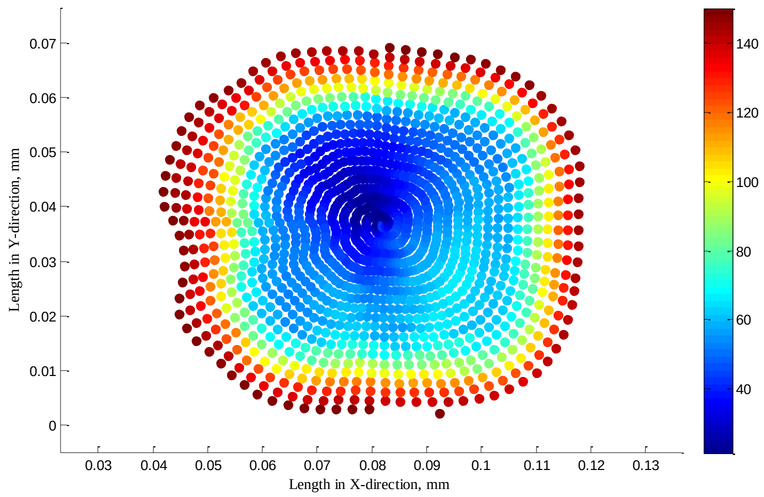

Figure 2.13 Distribution of nozzle traverse speed obtained by speed adaptation according to

the depth at each target point.

2.2.3 Target points simplification

During the trajectory generation, the interval distance between adjacent points becomes increasingly shorter from the outer circle towards the centre point because the number of target points for each circle is the same, as illustrated in Figure 2.14. Although the high density of target points can improve the trajectory precision, it affects the robot performance or even results in the failure of trajectory execution. According to execution simulation of robot trajectory in OLP software RobotStudio™, the original trajectory with a constant target point interval cannot be executed by robot due to the extremely high target point density. Therefore, the robot movement should be simplified to reduce the workload on the robot controller.

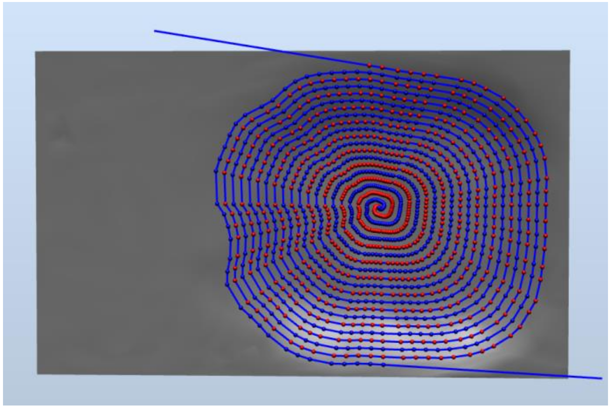

Figure 2.14 Generated spiral trajectory without target point simplification.

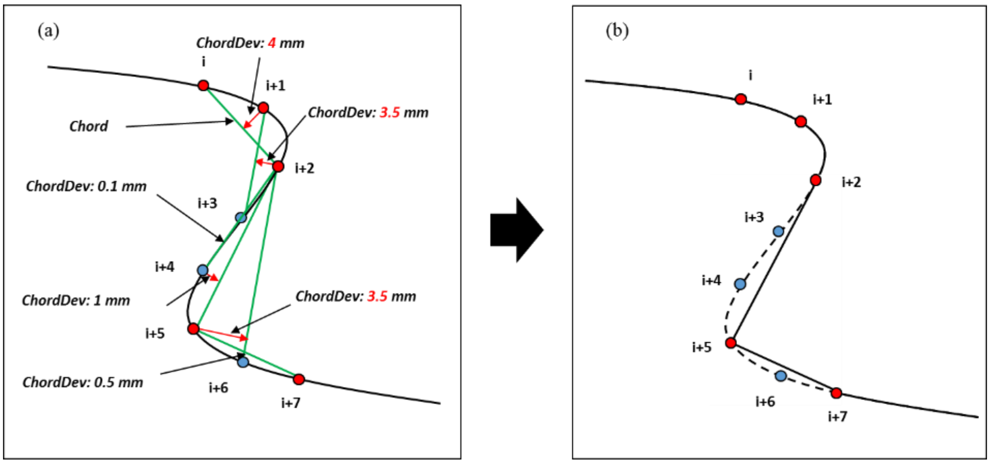

Figure 2.15 Schematic of trajectory simplification algorithm. (a) The original trajectory, (b) the trajectory optimised by ChordDev algorithm.

In this work, the optimisation algorithm called the Chord Deviation (ChordDev) Method was used to reduce the target point number of trajectory without affecting the precision of the trajectory. Figure 2.15 shows the schematic of trajectory simplification algorithm. As shown in Figure 2.15 (a), the segments between the points *i* and *i*+*n* ($n \geq 1$) are called Chord. The perpendicular distance between the point *i*+*m* ($0 < m < n$) and the Chord is considered as the ChordDev. To perform this algorithm, a threshold of ChordDev should be set as a reference value to remove the target points that possess smaller ChordDev values. In this example, the threshold chord deviation value is 3 mm. The optimisation algorithm starts from the point P_i. The chord between the point Pi and the point P_{i+2} is considered as $C_{i, i+2}$. The ChordDev of P_{i+1}, that is the perpendicular distance between the point P_{i+1} and the chord $C_{i, i+2}$ is 4 mm, is larger than the threshold value of 3 mm. This means that the point P_{i+1} should remain in the trajectory. For the next point P_{i+2}, the ChordDev that is the distance between the point P_{i+1} and the chord $C_{i+1, i+3}$, is 3.1 mm. The point P_{i+2} should also remain in the trajectory. As for the point Pi+3 and the chord $C_{i+2, i+4}$, the ChordDev is 0.1 mm, which means that the elimination of point Pi+3 will not affect the curvature of the trajectory at this point. The point P_{i+3} will then be deleted from the trajectory. The algorithm continues to test the point P_{i+4} and the chord $C_{i+2, i+5}$, which is 1 mm. Thus, the point P_{i+4} should also be deleted. As for the point P_{i+5}, the ChordDev between this point and $C_{i+2, i+6}$ is 3.2 mm and larger than the threshold value. So the point P_{i+5} should remain. The lateral points in the trajectory always remain to define the start and the end points for a pass. As shown in Figure 2.15 (b), the blue points are deleted and the red points remain in the trajectory to maintain their precision and shape. Thus, a simplified trajectory is generated and composed of red points and black segments. In summary, the principle of this optimisation algorithm is to simplify the trajectory by eliminating the target points that have slight effects on the trajectory precision and shape. A proper threshold value for ChordDev is important to guarantee the precision of the trajectory. Small threshold values lead to no obvious simplification of the trajectory, while large values bring serious deviation to the trajectory. According to the specific thermal spray process, the value of threshold is determined based on the value of scanning step and the maximum deviation of a point in the trajectory.

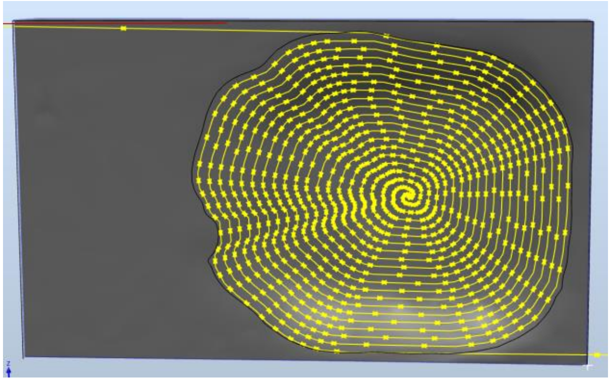

Figure 2.16 Simplified spiral trajectory after applying ChordDev algorithm.

By applying the ChordDev algorithm and a threshold of 0.5 mm to the created spiral trajectory in this study, a simplified trajectory was obtained and is shown in Figure 2.16. The value of threshold for the trajectory simplification is determined as 0.5 mm according to the half of the maximum deviation (1mm) of a point in the trajectory based on the scanning step of 2 mm in cold spray. Compared with the original spiral trajectory shown in Figure 2.14, the shape of the trajectory has no difference, but the point number decreased from 1338 to 646. The number of target points on the straight trajectory line is greatly reduced, while those on the areas with a large curvature remain.

2.2.4 Simulation results

The spiral trajectory shown was simulated by the virtual robot controller. In the simulation, a virtual workstation with spray equipment was created to simulate the cold spray process. As a result, the robot kinematics data including TCP (tool centre point) speed and position can be obtained. Note that the TCP speed is a robot kinematic concept that equals the nozzle traverse speed. By retrieving the TCP position and the corresponding TCP speed for every 24 ms, a TCP speed distribution on the spiral trajectory was generated and is presented in Figure 2.17. It was found that the simulation results of TCP speed are in good agreement with the depth distribution (Figure 2.9 (d)) and speed definition (Figure 2.13). In this case, it is reasonable to consider that the developed spiral trajectory in this work is applicable in the real cold spray process for repairing the damage workpiece with the crater defect.

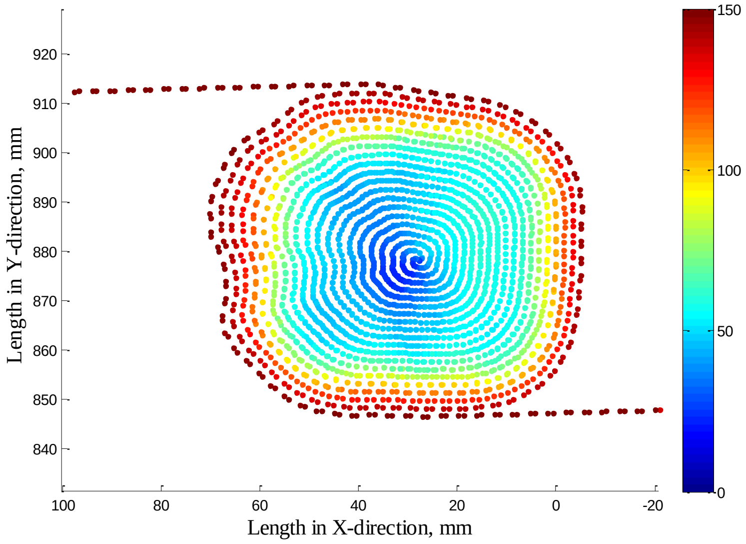

Figure 2.17 TCP speed distribution obtained by process simulation in RobotStudio™.

2.3 Defect repair by cold spray

In this section, a manually manufactured defect on aluminium was repaired by using the Archimedean spiral trajectory introduced above with cold spray technology. The experimental details as well as experimental results will be presented.

2.3.1 Experimental details

The cold sprayed coating was produced by CGT K3000 cold spray system equipped with a de-Laval type nozzle (SiC-Out1, Impact Innovation GmbH). The nozzle has a circular cross-section with an approximate expansion ratio of 5.6 and a divergent section length of 132 mm. High-pressure compressed nitrogen was applied as the propellant gas with an inlet temperature of 500 °C and pressure of 30 bars. The nozzle was cooled by a home-made water circulation system to avoid nozzle overheating and clogging. The standoff distance between the nozzle exit and the top surface of substrate was 30 mm without considering the crater depth. The spray angle was set as 90° to the substrate surface. The nozzle traverse speed was adapted according to Eq. 5 with maximum and minimum nozzle traverse speed of 150 mm/s and 50 mm/s, respectively. The scan step between two successive turns of Archimedean spiral was set as 2 mm. Substrate was preheated before the coating deposition process to facilitate the deposition. According to the coating thickness by a single pass of trajectory, the trajectory was repeated for 30 times for the purpose of a full restoration of crater defect.

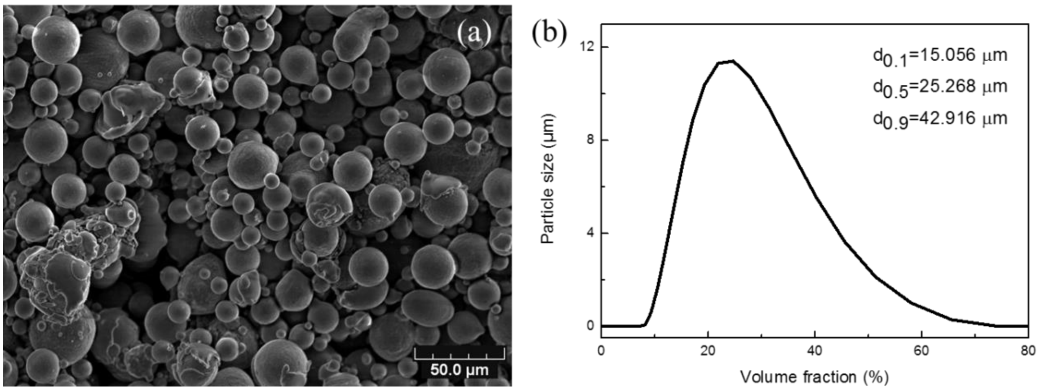

Figure 2.18 (a) SEM morphology and (b) powder size distribution of the Al5056 powders.

The gas-atomised Al5056 powder with near-spherical shape was selected as the feedstock, whose morphology is given in Figure 2.18 (a). The chemical composition of the powder and substrate is given in Table 2.1. The microhardness of the powder was 84.6+8.6 HV0.01. The size distribution of powder was measured by Mastersizer 2000 (Malvern Instruments Ltd., UK), which is shown in Figure 2.17 (b). The surface morphology of the as-sprayed coating on the damaged workpiece was measured by Profilometer (AltiSurf 500, Altimet, France). The polished coating cross-section was etched by Keller's reagent (95 mL of H_2O, 1.5 mL of HCl, 2.5 mL of HNO_3 and 1 mL of HF) and then the microstructure was observed by a scanning electron microscope (SEM) (JSM5800LV, JEOL, Japan). In order to evaluate the potential effect of inclination wall on the cohesion strength, a separate experiment was introduced, where three groups of tensile test specimens at spray angles of 70°, 80° and 90° were prepared. The as-sprayed workpiece was placed between two tensile test rods and adhered with each other by two glue layers (yield pressure: 59±3 MPa, FM1000 Adhesive, Couche Sales, LLC, USA). The tensile specimens were heated in the preheated oven for two hours at 185 °C and cooled to room temperature. The assembled tensile specimens were then measured by a tensile machine (IC ESCOFFIER, Estotest 50, France) at a crosshead speed of 1.26 mm/min.

Table 2.1 Chemical composition of Aluminium 5056 powder and Aluminium 2017A substrate

Element	Al	Mg	Cr	Cu	Fe	Mn	Si	Zn
Al5056	94.6	4.7	0.11	0.1	0.13	0.11	0.04	0.02
Al 2017A	Rest	0.4	0.1	3.5	0.7	0.4	-	0.25

2.3.2 Results and discussion

2.3.2.1 Spray efficiency

With the growing number of commercial applications of cold spray in automobile, aviation and electrical industry [10, 11], cost control and estimation of cold spray processes are showing more and more importance. For example, a cost structure model [12] of cold spray including various CS systems and various applications has been developed at Siemens and used to support decisions with sufficient accuracy. In this study, the spray efficiency by Archimedean spiral trajectory in the damage repair process was also investigated according to a comparison with a traditional round-trip trajectory.

Repair of the defect was made by a traditional round-trip trajectory with constant nozzle traverse speed of 150 mm/s and the same spray parameters, and the trajectory was repeated 30 times, which is the same as the experiments by the Archimedean spiral trajectory. It was found that the process took 14 min 40 s and the maximum coating thickness was 591 μm. As shown in Figure 2.19 (a) and (b), the coating deposited by round-trip trajectory did not restored the crater defect. According to the maximum depth of 4.3 mm at the crater, it can roughly estimate that it will take 104 min to fully restore the crater including the area with maximum depth. However, as for the Archimedean spiral trajectory, the process duration was shortened to 12 min. Although the nozzle traverse speed was decreased according to the depth in the crater in the case of the Archimedean spiral trajectory, the time that it took to cover the crater area has been shorted significantly compared with the round-trip trajectory. Based on the assumption of constant powder feed rate and power consumption, the reduced process duration can largely decrease the powder consumption as well as the energy consumption of the cold spray system.

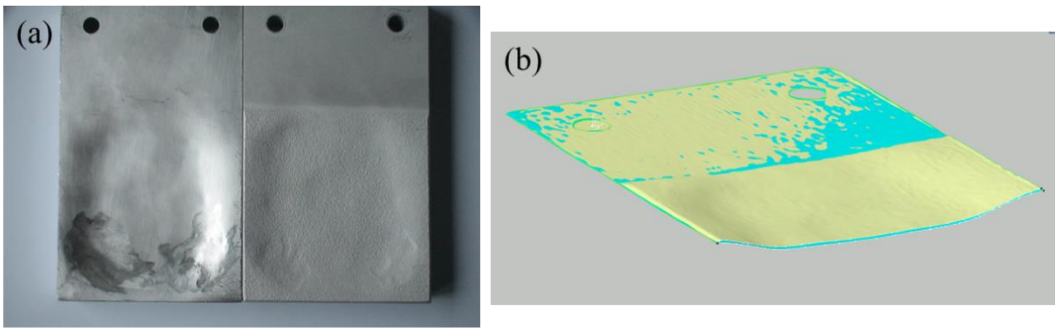

Figure 2.19 (a) The as-sprayed workpiece by round-trip trajectory and (b) coating profile by Profilometre.

Moreover, the traditional round-trip trajectory generates a rectangular coating that covered not only the crater defect area, but also the area outside the defect, which caused large unnecessary powder waste. On the contrary, the Archimedean spiral trajectory produced a coating based on the crater defect contour, which efficiently avoids excess powder deposition on the area outside the crater defect. It can be concluded that the Archimedean spiral trajectory can largely economise the spray process by reducing the process duration and powder consumption. Similarly, the case in defect can predict that the application of Archimedean spiral trajectory will avoid excess deposition and save consumption in terms of energy and powder.

2.3.2.2 Topography of as-spray workpiece

Figure 2.20 shows the comparison of the as-sprayed workpiece by the means of spiral trajectory and the original workpiece with a crater defect. It can be seen that the crater defect area was fully restored by Al5056 coating without excess deposition outside the defect area except the single straight track caused by entrance and exit trajectories. In addition, the coating was fabricated slightly higher than the substrate surface in order to ensure the sufficient margin for post-processing. The coating thickness only slightly increased from the crater edge towards the central region because of nozzle speed adaption. On further investigation of the coating thickness distribution on the crater defect, the coating surface morphology was measured by Profilometer and is shown in Figure 2.21, where three zones are indicated for microstructure observation in the following sections. The coating roughly shows a flat surface with some ridges and a central peak. The formation of the peak at the centre was due to the extremely low nozzle speed caused by the high target point density and high curvature of trajectory. More specifically, in order to reach the target point, the servomotor reducer needs a longer time to overcome the centrifugal force brought by the large trajectory curvature. Thus, the nozzle speed at the central region is much lower compared with that of the other regions. Moreover, an unavoidable inclined surface was formed at the edge of coating, which is due to the Gaussian coating profile of single deposition. This fact is in accordance with the edge loss phenomenon reported by Pattison [13].

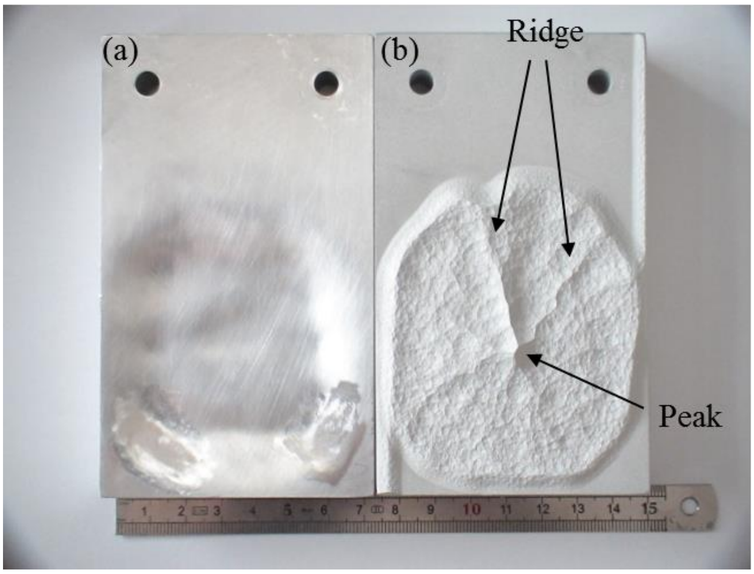

Figure 2.20 (a) The original damaged workpiece, (b) as-sprayed workpiece by spiral trajectory.

In order to evaluate the recovery quality, the as-sprayed workpiece was milled to remove the excess materials from the damaged workpiece. Figure 2.22 shows a comparison of digital photos between the original damaged and the repaired workpieces. As can be seen, the crater defect was fully filled by the Al5056 coating material. The boundary between the coating and substrate can be clearly observed without any gap, which indicates good consistency between the spiral trajectory and the crater contour. In addition, no detachment of the coating occurred during the milling process, which may indicate the good bonding between the coating and substrate. A detailed bonding strength investigation will be provided in the following section.

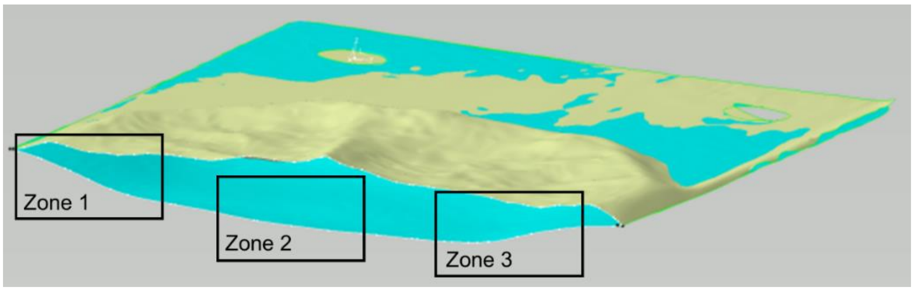

Figure 2.21 Coating profile obtained by Profilometer.

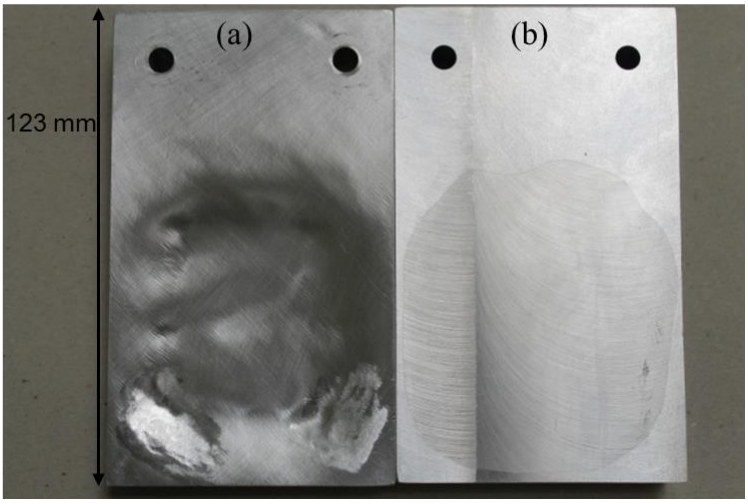

Figure 2.22. Workpiece after machinery. (a) The comparison between original damage workpiece, (b) the restored workpiece after traversal cutting the excess coating.

2.3.2.3 Bonding strength evaluation

Bonding strength including the adhesion strength between coating and damaged workpiece as well as the coating cohesion strength are of great importance to the dimensional recovery. It determines whether the repaired workpiece meets the requirement for real application [5, 14]. In this work, the nozzle was kept at 90° to the workpiece surface during the spraying process, but part of the crater has an inclination wall with the angle of 70°–80°. Therefore, the effective spray angle over the crater surface is inconsistent. As reported in previous works [15-17], the particle tended to deform towards the tangential-component direction in the angular spraying process, which resulted in a low contact area and deposition efficiency. However, Li et al. reported an interesting result—the maximum coating deposition efficiency not present in the case of 90° spraying but appears at somewhere around 80° because of the shear friction heating the interface and possibly improving the interfacial bonding [18]. This fact suggests that the spraying angle may not seriously affect the coating deposition when it is not far from 90°. Therefore, in order to confirm whether the spray angle between 70° and 90° will influence the bonding strength, Figure 2.23 provides the measured results of bonding strength as a function of spraying angle. It was found that the bonding strength had no significant change as the spray angle decreased from 90° to 70°. Based on this result, it is sensible to conclude that the bonding strength between the coating and damaged workpiece is roughly same over the entire crater surface.

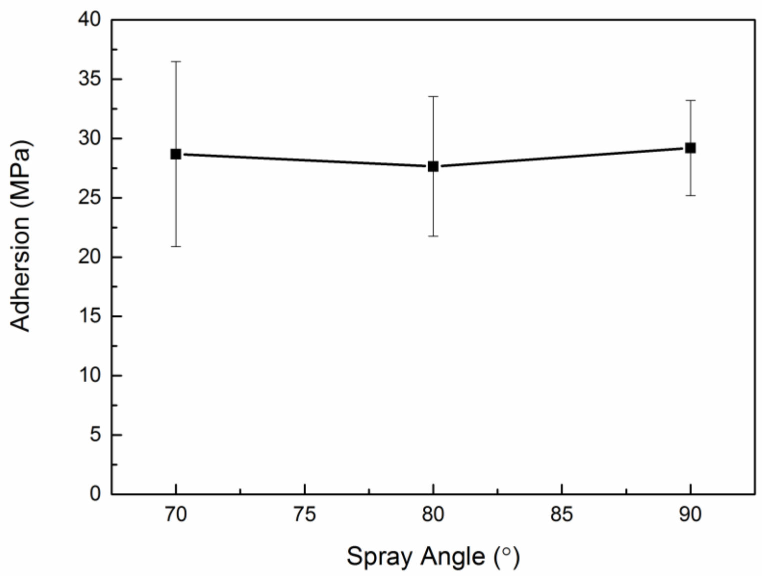

Figure 2.23 Effects of spray angle on adhesion strength of Al5056 coating.

2.3.2.4 Cross-sectional microstructure

The coating microstructure is another important factor that determines the coating quality. Figure 2.24 shows the cross-sectional SEM microstructure at different locations. Three typical zones (Zone 1, 2, 3) marked in Figure 2.21 were selected for observation. Zones 1 and 3 represent the inclination area on two sides, and zone 2 represents the flat area at the crater central region. As can be seen from Figure 2.24, the coating porosity at each zone was at a very low level regardless of the inclination angle, which indicates that the coating density and porosity are the same over the entire crater surface. This fact further confirms that the repair quality of the damaged workpiece is remarkable.

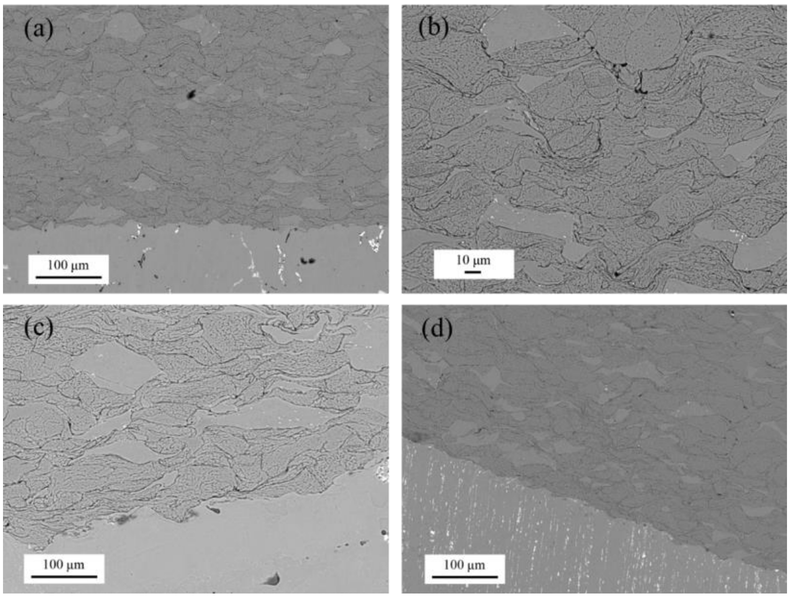

Figure 2.24 Cross-sectional microstructure between coating and substrate: (a) flat area of zone 2 and its high magnification figure, (c) and (d) inclined area of zone 1 and 3.

2.4 Conclusion

In this chapter, the generation of trajectory through the off-line programming method is presented. Firstly, the TST is embedded as a ribbon in the RobotStudio™, which gives a unified user interface. Meanwhile, a few improvements have been made. The meander trajectory for defect repair and workpiece pre-heating was also developed. Only a rectangular area in the middle needs to be deposited. Compared with a traditional round-trip trajectory, the meander trajectory is able to save powder consumption by avoiding excess deposition outside the strict area. Additionally, in order to maintain a constant scan step, an improvement in the trajectory generation algorithm for the curved substrate surface was made. In the optimised algorithm, the movement of the orthogonal surface corresponds to the substrate curvature, so that the constant scan step can be ensured even though the intersection is performed on a curved substrate.

Secondly, a novel Archimedean spiral trajectory was developed for a damage component recovery application by cold spray. Combined with the scaling method, the spiral trajectory was generated based on the defect area contour, which can decrease material waste outside the recovery area. Furthermore, the nozzle speed was adapted according to the crater depth, which enables the progressive change of coating thickness to compensate the variation of crater depth. An experiment of an Al5056 coating depositing on a manually manufactured workpiece with a crater defect was carried out to validate the effects of the spiral trajectory with an adapted nozzle speed. The experimental results showed that the cold sprayed Al5056 coating had fully filled the crater area on the substrate based on its contour. No excessive deposition was found outside the defect contour. The coating surface profile obtained by Profilometer measurement showed that a flat coating surface was achieved by adapted nozzle speed. Compared to the round-trip trajectory, the Archimedean spiral trajectory can significantly save the process duration as well as the consumption of powder and spray system energy, which leads to the increase of spray efficiency.

Both cross-section morphologies obtained from a different area show an Al5056 coating with high density and low porosity. By evaluating the bonding strength at different spray angles, it was found that the spray angle has little effect on Al5056 coating. It can be concluded that the proposed spiral trajectory is efficient for the application of damage component recovery and additive manufacturing with cold spray technology. With the scaling method, such an Archimedean spiral trajectory can be further applied to the repair of defects with other irregular shapes.

References

1. V. Champagne and D. Helfritch, Critical Assessment 11: Structural repairs by cold spray. *Mater Sci Technol*, 2015. **31**(6), p 627-634.
2. A. Moridi, S.H. Gangaraj, S. Vezzu, and M. Guagliano, Number of passes and thickness effect on mechanical characteristics of cold spray coating. *Procedia Engineering*, 2014. **74**, p 449-459.
3. N. Bala, H. Singh, J. Karthikeyan, and S. Prakash, Cold spray coating process for corrosion protection: a review. *Surf Eng*, 2014. **30**(6), p 414-421.
4. S. Yin, M. Meyer, W. Li, H. Liao, and R. Lupoi, Gas Flow, Particle Acceleration, and Heat Transfer in Cold Spray: A review. *J Therm Spray Technol*, 2016. **25**(5), p 1-23.
5. V.K. Champagne, The repair of magnesium rotorcraft components by cold spray. *Journal of Failure Analysis and Prevention*, 2008. **8**(2), p 164-175.
6. M. Faccoli, G. Cornacchia, D. Maestrini, G.P. Marconi, and R. Roberti, Cold Spray Repair of Martensitic Stainless Steel Components. *J Therm Spray Technol*, 2014. **23**(8), p 1270-1280.
7. D. Harvey and T. Marrocco, The Potential of the Cold Spray Process for the Repair and Manufacture of Aluminium Alloy Parts. *Proceedings of the 13th International Conference on Aluminum Alloys (Icaa13)*, 2012, p 257-263.
8. Z. Cai, S. Deng, H. Liao, C. Zeng, and G. Montavon, The Effect of Spray Distance and Scanning Step on the Coating Thickness Uniformity in Cold Spray Process. *J Therm Spray Technol*, 2014. **23**(3), p 354-362.
9. D. Fang, S. Deng, H. Liao, and C. Coddet, The effect of robot kinematics on the coating thickness uniformity. *J Therm Spray Technol*, 2010. **19**(4), p 796-804.
10. V.K. Champagne and D.J. Helfritch, Mainstreaming cold spray—push for applications. *Surf Eng*, 2014. **30**(6), p 8.
11. R.G. Maev and V. Leshchynsky, *Introduction to low pressure gas dynamic spray: physics and technology*. John Wiley & Sons. 2009.
12. O. Stier, Fundamental Cost Analysis of Cold Spray. *J Therm Spray Technol*, 2014. **23**(1-2), p 131-139.
13. J. Pattison, S. Celotto, R. Morgan, M. Bray, and W. O'Neill, Cold gas dynamic manufacturing: A non-thermal approach to freeform fabrication. *Int J Mach Tool Manu*, 2007. **47**(3–4), p 627-634.

14. V.K. Champagne, P. Leyman, and D. Helfritch, *Magnesium repair by cold spray*. 2008, DTIC Document.
15. C. Li, W. Li, Y. Wang, and H. Fukanuma, *Effect of spray angle on deposition characteristics in cold spraying*, in *Thermal Spray 2003, Advancing the Science & Applying the Technology* 2003, ASM International: Materials Park, Ohio, USA. p. 5-8.
16. S. Yin, X. Suo, J. Su, Z. Guo, H. Liao, and X. Wang, Effects of Substrate Hardness and Spray Angle on the Deposition Behavior of Cold-Sprayed Ti Particles. *J Therm Spray Technol*, 2014. **23**(1-2), p 76-83.
17. C. Chen, Y. Xie, S. Yin, M.-P. Planche, S. Deng, R. Lupoi, and H. Liao, Evaluation of the interfacial bonding between particles and substrate in angular cold spray. *Mater Lett*, 2016. **173**, p 76-79.
18. W.-Y. Li, S. Yin, and X.-F. Wang, Numerical investigations of the effect of oblique impact on particle deformation in cold spraying by the SPH method. *Appl Surf Sci*, 2010. **256**(12), p 3725-3734.

Chapter 3

Effects of operating parameters on coating properties and coating thickness

3.1 Introduction

As presented in the previous section, the thermal spray operating parameters can be classified into several categories according to published studies: the energy parameters, powder injection parameters and kinematic parameters. Among these parameters, the operating parameters can be directly controlled (speed of the torch, spray distance, scanning step, etc.), or indirectly controlled (speed and temperature of particles in flight, etc.) by the robot in thermal spraying process. Many publications [1-3] have described the relationship between the operating parameters and the coating characteristics as well as the coating structures. A. Kout et al. [4] investigated the planning trajectory-oriented spray-coating processes, they represented an optimisation method to compute and approximate the desired coating thickness with coating relative parameters. M. M. Fasching et al. [5] presented an approach for spraying layers using robotic thermal spraying system, they offered equations to optimize the spray angle, to generate more accurate robot trajectory. F. Trifa et al. [6] studied the interaction between the operating parameters and characteristics of the deposit, which allows selecting the proper settings. S. Guessasma et al. [7] developed an intelligent system based on fuzzy logic to assist the choice of parameters depending on the desired characteristics and desired deposit of the coatings. Therefore, operating parameters should be carefully chosen and kept constant during the thermal spray process in order to obtain desired and optimised coating properties.

Among various spray technologies, cold spray has drawn more and more attention due to its low porosity, high adhesion strength and low particle oxidation. In this process, particles in solid state with relatively low temperature are accelerated to high velocity ranging from 300 to 1200 m/s by heated and compressed driving gas through a converging-diverging nozzle, deposited onto substrate or layer already deposited [1-3]. Differing from traditional thermal spray processes where molten or semi-molten particles deposit at a low velocity, cold sprayed particles with low temperature and high velocity upon impact can prevent the occurrence of particle oxidation as well as local thermal residual stresses [4]. Due to its features of high deposition efficiency, high adhesion strength, low oxidation and low residual stress, cold spray is considered as an effective technology of additive manufacturing (AM) or 3D printing [5-8]. Compared with other additive manufacturing technologies like selective laser melting (SLM) and direct metal deposition (DMD), the small heat transfer in the cold spray process can mostly retain the microstructure and mechanical and chemical properties of feedstock powders. Furthermore, the controllable spray jet by the nozzle mounted at the robot provides more degree-of-freedom to the process, which enables fabrication of complex forms and coating deposition on free-form workpieces [5].

Nowadays, most additive manufacturing or dimensional repairs done by cold spray are achieved by machinery on the cold sprayed block coating, which causes a great amount of unavoidable material waste. Less attention is focused on the design of the as-sprayed coating shape or coating profile control with high accuracy. For the purpose of effective additive manufacturing by cold spray, it is of great importance to determine the dependence of operating parameters such as spray angle, nozzle traverse speed, scanning step and standoff distance on the coating thickness distribution.

There has been a series of studies focusing on the coating deposition model in cold spray as well as thermal spray process. Djurić et al. [9] developed a metal spray deposition model to simulate the spatial mass flux distribution produced by the nozzle. The deposition efficiency was included by transferring the non-linear inverse problem to a boundary-value problem. Rayment et al. [10] investigated the distribution of temperature and temperature variance on the substrate by using the same model, which aimed at the path planning optimisation as well as the elimination of the thermal residual stress and distortion of the sprayed steel shell. Duncan et al. [11] also used the numerical model developed by Djurić to optimise the path separation in spray coating, which used the sampling theory to transfer the problem into the spatial frequency domain. However, the studies mentioned above did not include the influence of off-normal spray due to the compromise on workpiece geometry or spray strategy. Fasching et al. [12] achieved a coating thickness distribution with low standard deviation by optimising the robotic trajectory, which was done by using a nozzle spray tilting model. Similarly, Leigh et al. [13] evaluated the effects of the spray angle on the coating profile by various coating properties like micro-hardness and tensile adhesion strength of the plasma sprayed coating.

In this chapter, a numerical model of the coating profile based on Gaussian distribution was developed and added to the off-line programming software. The numerical model includes the facts of various spray parameters, such as spray angle, scanning step and nozzle traverse speed, while three groups of experiments by cold spray were made to validate the numerical model. Afterwards, the coating thickness model was integrated into the off-line programming software RobotStudio™ as a module in the software Thermal Spray Toolkit (TST) [14, 15]. It enables the coating thickness simulation based on the operating parameters in the spray process, robot trajectory and robot kinematic data obtained by process simulation. Combined with other modules in TST such as trajectory generation [15-17] on different kinds of substrate surfaces, users are able to improve the spray strategy, robot trajectory and the operating parameters according to the results of coating thickness simulation and robot kinematic data.

3.2 Coating profile model

3.2.1 Single coating profile modelling

According to the central limit theorem, the averages of random variables can be considered normally distributed when the amount of variable is sufficiently large. Thus, in the case of the thermal spray process, the feedstock jet distribution out of the nozzle as well as the coating thickness distribution on the substrate surface can be approximated by the mathematical expression of Gaussian distribution. As a result, for the coating deposited by the thermal spray process, its thickness distribution, also known as the coating profile, can be expressed by Gaussian approximation [8], as the equation below. The coating profile has been frequently used for the coating thickness distribution in the spray process, which can be experimentally measured from the cross-section of the coating deposited by a single nozzle path [5].

$$\phi = \zeta(\theta)\int_0^T \left(\int \frac{A}{\sigma\sqrt{2\pi}} e^{-\left(\frac{(x-\mu_x)^2}{2\sigma^2}+\frac{(y-\mu_y)^2}{2\sigma^2}\right)} dxdy\right) dt \qquad \text{Eq. 3-1}$$

Where A is the amplitude factor in relation to the feedstock flow rate obtained from experimental result, σ is the standard deviation of the coating profile, (μ_x, μ_y) is the centre coordinate of the coating profile on the substrate surface and $\zeta(\theta)$ is the deposition efficiency in function of the spray angle. The values of each variable are obtained through experiments for a certain powder/substrate material system and spray parameters.

Generally, the spray angle is 90° in order to obtain a maximum deposition efficiency and coating quality. However, in the real spray process, due to the limits of workpiece geometry and working conditions, the off-normal spray usually appears as a compromise on spray strategy. In this study, the effects of spray angle are included in the numerical model through mathematical transformation. As shown in Figure 3.1, for a perpendicular spray case, the coating profile is conical and symmetric with the central line of nozzle. In the off-normal spray case, the substrate is inclined clockwise according to the nozzle. The coating profile in off-normal cases can be deducted by transforming the perpendicular spray model in the Cartesian coordinate system to the polar coordinate system. The spray cone in polar coordinate system is divided into a series of rays with a constant interval angle. Exemplary rays in the polar coordinate are indicated as dash lines in Figure 3.1. In the polar coordinate system, any point on the coating surface in the perpendicular spray case can be described by two variables. As illustrated in Figure 3.1, one is the deflection angle β between each ray and the central line, and the other one is the spray length AC at this angle between the impacting point C on the substrate and the point A at the coating profile. Thus, it can describe the coating profile as a function of the deflection angle and the corresponding spray length.

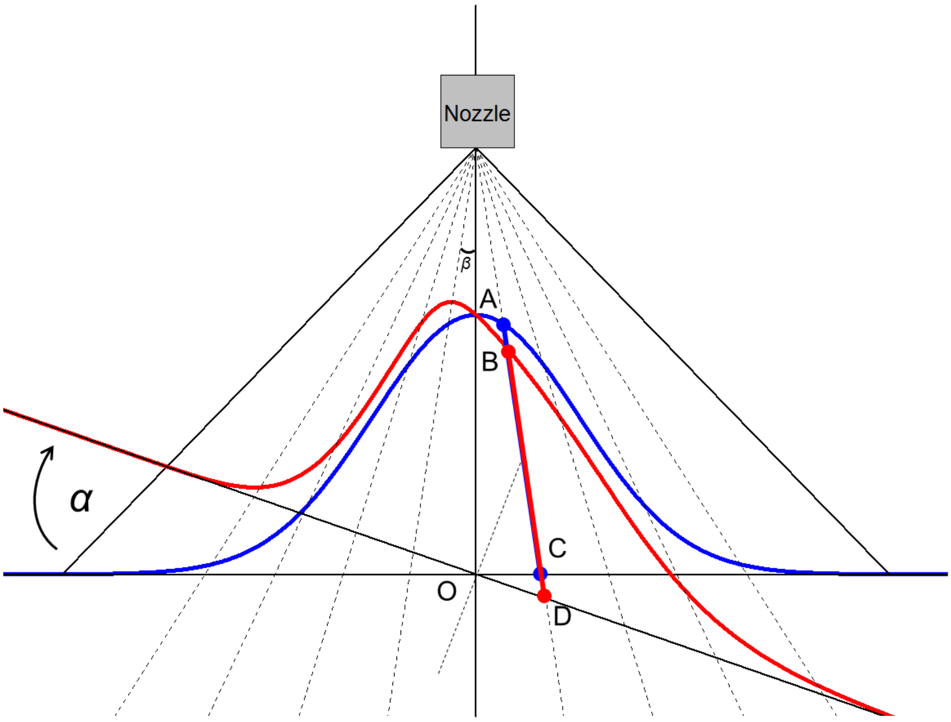

Figure 3.1. Schematic of coating profile in perpendicular (blue line) and off-normal (red line) spray cases. The substrate is inclined clockwise in off-normal spray case.

Due to the fact that mass distribution out of the nozzle is constant during nozzle inclination, an assumption can be made that the spray length at each deflection angle is constant during inclination. Thus, the coating profile of the off-normal spray can be established by spray length at each deflection angle in the standard model in the perpendicular case. For example, at the deflection angle of β as indicated in Figure 3.1, the spray length AC at the perpendicular spray case has the same value as BD at off-normal spray cases. The impacting point at each deflection angle is obtained by perspective projection through the nozzle exit point at the substrate surface. As a result, by applying the spray length at each deflection angle, the corresponding points can be obtained at the coating surface within the inclined spray cone area. The coating profile for off-normal spray cases is given in Figure 3.1, where the off-normal coating profile is marked as red, and the perpendicular one is marked as blue.

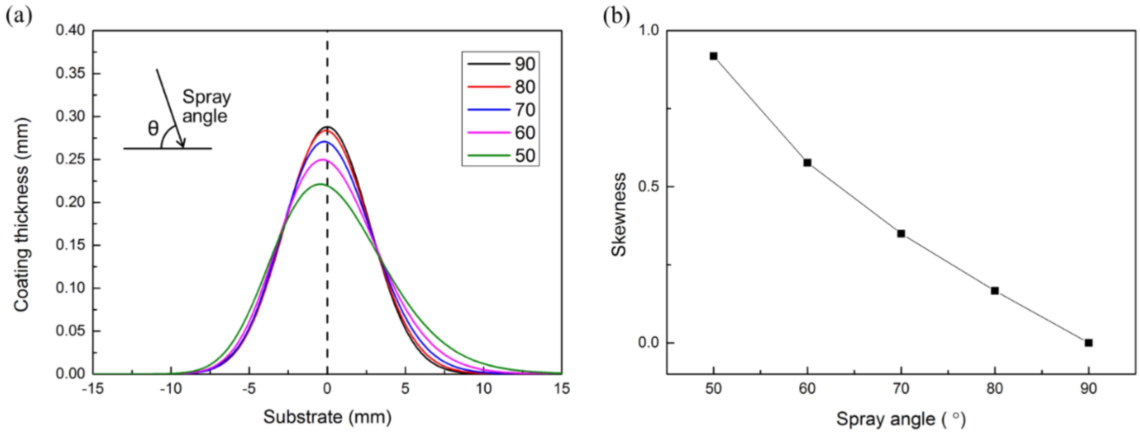

Figure 3.2 (a) Coating profile at different spray angles, (b) skewness of coating profile at different spray angles.

As shown in Figure 3.2 (a), exemplary coating profiles at different spray angles from 90° to 50°, obtained by the methodology above without accounting deposition efficiency are given, where the nozzle is inclined counter-clockwise according to the original point, the standoff distance is 30 mm. It was found that for off-normal spray cases, as the spray angle decreases from 90°, the mass distribution is gradually concentrated on the left side, and its asymmetry becomes more evident. Due to the decrease in the spray angle, particles are dispersed on a larger area, which causes the decrease of the maximum coating profile height and increase of the coating profile width, as observed in Figure 3.2 (a). The effects of the spray angle on deposition efficiency will be presented in the following parts by experimental data. In order to evaluate the coating profile asymmetry with the spray angle, the parameter of skewness, which is usually used to characterise the symmetry of the probability distribution of a set of random values, was applied and its variation is given in Figure 3.2 (b). For the spray angle of 90°, the skewness of the coating thickness distribution is zero, which indicates the perfect symmetric distribution. With the decrease in the spray angle, the skewness increases, which indicates the asymmetric distribution as well as the fact that the coating profile is gradually concentrated in the same direction of nozzle rotation. The skewness variation with the spray angle has good consistency with the coating profile variation in Figure 3.2 (a).

3.2.2 Coating thickness distribution modelling

Based on the numerical model of a single coating profile, a model can be built of coating thickness distribution on the substrate surface deposited by a nozzle trajectory. The schematic is shown in Figure 3.3, where an exemplary nozzle trajectory is illustrated on the surface of the substrate meshed by mapped grid. Firstly, the trajectory is dispersed into a series of target points separated by constant time step. The target points for thickness simulation are obtained according to the constant time step and nozzle speed interpolation based on the process simulation result, which is collected for every 24 ms by virtual robot system in RobotStudio™. Thus, the distance between two adjacent points is the product of time step and nozzle traverse speed of the previous point obtained by interpolation. An appropriate time step value is important for the thickness simulation result due to the fact that a large time step can lead to a less accurate result and a small one can lead to excess computation. The time step of 1 ms is chosen in this study.

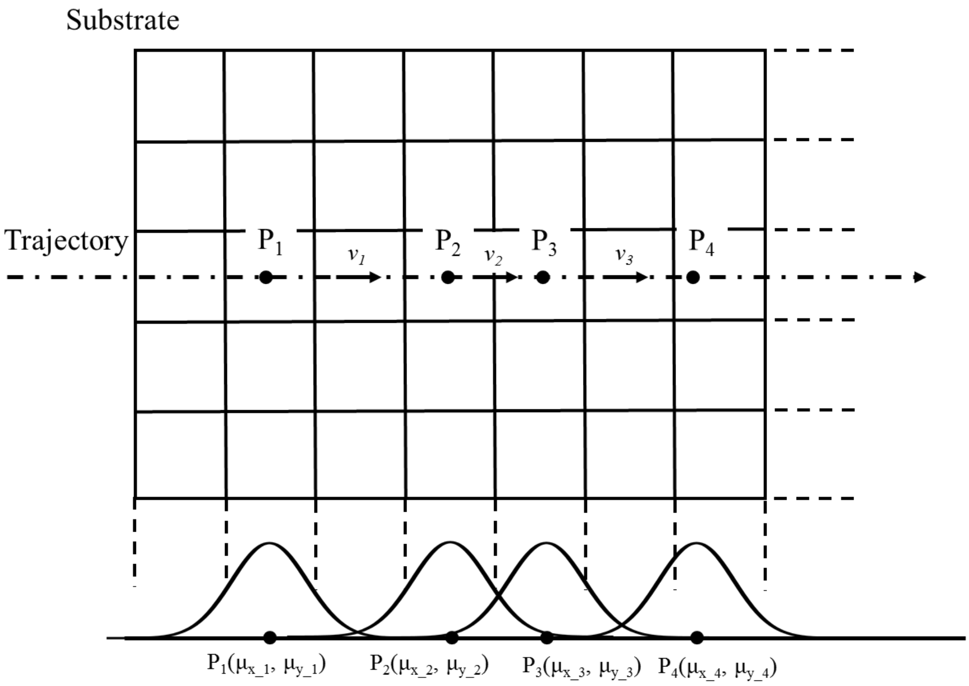

Figure 3.3 Schematic of coating thickness distribution model of trajectory from P1 to P2: the mapped mesh-grid nodes on substrate surface and the single coating profiles at target points P1 and P2.

By repeating this procedure, the points consisting the trajectory can be deduced. Secondly, by integrating the Gaussian distribution at each point along the trajectory, coating thickness distribution on the entire substrate surface can be obtained. In this process, the substrate surface is meshed as a mapped grid with constant grid size. For each target point P (μ_x, μ_y) on the trajectory, the thickness value at each mesh-grid node can be obtained by substituting the node coordinate (x, y) into the corresponding single coating profile model ϕ (σ, μ_x, μ_y). By integrating the thickness value of each mesh-grid node on the substrate surface along the trajectory, coating thickness distribution is able to be calculated according to the trajectory. Thus, it is able to describe the influence of the nozzle traverse speed in the model of coating thickness distribution. Additionally, the effects of operating parameters like the spray angle have already been included in the single coating profile model. The numerical model is developed by the software Matlab 2012b. Thus, based on the simulation result, it is able to optimise the nozzle trajectory and operating parameters as well as spray strategy.

3.3 Effects of operating parameters on coating properties

3.3.1 Experimental details

In order to study the effects of the spray operating parameter on coating thickness and validate the proposed coating thickness modelling, the experimental study on cold spray was carried out. Cold sprayed coating was produced by a homemade cold spray system (LERMPS, UTBM, France), which was equipped with a de-Laval type converging-diverging nozzle. The nozzle was cooled by a homemade circulating water system. The pure Al5056 powder (ECKA Granules Metal Powders Ltd., Germany) with spherical morphology was chosen as the feedstock, which was used and introduced in section 2.3.1. High-pressure compressed air gas was applied as the propellant gas with a temperature of 450 °C and pressure of 2.8 MPa. The standoff distance was 30 mm away from the substrate. In order to validate the numerical model, the coatings were produced by a single round-trip of nozzle as well as the full deposition. The coating thickness distribution was measured by the Profilemeter (AltiSurf 500, Altimet, France). The relative deposition efficiency was characterised as the ratio of weight gain of each sample to the maximum weight gain among all the samples at different spray angles. Microstructures of powder and coatings were examined by scanning electron microscope (SEM, JSM5800LV, JEOL, Japan) and optical microscope (OM, Nikon, Japan), respectively.

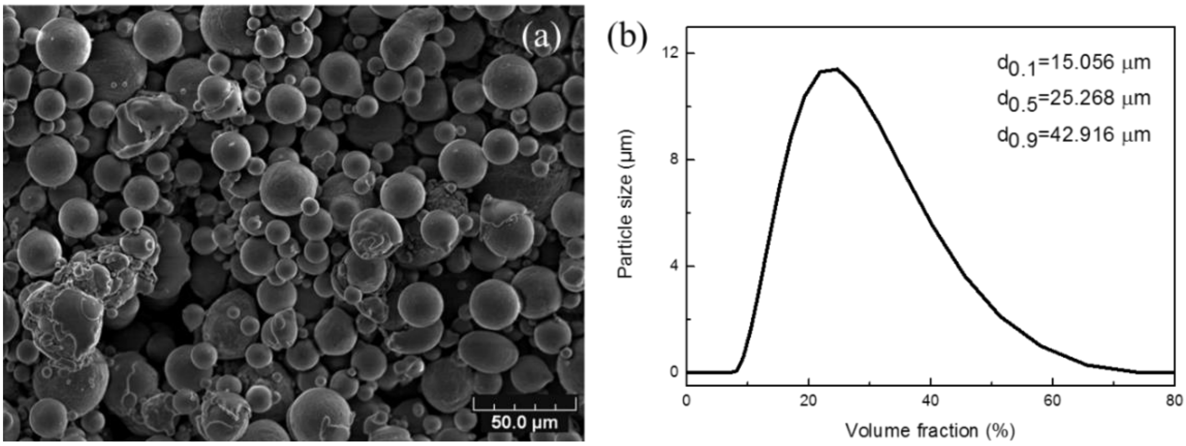

Figure 3.4 Morphology of the Al5056 powders observed by SEM.

Table 3.1 Detailed description of different operating parameters.

Group	Substrate	Nozzle traverse speed (mm/s)	Spray angle (°)	Scanning step (mm)	Nozzle pass
1	Stainless steel	150	90	None	32
			80		
			70		
			60		
			50		
2	Stainless steel	50	90	None	32
		100			
		150			
		200			
		300			
3	Aluminium	150	90	From 1 to 6	20

A detailed description of different operating parameters is listed in Table 3.1, where different spray angles, nozzle traverse speeds and scanning steps were studied. For groups 1 and 2, a coating deposited by single nozzle path was made to study the effects of the spray angle and nozzle traverse speed on a single coating profile, respectively. The trajectory was repeated 32 times to ensure a thick coating. Polished stainless steel with a thickness of 2 mm was used as a substrate for groups 1 and 2. As for group 3, a trapezoid round-trip trajectory with changing scanning step was generated in the off-line programming software RobotStudio™, as shown in Fig. 5, where the scanning step gradually increases from 1 mm on the right to 6 mm on the left. As shown in Figure 3.5, a coating composed of 11 nozzle paths is deposited on the substrate with a width of 100 mm. An over-length of 10 mm on the trajectory is reserved to maintain the stable nozzle traverse speed within the area of the substrate. In this group, polished aluminium block with a thickness of 20 mm was used as the substrate, which is thick enough to avoid substrate deformation caused by residual stress.

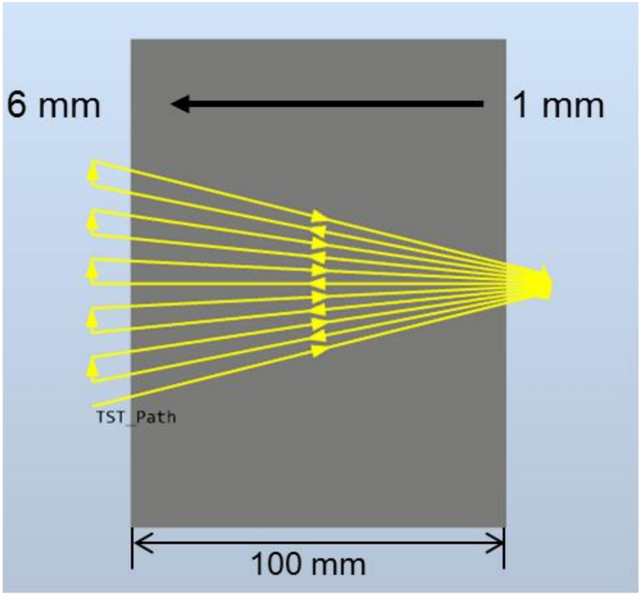

Figure 3.5 Trapezoid round-trip trajectory with changing scanning step from 1 mm to 6 mm.

3.3.2 Effects of spray angle

The effects of the spray angle on a single coating profile were investigated both experimentally and numerically, where the cases of a spray angle of 90°, 80°, 70°,60° and 50° were studied. Firstly, the relative deposition efficiency obtained by the experiments was introduced into the numerical model. As shown in Figure 3.6, the relative deposition efficiency decreases with the decreasing spray angle. The maximum deposition efficiency can be obtained for a spray angle between 80° and 90°. As for the spray angle between 60° and 80°, a rapid drop of deposition efficiency can be observed, which is because increasing the tangential component of the particle impacting velocity increases the possibility of particle rebounding from the substrate, and decreases the bonding strength between substrate and particle. As the spray angle decreases below 60°, the relative deposition efficiency reaches the minimum value. It can be expected that the deposition efficiency will reach zero with a further decrease in the spray angle, which is indicated in Figure 3.6 as a dotted line. Such a result was also reported by Li [9] using copper and titanium powder, Binder [10] using titanium powder and Luo [11] using nickel powder.

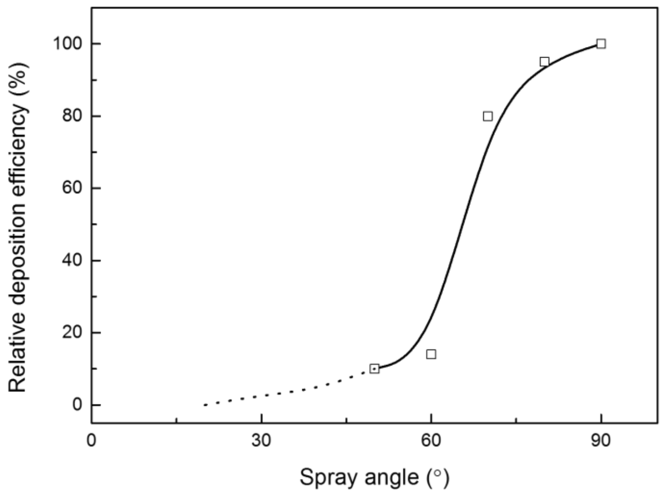

Figure 3.6 Effects of spray angle on relatively deposition efficiency of Al5056 coating.

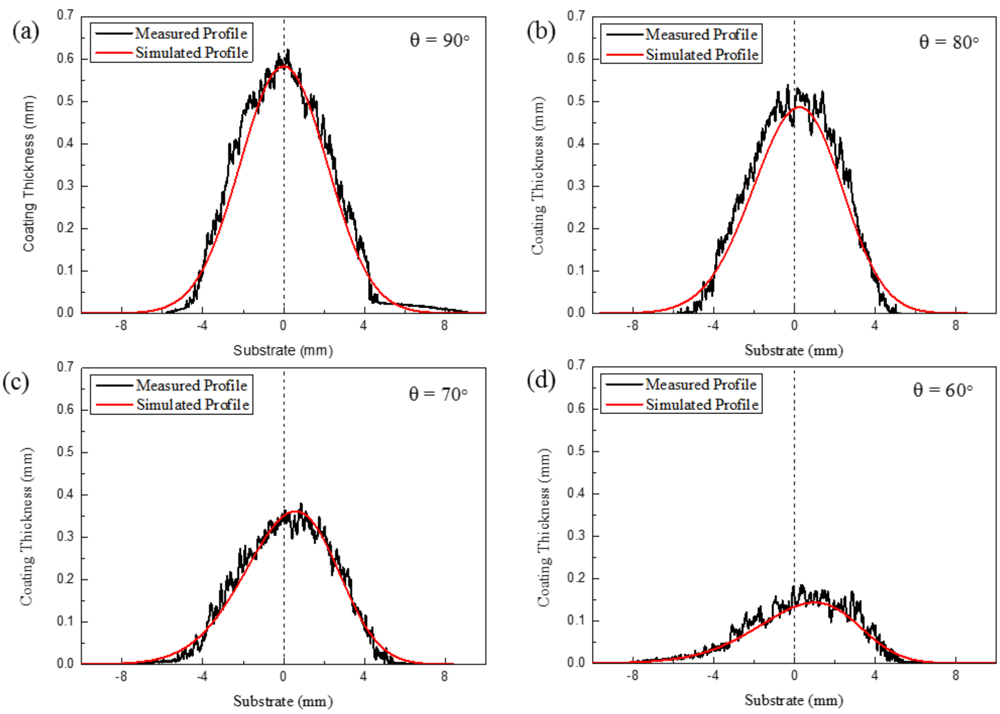

Figure 3.7 Single coating profile comparison between experimental and numerical results at different spray angles.

By introducing the effects of deposition efficiency obtained by experimental results, the coating profiles at different spray angles are simulated. The numerical results are compared with experimental results as shown in Figure 3.7. It was found that with the decreasing spray angle, the maximum coating thickness decreases and its asymmetry becomes more evident. As shown in Figure 3.7, the simulated coating profile fits well with the experimental ones. However, due to the rugosity of cold sprayed Al5056 coating, the fluctuation of the measured coating profile can be observed in Figure 3.7. In order to further evaluate the simulated coating profile, the relative error under different spray angles compared with experimental results is given in Table 3.2. Due to the rugosity of as-sprayed coating, a low relative error exists but cannot be avoided.

Table 3.2 Relative error of simulated coating profile under different spray angles compared with experimental results.

Spray angle (°)	90	80	70	60
Relative error (%)	25.2	20.9	24.2	32.8

Afterwards, the coating profile of a single deposition spot obtained by 3D simulation is shown in Figure 3.8, where coating thickness is specified by colour and its range is indicated in the colour legend on the right. Similar to the 2D simulation result shown in Figure 3.7, the 3D simulation results of the coating profile present the same trend of coating thickness and asymmetry at different spray angles.

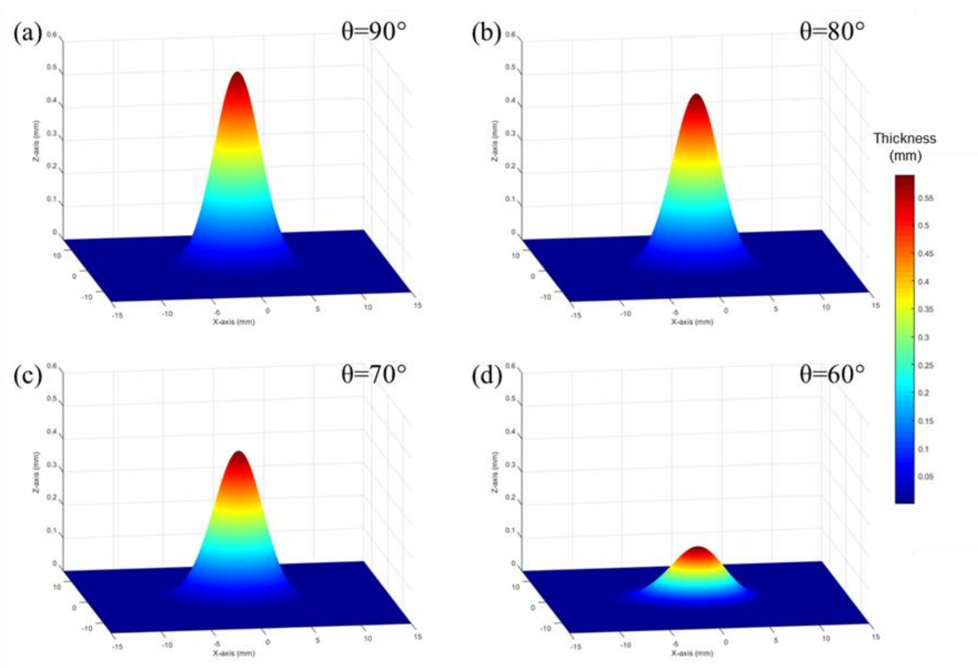

Figure 3.8 3D numerical results of single coating profile at different spray angles.

Furthermore, the cross-sectional OM micrographs of the cold-sprayed Al coatings on SS substrate at different spray angles are given in Figure 3.9. For each case, an Al coating with different thickness values can be formed without obvious porosity. The coating shows similar thickness distribution at the spray angle of 90° and 80°. By further decreasing the spray angle, it can be seen that the thickness decreases as the spray angle decreases. Thus, the 3D coating profile model is able to be used in the simulation of coating thickness distribution.

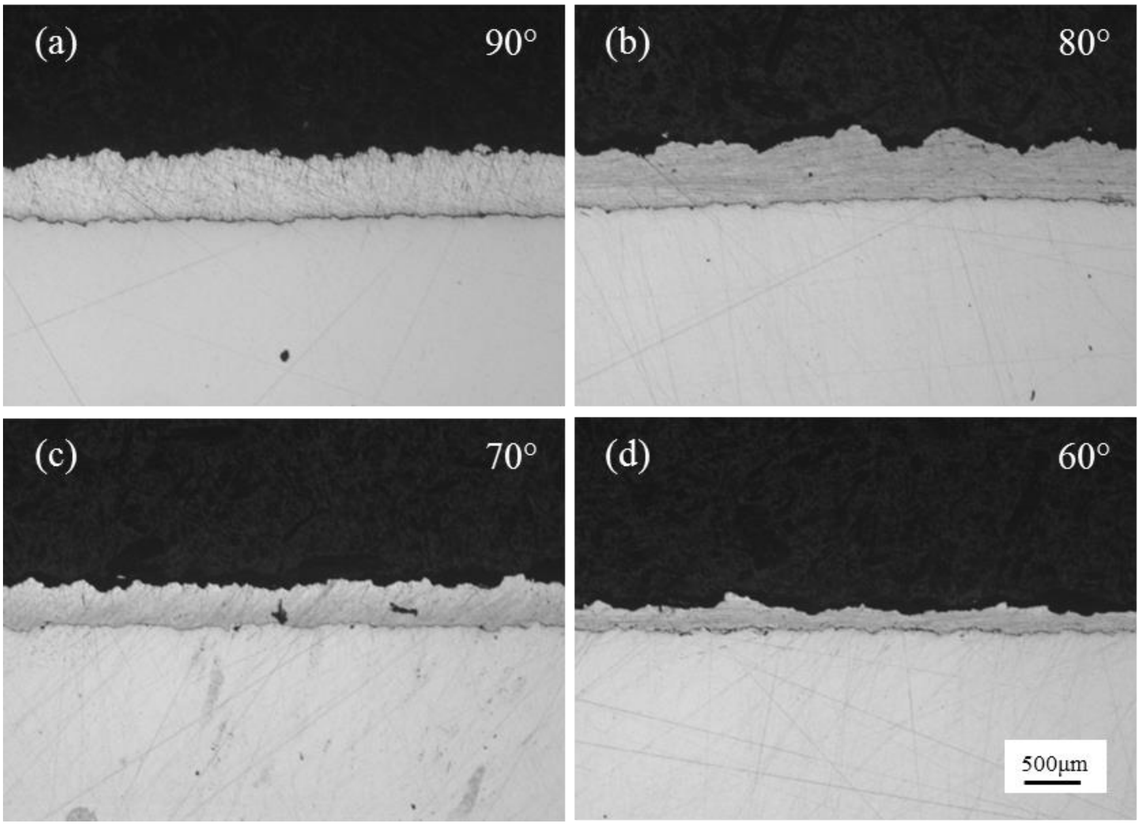

Figure 3.9 Cross-sectional OM micrographs of the cold-sprayed Al5056 coatings on SS substrate at different spray angles: (a) 90, (b) 80°, (c) 70° and (d) 60°.

3.3.3 Effects of nozzle traverse speed

The effects of nozzle traverse speed on the coating profile as well as maximum coating thickness were studied through a numerical model and experiments. Nozzle traverse speeds of 50 mm/s, 100 mm/s, 150 mm/s, 200 mm/s, 300 mm/s were included. Based on the coating thickness model on the substrate surface, the effects of nozzle traverse speed are included. As shown in Figure 3.10 (a-e), the coating profiles at different nozzle traverse speeds are presented and marked in red. The relative error of the simulated coating profile compared with experimental ones is given in Table 3.3, which shows an acceptable value. According to the good fitness between numerical and experimental coating profiles, no difference of deposition efficiency can be found for different nozzle traverse speeds, which was also reported by Wong with pure Ti and Ti-6Al-4V powder [12]. Thus, it can be concluded that deposition efficiency is independent of the nozzle traverse speed. Figure 3.10 (f) shows that the maximum coating thickness decreases with increasing nozzle traverse speed, which means that less powder was deposited for a higher nozzle traverse speed.

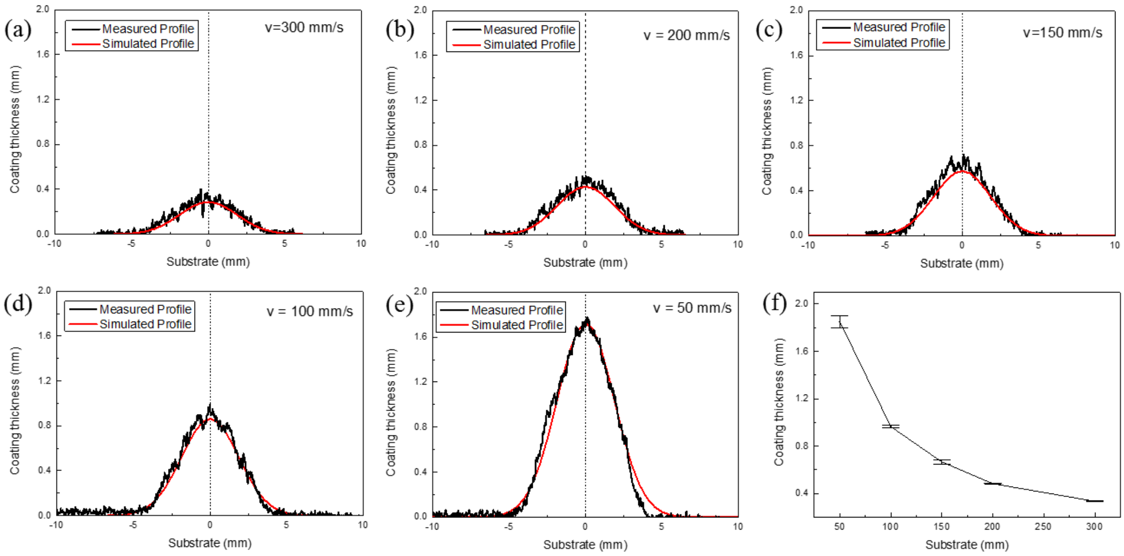

Figure 3.10 (a-e) Single coating profile at different nozzle traverse speeds, (f) maximum coating thickness with different nozzle traverse speeds.

Table 3.3 Relative error of simulated coating profile under different nozzle traverse speeds compared with experimental results.

Nozzle traverse speed (mm/s)	300	200	150	100	50
Relative error (%)	23.6	24.3	15.0	24.4	13.7

As shown in Figure 3.11, microstructures of cold sprayed Al5056 coating as a function of nozzle traverse speeds is given. Clearly, the nozzle traverse has a prominent influence on coating thickness. The coating thickness increases significantly as the nozzle traverse speed increases. Thus, by understanding the effects of the nozzle traverse speed on coating thickness, the coating thickness distribution can be adjusted and controlled.

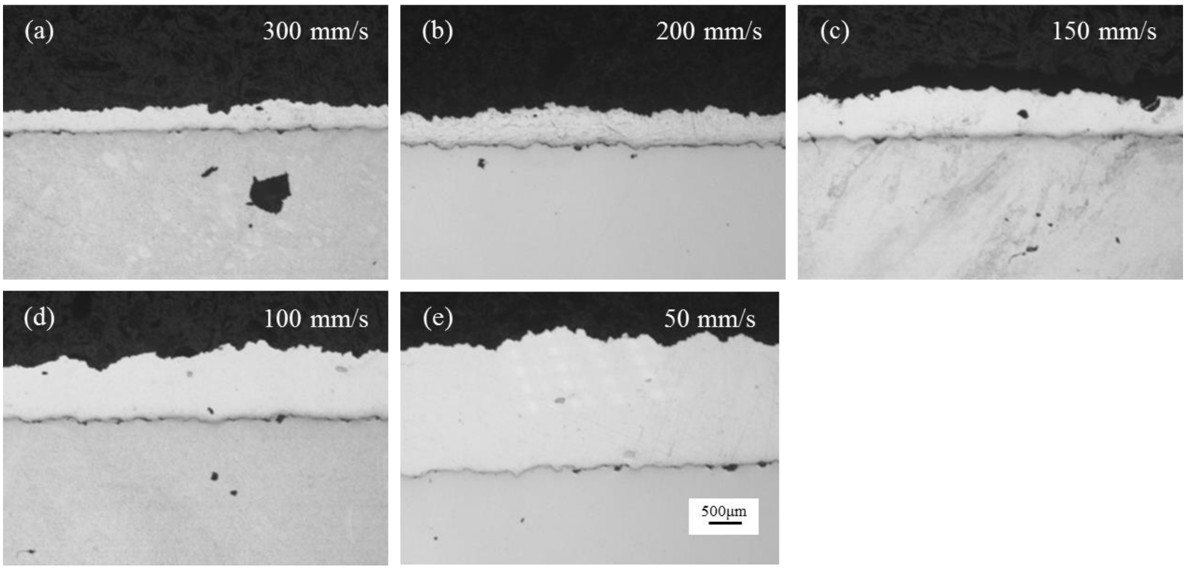

Figure 3.11 Cross-sectional OM micrographs of the cold-sprayed Al5056 coatings on SS substrate as a function of nozzle traverse speed: (a) 50 mm/s, (b) 100 mm/s, (c) 150 mm/s, (d) 200 mm/s and (e) 300 mm/s.

3.4 Evaluation of coating thickness by ProfileKit

An add-in software package called Thermal Spray Toolkit (TST) was developed by Deng et al. [13-15] in the off-line programming software RobotStudio™. It aims to provide a complete solution for the application of an ABB robot in the thermal spray process, which consists of three modules: PathKit, ProfileKit and MonitorKit. Among these modules, PathKit [13] provides the function of trajectory generation on various substrate geometries. Afterwards, the single coating profile of the generated trajectory can be simulated by ProfileKit [14], and the real-time robot trajectory can be monitored in MonitorKit [16]. At the same time, efforts have also been made to improve the functionality of TST, such as the application of an external axis [17], and trajectory generation with mesh-grid method on curved surface [18].

In this study, based on the coating thickness model and experiments validation, a simulation of the coating profile in 2D and coating thickness in 3D is introduced to ProfileKit. Compared with previous work [14], ProfileKit is improved by introducing the simulation and presentation of 3D coating thickness distribution and the dependence on robot kinematic data such as spray angle and real-time nozzle traverse speed. The cross-sectional coating profile can be observed based on different operating parameters in ProfileKit 2D, and simulate the coating thickness distribution by a nozzle trajectory and operating parameters in ProfileKit 3D. The ProfileKit 2D and 3D are written by C# language and embedded in RobotStudio™ as an add-in programme. The data exchange between ProfileKit and RobotStudio™ is based on API function, which makes it possible for ProfileKit to obtain the robot kinematic data from RobotStudio™, transfer the simulation results to RobotStudio™ and present them in a graphic form. In the following sections, a numerical simulation was made by ProfileKit 2D and 3D for comparison with the experimental results and to validate their reliability.

3.4.1 Coating thickness simulation by ProfileKit 3D

Due to the manipulation of the industrial robot, the coating quality is directly influenced by the stability of the robot motion. The instability of the robot motion can lead to the fluctuation of the nozzle traverse speed [19], which results in the low flatness of the coating surface. Meanwhile, a lot of effort have been made to improve the coating quality as well as robot motion through kinematic optimisation of the robot trajectory [5, 19, 20]. In order to present the coating thickness distribution affected by the robot kinematic data and provide evidence of kinematic optimisation, the coating thickness distribution on the substrate surface is integrated into the ProfileKit 3D, while the coating thickness simulation is based on the robot motion simulation results.

The user interface (UI) of ProfileKit shown in Figure 3.12(b) consists of two panels that refer to different operation steps. The robot trajectory can be simulated by the virtual robot system in RobotStudio™ and the robot kinematic data such as TCP (tool centre point) speed and position are collected and then displayed in the diagram below. Afterwards, in the right panel, based on the collected TCP data and operating parameters, the coating thickness distribution can be simulated after specifying the simulation parameters. Then displayed on the substrate surface in the operating window of RobotStudio™ as a coloured parametric surface on the substrate, with the colour specified by thickness value. The colour legend is given on the right side, which indicates the colour map as well as the range of thickness value. As shown in Figure 3.12(b), the robot kinematics data is illustrated in the diagram, where the data is collected for every 24 ms. By defining the time step of 1 ms, a series of points are generated on the trajectory according to the primary target points collected by RobotStudio™. By integrating the Gaussian coating profile at each point, the simulation results of the trapezoid trajectory with changing scanning steps is given on the substrate surface with a colour indicating the thickness value. The coating thickness increases from left to right where the scanning step decreases, while the surface flatness increases correspondingly.

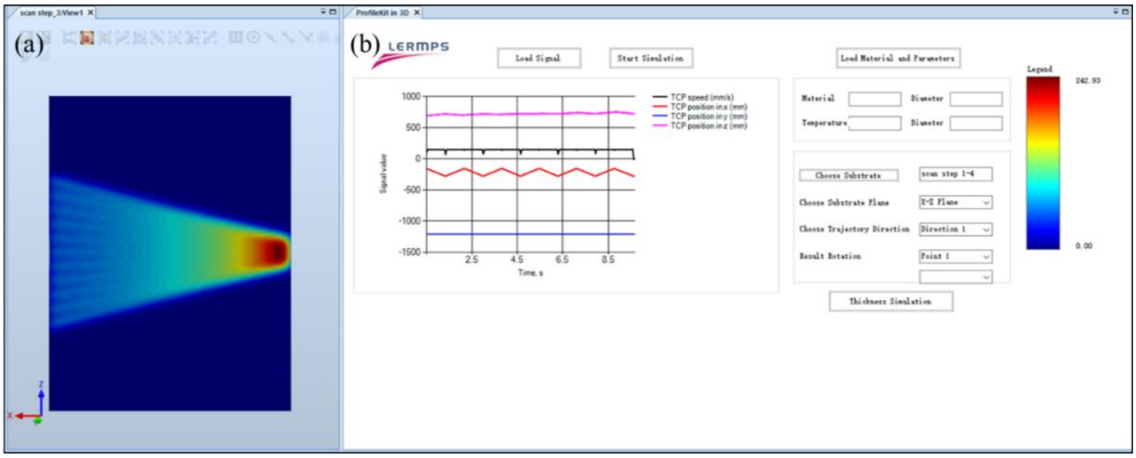

Figure 3.12 (a) Result display on substrate surface in operating window of RobotStudio™, (b) the user interface (UI) of ProfileKit of coating thickness simulation in 3D.

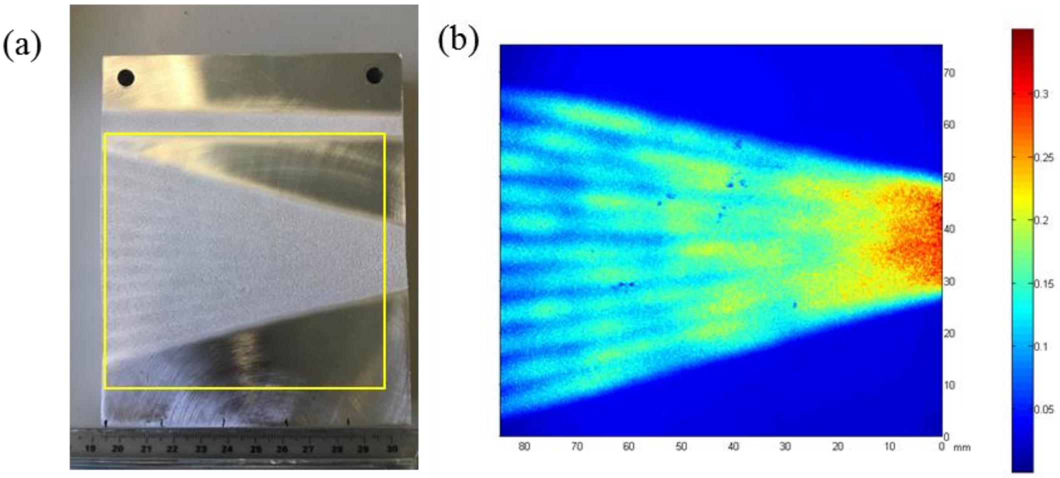

Figure 3.13 (a) Digital photo of as-sprayed workpiece by the trajectory with changing scanning step, (b) coating thickness (mm) of the coating surface by Profilometre.

The effects of the scanning step were experimentally investigated according to the parameters of group 3 in Table 3.1. As shown in Figure 3.13, the scanning step of the trajectory is gradually increasing from 1 mm on the right to 6 mm on the left, which forms a trapezoid trajectory. The as-sprayed Al 5056 coating deposited on the Al substrate by the trapezoid trajectory is shown in Figure 3.13 (a). A coating by a single nozzle path is found next to the trapezoid coating, which is caused by the return of the nozzle and used as the standard coating profile model. From the as-sprayed coating surface, it can be roughly observed that coating surface flatness decreases from right to left where scanning step decreases correspondingly. On the left of trapezoid coating, each individual nozzle path can be clearly observed. In order to further understand the coating thickness distribution, the as-sprayed trapezoid coating was scanned by Profilometre and the result is given in Figure 3.13 (b) with the colour legend indicating the thickness value. According to the colour distribution, it can be found that the coating thickness increases from left to right with the decreasing scanning step. By extracting the thickness value, the average coating thickness at different scanning steps is given in Figure 3.14. The decreasing coating surface flatness can be observed from right to left, with an increasing scanning step. On the left with a maximum scanning step value, coating by each individual nozzle path can clearly be observed, which shows an undesired coating surface quality and extremely low surface flatness.

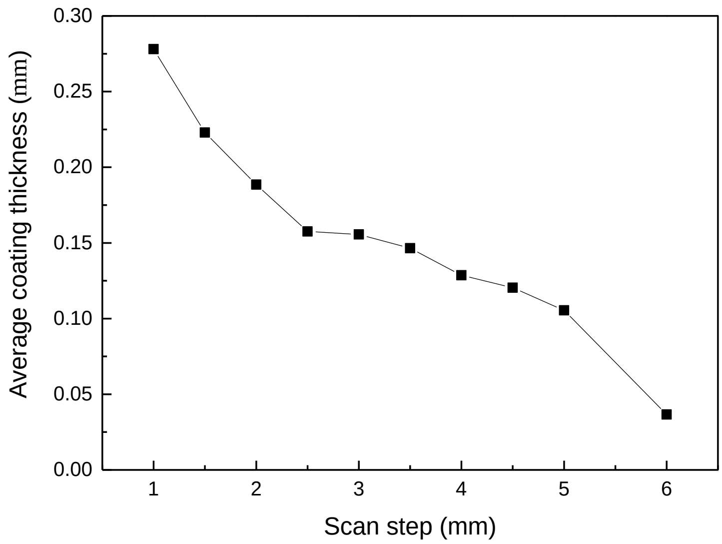

Figure 3.14 Average coating thickness at different scanning steps.

3.4.2 Single coating profile simulation by ProfileKit 2D

In order to further investigate the influence of different scanning steps, the coating profiles at each scanning step were simulated by ProfileKit 2D and then compared with the experimental results. In this module, it is able to obverse the single coating profile based on different operating parameters including spray angle, scanning step, nozzle traverse speed and so on. The UI of ProfileKit 2D is given in Figure 3.15 (a), which consists of the parameter input panel on the left and the result display panel on the right. By altering the operating parameters, coating profiles of each individual nozzle path that are coloured in blue and separated by scanning steps are shown in the display panel on the right. The integrated coating profile that is the superposition of all individual nozzle paths above is coloured in red and shown in the display panel on the right. From this diagram, the integrated coating profile as well as each nozzle path can be observed, which can be used to find the influence of operating parameters and to optimise the trajectory.

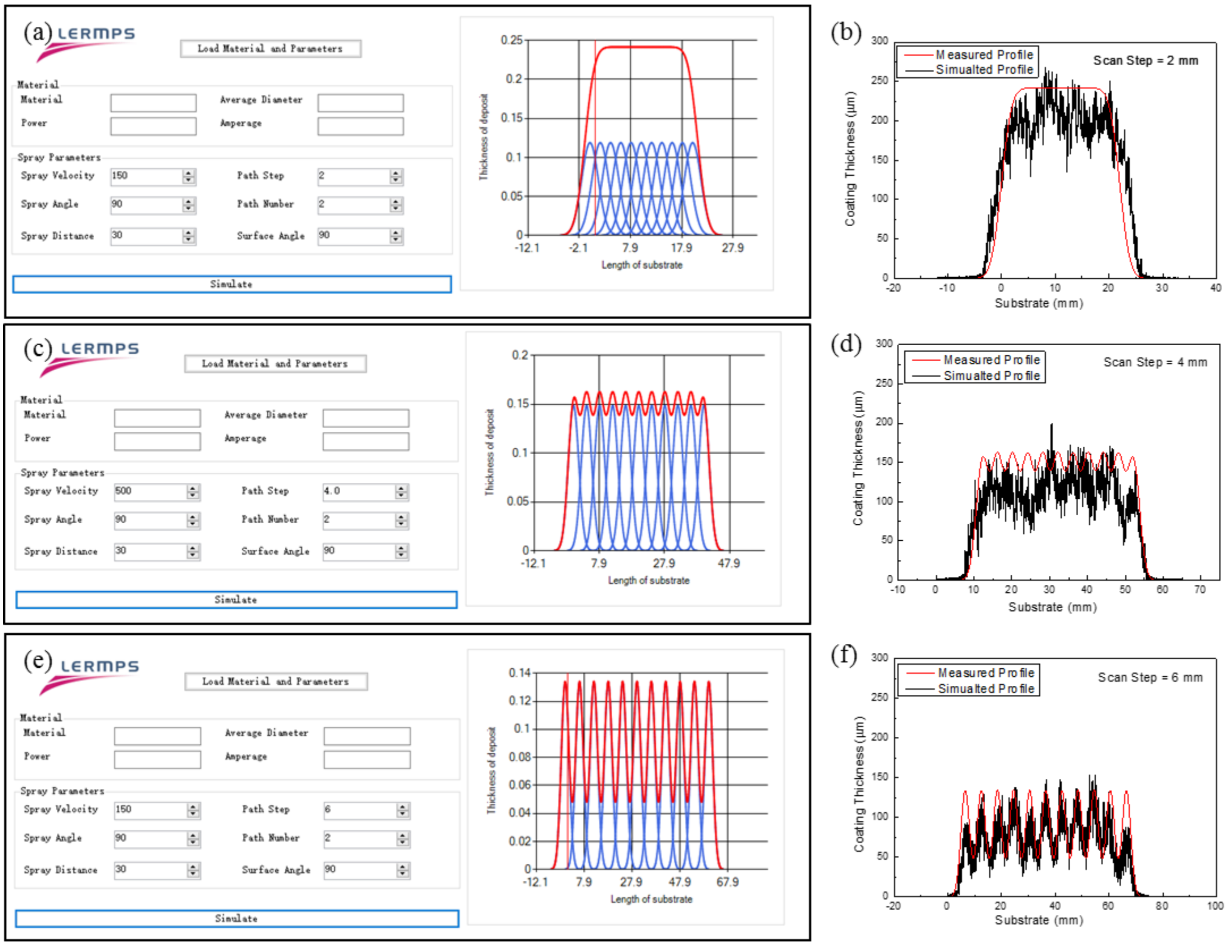

Figure 3.15 User interface of ProfileKit 2D and comparison of experimental and numerical results.

Coating profiles at scanning steps of 2 mm, 4 mm and 6 mm simulated by ProfileKit 2D are shown in Figure 3.15 (a), (c) and (e). It can be found that the surface flatness decreases with the scanning step increasing from 2 mm to 6 mm, which is in good accordance with the thickness distribution result in Figure 3.14. In order to validate the simulation result, the coating profile at positions where scanning steps are 2 mm, 4 mm and 6 mm were extracted from the thickness distribution measured from the as-sprayed workpiece. Coating profiles at different scanning steps obtained by experiment and simulation are compared and shown in Figure 3.15 (b), (d) and (f). An acceptable deviation can be observed between the numerical and experimental results, and a further discussion of relative error will be given below. As shown in Figure 3.15 (f) with scanning step of 6 mm, obvious coating thickness fluctuation can be observed from both experimental and numerical results. Figure 3.15 (e) shows that final coating profile matches well with each single profile by individual nozzle trajectory. According to the experimental results, the standard deviation σ of single coating profile is 2.7 mm. As the scanning step decreases to 4 mm, less coating profile fluctuation is found in Figure 3.15 (d). As for the scanning step of 2 mm in Figure 3.15 (b), a perfect flat coating surface is obtained, which indicates that the scanning step value equals or is below the value of σ can ensure the flatness of the coating surface. This result was also reported by Fasching [5] with electric arc spray and Cai [14] with a simulation study.

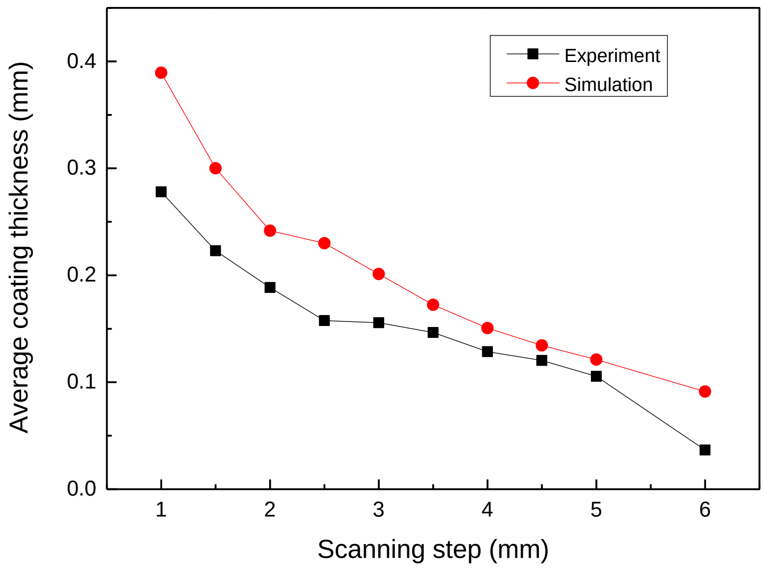

Figure 3.16 Comparison of average coating thickness at different scanning steps between experimental and numerical results.

In order to further understand the effect of scanning steps on average coating thickness, the coating profile is simulated by ProfileKit 2D at scanning steps ranging from 1 mm to 6 mm. The average coating thickness values are compared with the experimental ones and shown in Figure 3.16. Both experimental and numerical results show that the coating thickness decreases as the scanning step increases. The relative errors of average coating thickness obtained by simulation are given in Table 3.4, which shows that the simulation result is acceptable compared with the experimental result. Differences between numerical and experimental results that are found in Figure 3.15 (b), (d), (f) and Figure 3.16 can be considered as the deposition efficiency change and material loss in the coating deposited by round-trip trajectory. For a coating deposited by two parallel nozzle trajectories separated by a scanning step, the deposition efficiency of the upcoming track will be affected by Gaussian profile of the track already deposited, which can cause material loss during position.

Table 3.4 Relative error of simulated coating profile under different scanning steps compared with experimental results.

Scanning step (mm)	1	2	3	4	5	6
Relative error (%)	28.6	21.9	22.6	14.6	12.9	59.8

3.5 Conclusion

Cold spray is considered as an effective method for additive manufacturing due to its advantage of low particle temperature, low oxidation and residual stress. Although the terms like coating quality, coating microstructure and bonding theory of cold spray have been widely studied, the control of the coating thickness and coating surface quality is rare. In this study, a coating thickness simulation model was developed and integrated in off-line programming software to assist the optimisation of robot trajectory and spray strategy. The mathematical model consists of the coating profile by single nozzle path and coating thickness distribution on a substrate surface. The achievements in this section are given as follows.

A numerical model of a single coating profile based on standard experimental results was established, which included the effects of spray angle, nozzle traverse speed as well as scanning steps. According to the experimental studies of a cold sprayed Al5056 coating by a single nozzle path, the numerical model was well validated. Afterwards, a coating thickness model was developed based on the single coating profile model, which enables the thickness distribution on the entire substrate surface. It includes the effects of kinematic parameters such as spray angle, nozzle traverse speed, scanning step and so on. Based on the model above, the coating thickness simulation model is developed and integrated in the add-in software TST as a module called ProfileKit. Two parts are included in ProfileKit—a simulation of coating profile in 2D and coating thickness distribution in 3D. In ProfileKit 2D, by altering the operating parameters, it is able to account the effects on coating profile and optimise the parameter choice. In the ProfileKit 3D, coating thickness distribution can be simulated based on the nozzle trajectory on a substrate surface, and robot kinematics data by process simulation in RobotStudio™. The functionality of ProfileKit 2D and 3D were validated respectively by the trapezoid cold sprayed coating with changing scanning steps. It can be concluded that with

ProfileKit 2D and 3D, coating thickness can be simulated and predicted, which also provides evidence to optimise the operating parameters, nozzle trajectory and spray strategy.

References

1. R.L. Williamson, J.R. Fincke, and C.H. Chang, Numerical study of the relative importance of turbulence, particle size and density, and injection parameters on particle behavior during thermal plasma spraying. *J Therm Spray Technol*, 2002. **11**(1), p 107-118.
2. J. Disam, K. Lubbers, U. Neudert, and A. Sickinger, Effect of Spraying Parameters of the LPPS Method on the Structure of Ceramic Coatings. *Thermal Spray Coatings: Research, Design and Applications*, 1993, p 487-491.
3. A. Arcondeguy, A. Grimaud, A. Denoirjean, G. Gasgnier, C. Huguet, B. Pateyron, and G. Montavon, Flame-sprayed glaze coatings: effects of operating parameters and feedstock characteristics onto coating structures. *J Therm Spray Technol*, 2007. **16**(5-6), p 978-990.
4. A. Kout and H. Müller, Parameter optimization for spray coating. *Adv Eng Softw*, 2009. **40**(10), p 1078-1086.
5. M. Fasching, F. Prinz, and L. Weiss, Planning robotic trajectories for thermal spray shape deposition. *J Therm Spray Technol*, 1993. **2**(1), p 45-57.
6. F.-I. Trifa, G. Montavon, and C. Coddet, On the relationships between the geometric processing parameters of APS and the Al 2 O 3–TiO 2 deposit shapes. *Surface and Coatings Technology*, 2005. **195**(1), p 54-69.
7. S. Guessasma, M. Bounazef, and P. Nardin, Neural computation analysis of alumina–titania wear resistance coating. *International Journal of Refractory Metals and Hard Materials*, 2006. **24**(3), p 240-246.
8. R. Bolot, S. Deng, Z. Cai, H. Liao, and G. Montavon, A Coupled Model Between Robot Trajectories and Thermal History of the Workpiece During Thermal Spray Operation. *J Therm Spray Technol*, 2014. **23**(3), p 296-303.
9. C. Li, W. Li, Y. Wang, and H. Fukanuma, *Effect of spray angle on deposition characteristics in cold spraying*, in *Thermal Spray 2003, Advancing the Science & Applying the Technology*, 2003, ASM Internatiaonal: Materials Park, Ohio, USA. p 5-8.
10. K. Binder, J. Gottschalk, M. Kollenda, F. Gärtner, and T. Klassen, Influence of impact angle and gas temperature on mechanical properties of titanium cold spray deposits. *J Therm Spray Technol*, 2011. **20**(1-2), p 234-242.

11. X.-T. Luo, Y.-J. Li, C.-X. Li, G.-J. Yang, and C.-J. Li, Effect of spray conditions on deposition behavior and microstructure of cold sprayed Ni coatings sprayed with a porous electrolytic Ni powder. *Surf Coat Technol*, 2016. **289**, p 85-93.
12. W. Wong, A. Rezaeian, E. Irissou, J.G. Legoux, and S. Yue. Cold spray characteristics of commercially pure Ti and Ti-6Al-4V. *Advanced Materials Research*. 2010, Trans Tech Publ. 2010. p 639-644
13. S. Deng, Z. Cai, D. Fang, H. Liao, and G. Montavon, Application of robot offline programming in thermal spraying. *Surf Coat Technol*, 2012. **206**(19-20), p 3875-3882.
14. Z. Cai, S. Deng, H. Liao, C. Zeng, and G. Montavon, The Effect of Spray Distance and Scanning Step on the Coating Thickness Uniformity in Cold Spray Process. *J Therm Spray Technol*, 2014. **23**(3), p 354-362.
15. S. Deng, H. Liao, C. Zeng, P. Charles, and C. Coddet. Robotic trajectory autogeneration in thermal spraying. *International Thermal Spray Conference* 2005 (Seattle, Washington, USA), 2005. p 481-485.
16. S. Deng, *Robot offline programming and real-time monitoring of trajectories: development of an add-in program of robotstudio™ for the thermal spraying*, in *Graduate School of Physics for Engineers and Microtechnology*. 2006, University of Technology of Belfort-Montbéliard, France.
17. S. Deng, D. Fang, Z. Cai, H. Liao, and G. Montavon, Application of External Axis in Robot-Assisted Thermal Spraying. *J Therm Spray Technol*, 2012. **21**(6), p 1203-1215.
18. Z. Cai, H. Liang, S. Quan, S. Deng, C. Zeng, and F. Zhang, Computer-Aided Robot Trajectory Auto-generation Strategy in Thermal Spraying. *J Therm Spray Technol*, 2015. **24**(7), p 1235-1245.
19. S. Deng, H. Liang, Z. Cai, H. Liao, and G. Montavon, Kinematic Optimization of Robot Trajectories for Thermal Spray Coating Application. *J Therm Spray Technol*, 2014. **23**(8), p 1382-1389.
20. D. Fang, S. Deng, H. Liao, and C. Coddet, The effect of robot kinematics on the coating thickness uniformity. *J Therm Spray Technol*, 2010. **19**(4), p 796-804.

Chapter 4

Kinematic optimisation of robot trajectory

4.1 Introduction

Although the robots are designed as highly accurate manipulators, the weight of electric cables, torch and accessories (payloads) can cause dynamic divergences between the expected and the actual robot trajectories during the thermal spraying process. These divergences are represented in two kinds of issues: trajectory issues and speed issues. These problems, which are commonly ignored in thermal spray, will be presented and discussed with two experimental examples. All the simulations are performed under RobotStudio™, which is an off-line programming software provided for ABB robots.

4.1.1 Failure to comply with the trajectory

The first example presents the spraying on a complex workpiece that has a curved shape in the middle. Figure 4.1 (a) and (b) show the spray configurations and the corresponding trajectory of robot. The torch (Type F4, Sulzer Metco AG, Switzerland) was guided by a six-axis robot (Type IRB4400-45, ABB, Sweden) and kept normal to the substrate when scanning the workpiece. The spray distance was set to 110 mm and the relative scanning speed was programmed at 500 mm/s. With the help of an add-in software of RobotStudio™ named TST [1, 2], a robot trajectory according to the surface profile was generated. For one pass of scanning, 13 points were connected linearly to approach the curved profile of the surface. This trajectory was then simulated off-line and downloaded into the real robot for spraying. The robot movement data including TCP position and orientation versus time were recorded in real-time by the monitoring module of TST.

Figure 4.2 shows the comparison of robot trajectories. The white curve was the programmed TCP trajectory; the yellow spheres were the sample points recorded in real-time, which represented the actual TCP movement during the spray process. From this image, it can be observed that the centres of the yellow spheres were not exactly situated on the white curve, which means that the robot did not respect the designed trajectory in this process. The maximum discrepancy between the real trajectory and programed trajectory was up to 3.8 mm. This divergence causes inaccuracies in the coating formation, which affects the final coating quality especially for the process, which is sensitive to the spray distance (e.g. cold spray). Unfortunately, the failure of the trajectory was not always found nor noticed exactly, but often ignored because the robot manipulators were considered to be completely accurate.

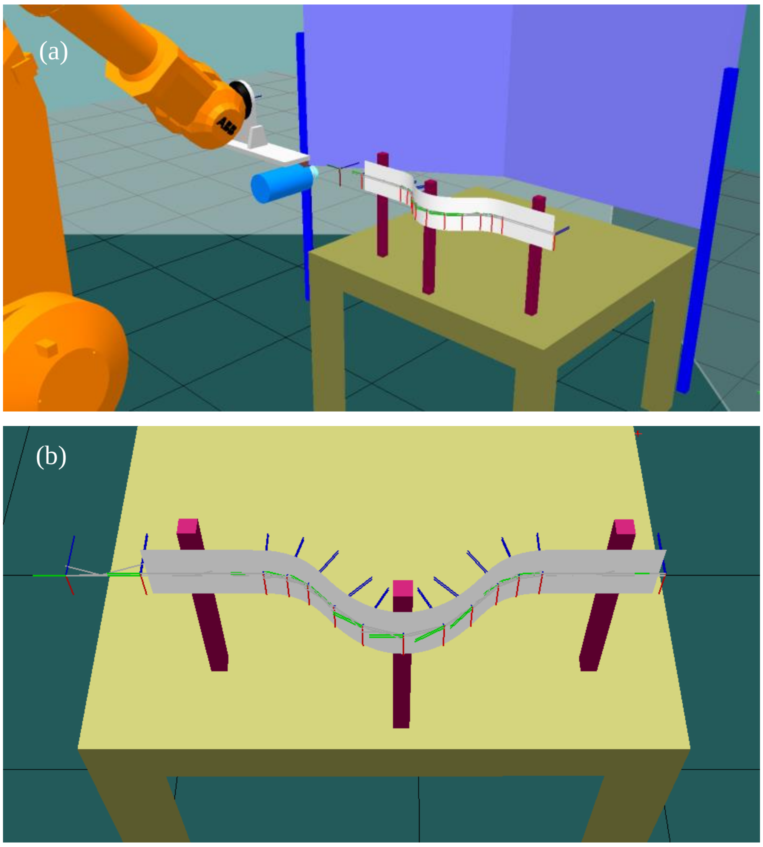

Figure 4.1 Spraying configurations and robot trajectory: (a) view of workshop, (b) robot trajectory.

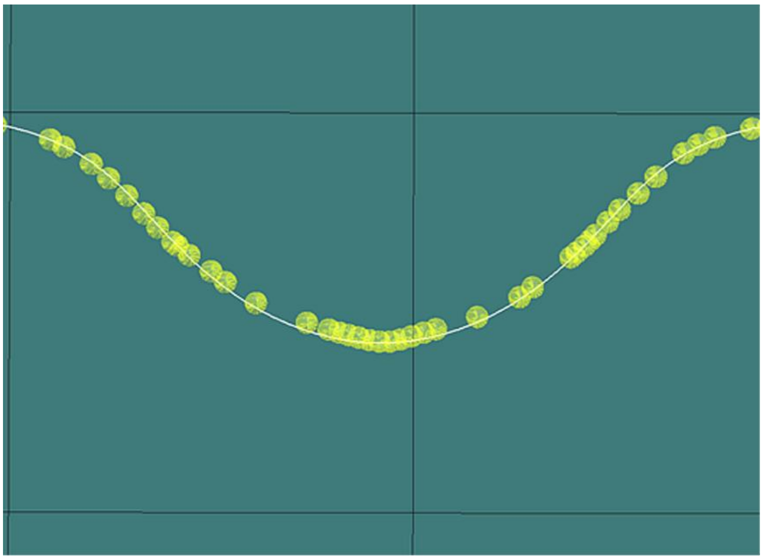

Figure 4.2 Failure to comply with the trajectory.

4.1.2 Failure to comply with the speed

In the second example, the robot was planned to spray on a simple rectangular workpiece in an equipped workshop, which is a common case in research works. The workpiece was placed on a worktable fixed in front of the robot (Type 2400-16, ABB, Sweden) for spraying. The central axis of the worktable was placed on the x-axis of the robot coordinate system. The best placement of the workpiece was unknown initially; so the workpiece was just placed at the front edge of the worktable, and axis-symmetrical on the x-axis of the robot coordinate system in the same manner as the worktable (shown in Figure 4.3). For the study purpose, a simple round-trip trajectory was created on the workpiece and simulated in RobotStudio™. The length of scanning was 400 mm, the predefined TCP speed was 500 mm/s. The real TCP speed was then recorded by the analyser module of RobotStudio™.

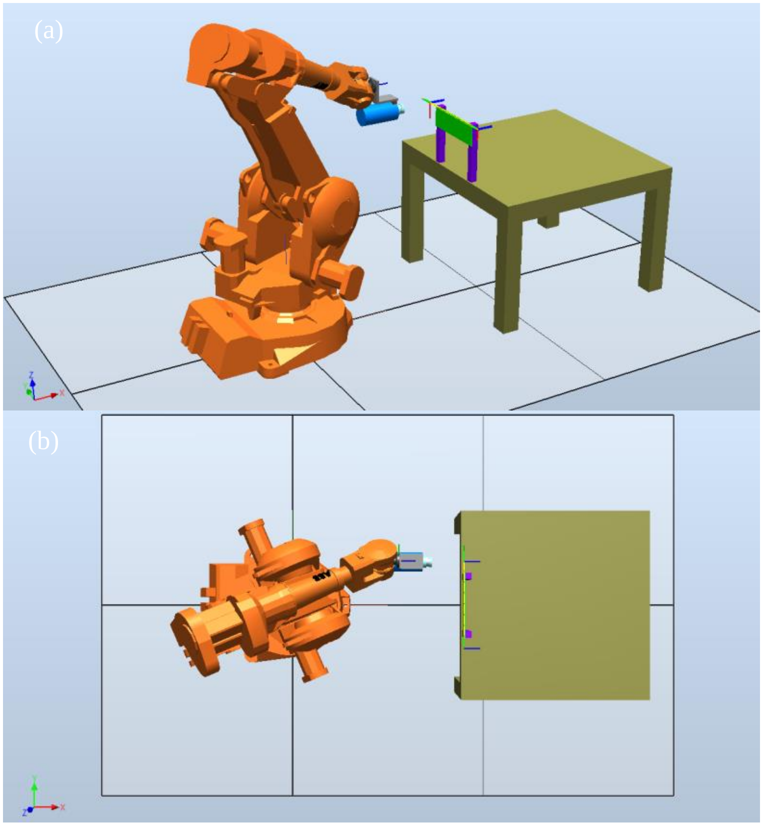

Figure 4.3 Workshop configuration: (a) global view, (b) top view.

Figure 4.4 shows the TCP speed in the simulation. It can be observed that the TCP speed was not constant when the torch was scanning on the substrate. The predefined speed was 500 mm/s, however the real speed varied from 485.3 mm/s to 515.4 mm/s. As known, the deposit properties such as coating structure and surface profile (e.g. coating thickness, coating roughness) are highly influenced by the scanning speed. In order to keep the coating uniform, the scanning speed of the torch should be constant. The failure of the speed was often underrated because it lacks the means of speed monitoring. It was assumed that robots could achieve and maintain a prescribed speed during the process.

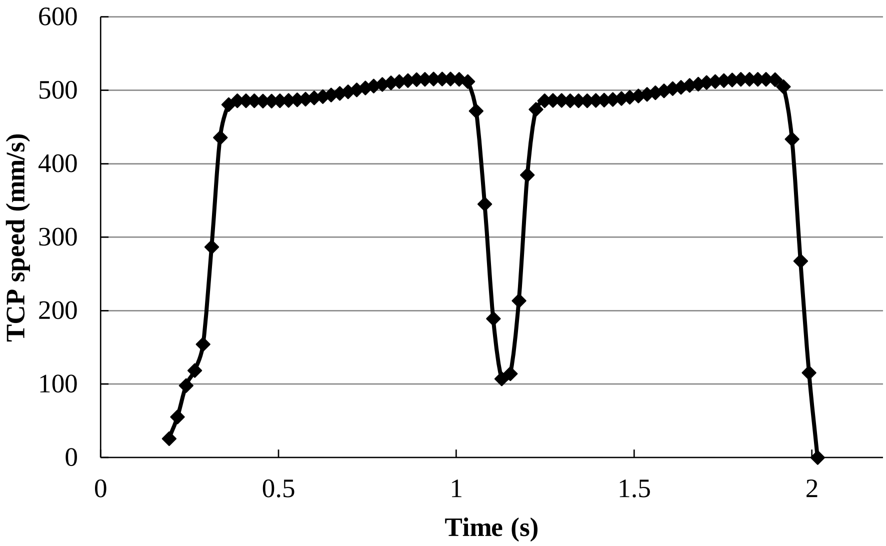

Figure 4.4 Simulated TCP speed.

From the two failure examples presented above, it can be confirmed that some neglected issues caused by robot manipulators may appear in the thermal spraying process, and lead to the quality deterioration of coatings. Therefore, it is necessary to determine and avoid these problems in the stage of off-line programming before performing the real spray process. Kinematic analyses of the robot manipulator become important and indispensable for thermal spray, especially for the cases containing complex workpieces. In the next session, attention will be paid to the second example of speed failure, which represents a more serious issue in thermal spray to find the optimisation solution.

Robot trajectory optimisation is a hot topic in the field of robotics. Much research has been carried out to investigate the trajectory planning problem for industrial robots. Fares J. Abu-Dakka et al. [3] and R. Saravanan et al. [4] proposed methods for trajectory planning in the presence of obstacles by using an evolutionary algorithm. T. Chettibi et al. [5] and Sezimaria F.P. Saramago et al. [6] introduced trajectory planning of robots taking into account certain criterion (e.g. minimum travelling distance, minimum mechanical energy, etc.). This research concerned the robot trajectory planning between fixed points in a Cartesian workspace with obstacle avoidance.

In this study, by taking into account robot kinematics according to the characteristics of thermal spray, two approaches were used to propose optimisation strategies and methods for robot aided thermal spray. According to the trajectory generation procedure and spray strategy, the kinematic optimisation can be made, based on the aspects below. Firstly, a workpiece for thermal spray will be chosen. Meanwhile, the corresponding torch setup will be chosen according to the geometry of workpiece. The torch setup will affect the motion of robot axes of the robot directly, which will influence the stability of robot speed. Furthermore, a proper torch setup will bring better robot performance. Then the trajectory is generated by the off-line programming method based on spray strategy and operating parameters. According to the simulation result and kinematic analysis, the best placement of the workpiece on the worktable can be decided. Thus, the trajectory optimisation can be considered complete.

4.2 Optimisation of nozzle mounting method

Due to the advantages in the terms of high precision for production, repeatability and protection for operators from dangerous working environment, industrial robots were introduced to the process of thermal spraying. On one hand, for a 6-axis industrial robot with a nozzle fixed on the last axis, the robot is endowed with large flexibility to reach the entire surface of a workpiece. Thus, industrial robots have brought the possibility to deposit coating onto the surfaces of workpieces with complex geometries that a manual operation cannot complete [7]. On the other hand, the high flexibility of the robot can provide a high-quality coating by accounting the thickness, roughness, hardness and porosity.

However, while industrial robot brings its power to the thermal spraying process, the problems are also emerging [8]. The optimisation of robot trajectory and motion in thermal spraying has become a hot topic. The focus mainly stays on the correlation between the coating quality and the thermal spraying operating parameters such as the spray angle, standoff distance, speed and so on [9-11]. The problem of trajectory optimisation is usually left out. Generally, the robot trajectory can be optimised based on two aspects. One is the trajectory planning optimisation to obtain a minimum cost in terms of time and energy. It has to take into account the factors such as the limits and dynamic evolution of joint positions, velocities and constraints of the manipulator [12]. For example, Chettibi et al. [5] discussed the planning of minimum cost trajectory for a robot manipulator by taking into account the dynamic equations of motion. Applications involving grasping a mobile object or obstacle avoidance show the efficiency of the proposed optimisation method. From the point of view of the cost-saving problem in the cold spray process, a cost model was proposed by Stier [13], where cost per unit quantity of deposited material is calculated by numerical model including deposition efficiency, mass loading ratio and He content of the propellant gas. As a result, the energy and time consumption is a key factor for industrial production as well as for experimental research.

Another aspect is to improve the robot performance with its kinematic constraints. The performance of a robot depends on a series of factors, such as the stability of TCP (tool centre point) speed, which is known as nozzle traverse speed [14], and its deviation from a predefined speed at each target point, as well as the joint motion of each axis. For example, in order to obtain smooth and flat coating layers by thermal spraying, Fasching et al. [15] optimised the trajectory by taking into account the effect of spray angle tilting and the spray distribution model. Based on the simulation results, the robot trajectory and spraying parameters are optimised. Based on robot kinematics, Deng et al. [16] studied the best workpiece placement in workspace by evaluating an overall parameter, which takes into account the maximum performance and joint motion of each robot axis. Fang et al. [17] also used the robot kinematic analysis method to evaluate the performance of different trajectories in the application of the external axis. Thus, by considering the TCP speed and joint motion of each axis, the performance of the robot can be evaluated and an optimisation method can be proposed.

Similar with the robot performance optimisation with its kinematic constraints, a novel optimisation method is proposed based on the nozzle mounting method. Actually, a designed trajectory is the motion of the nozzle fixed at the end-effector of the robot. Based on the robot kinematics theory, its movement is completed by a combination of six individual axes. There is a series of possibilities for the combination of axis configuration, each of which has a corresponding motion behaviour. But when the TCP orientation on the tool is defined, the corresponding configuration of robot motion is also defined. As a result, the mounting method of the nozzle decides the robot performance during the thermal spraying process. The robot performance includes aspects such as TCP speed and joint motion of each axis. The spray distribution, coating surface quality and coating thickness are affected directly by the variation of TCP speed. An instable nozzle speed leads to a rough coating surface and local overheating, which brings local re-melting and residual stress. As the study of Cinca et al. [18] shows, in the process of cold spray, the temperature distribution of particles as well as the substrate is determined directly by the nozzle speed, then influences the properties of already adhered layers. Recently, the role of substrate temperature in the cold spray process is attracting more and more attention. Fukumoto et al. [19] and Legoux et al. [20] have discussed the relationship between the deposition efficiency and the substrate temperature. Rech et al. [21] studied the influence of substrate temperature on the coating residual stress. Furthermore, Wong et al. [14] reported the influence of nozzle traverse speed on the density and micro-hardness of cold sprayed pure titanium coating, as well as the effects of substrate temperature on deposition efficiency.

Thus, in this part, the optimisation of the mounting method applied for type F4 nozzle was discussed from the stand point of robot kinematic analysis, in order to obtain a more stable TCP speed and a better coating quality. A thermal spraying example was proposed to test different mounting methods. A simple robot trajectory was intercepted to simulate the thermal spraying process. During the simulation, kinematic analysis was used to evaluate the robot performance with the different mounting methods. An improved robot performance can be defined as the low deviation between actual TCP speed and a predefined one, and the balanced joint motion of all axes. Thus, the kinematics data of different nozzle mounting methods were compared. At the same time, the energy consumptions were also compared. As mentioned above, energy consumption has become a crucial factor and constraint for both experimental research and industrial production. As a result, the introduction of energy consumption is of great importance.

4.2.1 Theory and methods

In this study, the simulation and off-line programming were done with the software RobotStudio^{TM} (ABB, Sweden). With this software, 3D models of workshops, robots and workpieces can be imported to form a virtual thermal spraying workshop, where the trajectory for the nozzle can be generated by manual composition or add-in software [22]. With the virtual robot, the reachability of targets and motion collision can be tested during the execution of the spraying process. With the signal analysis function in RobotStudio^{TM}, the kinematic parameters including speed, linear acceleration and orientation of TCP, joint position for each individual axis and the configuration of robot can be recorded for post-processing analysis. After simulation, post-processing and a series of trial tests, an optimal trajectory can be synchronised to the real robot in a work cell for the thermal spraying process.

4.2.1.1 Simulation method

In this section, the industrial robot (Type IRB2400-16, ABB, Sweden) as well as the plasma nozzle (Type F4, Sulzer Metco AG, Switzerland) [23] currently used for plasma spray experiments and production in the LERMPS were chosen for the process simulation. In order to correspond with the real thermal spray working environment, a virtual work station, virtual robot model, nozzle model together with its mounting were created in the off-line programming software RobotStudio™, as shown in Figure 4.5. Originally, the F4 nozzle was installed, as shown in Figure 4.6 (a), where the original tool centre faced the substrate. Thus, the nozzle could be perpendicular to the substrate. The spray distance, known as the standoff distance, between the nozzle and substrate was predefined as 100 mm. A rectangular workpiece with the dimensions of 300×200×10 mm was placed on a worktable in front of the robot, which was on the same central axis as the robot, as shown in Figure 4.5.

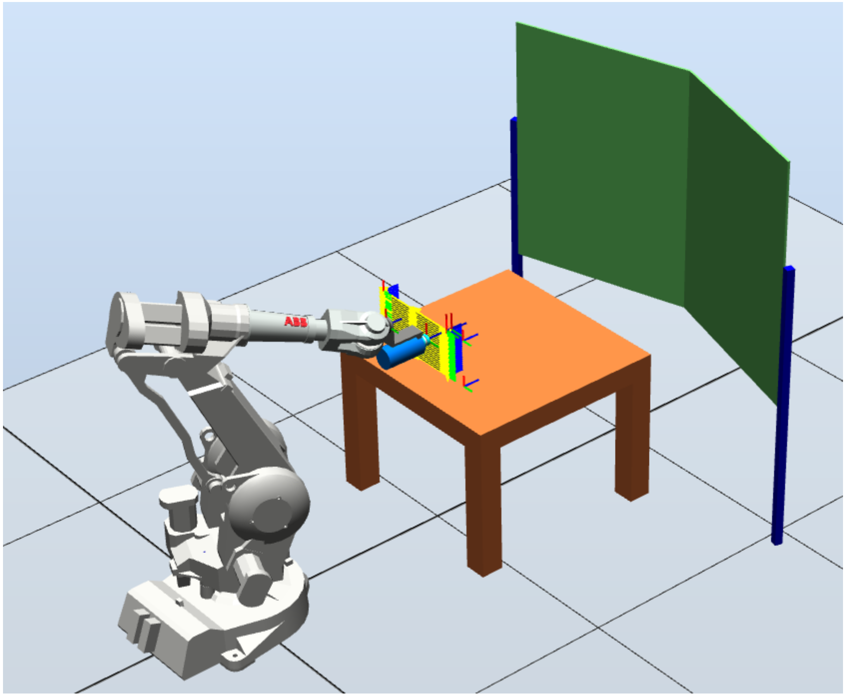

Figure 4.5 Virtual work cell in RobotStudio™.

In order to investigate the kinematic parameters of the robot during the spraying process, a simple round-trip trajectory was created at the top of the rectangle substrate, as shown in the Figure 4.6 (b), with the white arrows indicating the nozzle motion direction. The length of single scanning was 400 mm, with the predefined TCP speed of 1000 mm/s. After one scanning on the top, the nozzle moved 10 mm downwards in the z-axis to continue the second scanning. There was an over-length, which was the distance between the target point and the substrate edge. In order to avoid the fluctuation of TCP speed, this distance was reserved for the robot to accelerate and decelerate between two successive scanning paths. During the spraying process, the kinematics parameters including the TCP speed and joint positions of each individual axis were recorded by the function called the signal analyser in RobotStudio™, which was used for analysing robot kinematics.

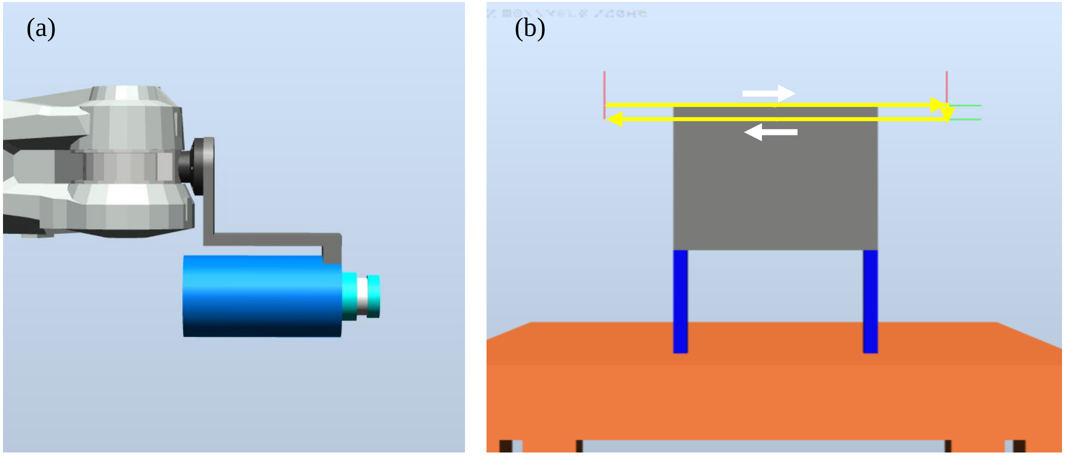

Figure 4.6 (a) Original F4 nozzle mounting on 6th axis of robot, (b) trajectory and target points on the workpiece with white arrows indicating the direction.

4.2.2 Robot kinematic analysis

4.2.2.1 TCP speed

The TCP speed variation with the original mounting method obtained by spraying simulation in RobotStudio™ is shown in Figure 4.7. Due to the existence of overlength, the robot can accelerate to the predefined TCP speed before entering the substrate area and decelerate and shift to the next path after leaving the substrate area. The regions marked by two horizontal lines indicate the corresponding TCP speed when the nozzle is within the substrate. A trough and two peaks of TCP speed are found in each path in Figure 4.7, which is due to the acceleration and deceleration of the spray nozzle. The TCP speed falls from the predefined 1000 mm/s to the lowest value of 400 mm/s, which is much lower than the predefined value. Obviously, such sudden ascent and descent of TCP speed is unfavourable for the thermal spray process and can cause a series of harm to the coating quality.

For the purpose of further study on the effective nozzle speed when the spray nozzle is within the area of substrate, which is between Y=-167 mm and Y=130 mm, the TCP speeds and spray nozzle movement direction of the Y-axis are illustrated in Figure 4.8. As shown in Figure 4.8, a fluctuation of TCP speed is found in the middle of the substrate, where the TCP speed falls to 400 mm/s from 1000 mm/s. The average speed within the substrate area is 709.573 mm/s, which is much lower than the predefined value. Meanwhile, the average error of 207.524 mm/s also demonstrates a large deviation of TCP speed from the predefined value.

The value of variance and standard deviation shows that the TCP speeds are widely spread around the predefined value, and a large fluctuation is presented as well. Obviously, both the values of maximum error and standard deviation are outside the tolerance.

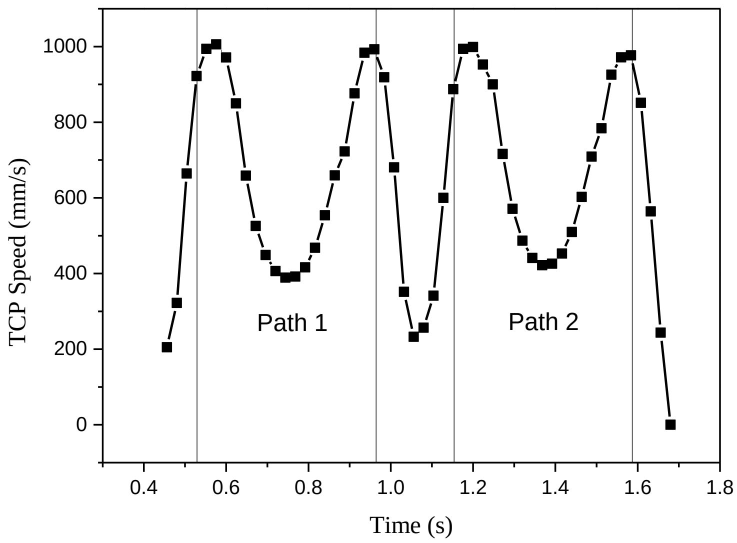

Figure 4.7 The TCP speed variation obtained with the original mounting method.

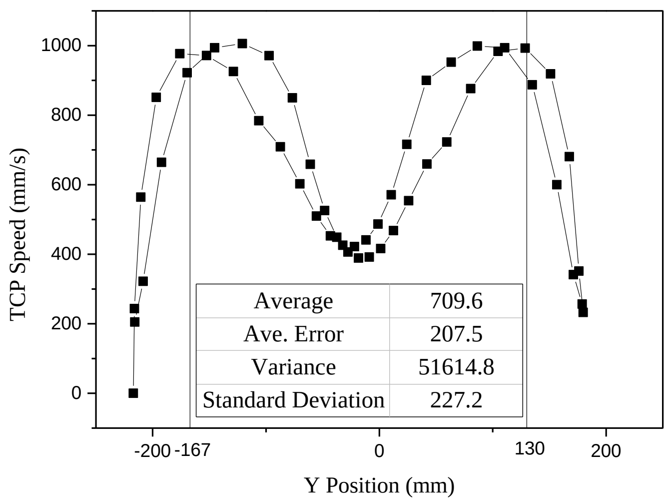

Figure 4.8 Effective TCP speed variation within substrate area along the Y-direction obtained with the original mounting method.

As mentioned above, the quality of coating mainly depends on the TCP speed. The problems of uneven coating thickness and varying roughness arise when the TCP speed cannot be kept constant. Such a sudden fall of nozzle speed can cause local overheating and corresponding thermal stress, which can deteriorate the coating quality.

4.2.2.2 Joint position and joint speed

Besides the configuration and kinematic parameters of robot, a simple robot motion between two target points is composed of the motion of each individual axis. Meanwhile, the position and orientation of TCP can be calculated by the variables of each individual axis. Thus, the TCP speed is largely influenced by the joint motion of each axis, which is also a presentation of the robot performance. The motion of each individual axis plays an important role to realize a robot movement. There are three parameters for a joint motion which are the joint position, joint speed and its acceleration.

For the joint position, it represents the value of axis rotation at a given time, with the unit of degree, which depends on mechanical limits of the robot joints. For a robot, a working envelope is the definition of its movement range, which is the space zone created when a manipulator reaches forward, backward, up and down. These distances are determined by the length of a robot's arm and the rotation limit of its axes. Each axis contributes its own range of motion. A robot can only perform within the confine of its working envelope. As a result, the joint position of each axis should be strictly maintained within its rotation limit. Meanwhile, a smooth changing of joint position within its rotation limit is favourable for a better motion performance. A sudden change of joint position will cost more energy for the servomotor of an axis to complete a designed robot motion, and also result in more fluctuation of TCP speed. As for the joint speed, it is the angular speed of an axis, defined by the derivative of the joint position with respect to time. It has a unit of degree per second (°/s). As another variable to evaluate the axis motion behaviour, the joint speed represents how fast an axis is rotating, whose limits base on the servomotor performance. A rapidly change of joint speed of a certain axis will bring risks of reaching electrical and mechanical limit. As a result, a constant or gradually changing value of the joint speed is better for the robot motion. As a result, for a single axis, two limits of joint position and joint speed exist and restrict each other. In order to improve the robot performance and stabilise the TCP speed, it is important to make sure that all the joint positions are within limits, and the joint speed is constant or changes smoothly.

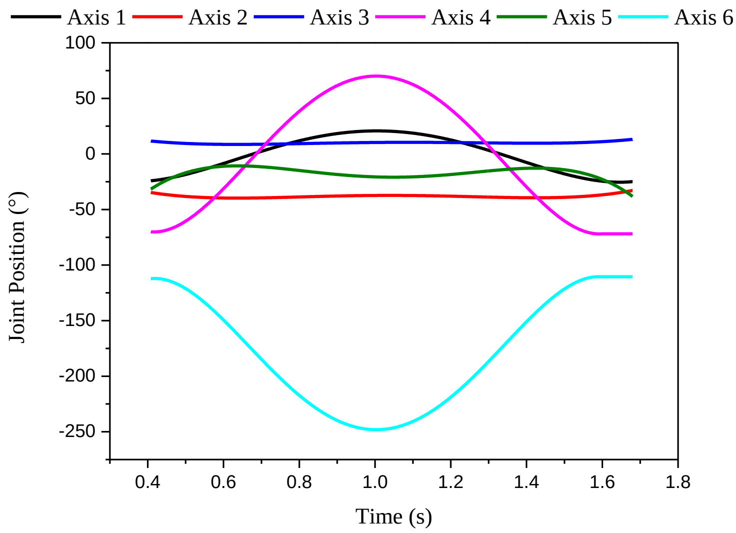

Figure 4.9 Joint position variation of each axis obtained with the original mounting method.

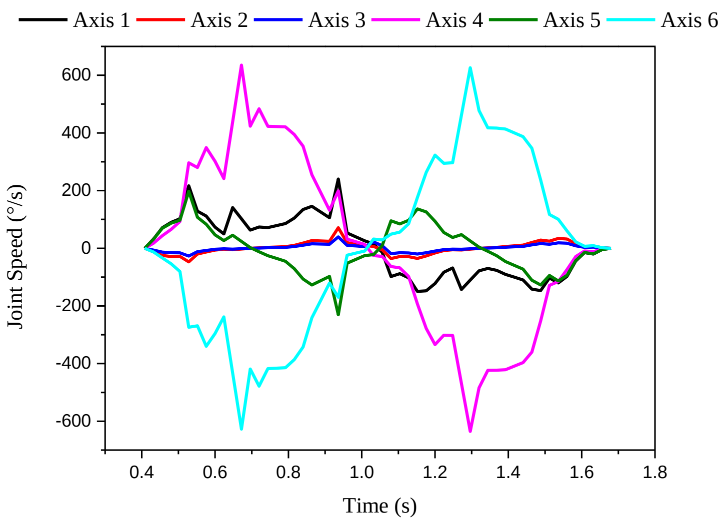

Figure 4.10 Joint speed variation of each axis obtained with the original mounting method.

As shown in the Figure 4.9, the joint positions of axes 4 and 6 have larger movement amplitudes than other axes. As the spray nozzle enters the substrate area, the joint position of axis 4 increases from -46.0 ° to 67.6 ° in 0.460 seconds, and that of axis 6 decreases from -118.9 ° to -244.7 ° simultaneously. Combining with the specification of each axis listed in As another variable to evaluate the axis performance, the joint speed represents how fast an axis is rotating, whose limit is based on the servomotor performance. A sudden change of joint speed of an axis will bring rapid change of joint position with the risk of reaching its limit. A constant or gradually changing value of the joint speed is suitable for the robot motion. In other words, joint acceleration can be used to evaluate the robot motion. Generally, the joint acceleration is to evaluate how joint speed varies, with a unit of °/s2. The larger the joint acceleration, the greater the power the servomotor has to provide. A joint acceleration that is low or constantly maintained can reduce the mechanical wear. As a result, for a single axis, three limits exist and restrict each other. In order to improve the robot performance and maintain the TCP speed, it is important to make sure that all the joint positions are within limits; moreover, the joint speed of all axes are constant or changing smoothly.

Table 1.3, the axes 4 and 6 are found both approaching their limits. The rapid changing axis joint in Figure 4.9 implies the risk of reaching the maximum axis speed. The joint speed curves of each axis obtained based on joint position data and time interval are shown in Figure 4.10. Sudden increments and decrements are found for axes 4 and 6. After increasing from 247 °/s to 635 °/s in 0.048 seconds, the joint speed of axes 4 falls to 423 °/s in 0.024 seconds. Such rapid joint speed variation continues appearing for axis 4 as well as joint 6 in the following movements. As shown in As another variable to evaluate the axis performance, the joint speed represents how fast an axis is rotating, whose limit is based on the servomotor performance. A sudden change of joint speed of an axis will bring rapid change of joint position with the risk of reaching its limit. A constant or gradually changing value of the joint speed is suitable for the robot motion. In other words, joint acceleration can be used to evaluate the robot motion. Generally, the joint acceleration is to evaluate how joint speed varies, with a unit of °/s2. The larger the joint acceleration, the greater the power the servomotor has to provide. A joint acceleration that is low or constantly maintained can reduce the mechanical wear. As a result, for a single axis, three limits exist and restrict each other. In order to improve the robot performance and maintain the TCP speed, it is important to make sure that all the joint positions are within limits; moreover, the joint speed of all axes are constant or changing smoothly.

Table 1.3, both joint motions of axes 4 and 6 surpass the axis speed limits, which are 360 °/s and 450°/s, respectively. The reason for such joint variation is due to the rapid joint motion of all 6 axes in order to reach the predefined TCP position as well as sampling instability, which leads to the acceleration and deceleration in a short time. Thus, the rapid joint motions concluded above including the axis position and speed result in a series of rapid actions for robot axes, which brings large shocks and frictions for each servomotor and higher energy consumption. As a result, in order to improve the robot performance, it is necessary to redistribute the axis motion among all 6 axes reasonably by optimising the mounting and changing the robot posture during movement.

Table 4.1 Specification of Robot IRB 2400/16.

	Range of Movement, °	Maximum axis speed, °/s
Axis 1	+180 to -180	150
Axis 2	+110 to – 100	150
Axis 3	+65 to -60	150
Axis 4	+200 to -200	360
Axis 5	+120 to -120	360
Axis 6	+400 to -400	450

4.2.3 Optimisation of mounting method

As is well known, the job of a robot is to move the TCP to a predefined target position with a predefined orientation in a predefined speed. For a typical 6-axis industrial robot, it takes a combination of joint motions of six individual axes to accomplish a robot action.

Combining the kinematics of a robot with the joint motion in Figure 4.11 (b), based on the flexibility and reachability of a 6-axis robot, it was found that the cooperation between the axes 1, 2 and 3 could approximately define the TCP position. As shown in Figure 4.11 (a), the working envelope of the 6-axis robot is obtained by the rotation range of axes 2 and 3, while the joint position of axis 1 defines the plane of the working envelope. As a result, axis 1 defines the working plane of the robot and the rest of the axes, while axes 2 and 3 can confirm the designed TCP position. The joint position of the rest of the axes (4, 5 and 6) can only provide a fine adjustment for the TCP orientation. As the nozzle is mounted on axis 6, its orientation to the substrate is mainly based on the joint position of axes 4, 5 and 6 as shown in Figure 4.11 (b). Based on this understanding, the mounting method should bring a more reasonable distribution of axis work load as described above, which will result in a better performance in kinematics and energy.

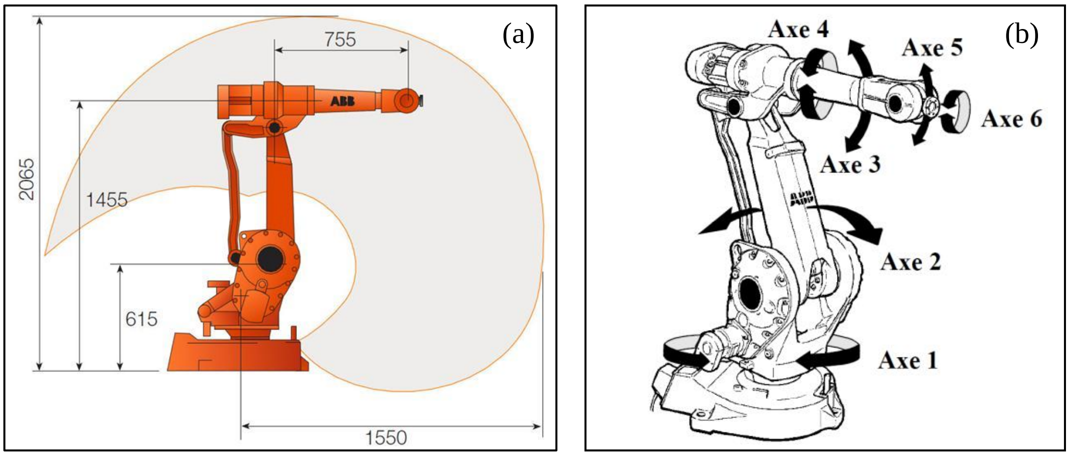

Figure 4.11 Schematic diagram of robot IRB 2400/16 by ABB: (a) working envelope of robot, (b) joint motion of each axis.

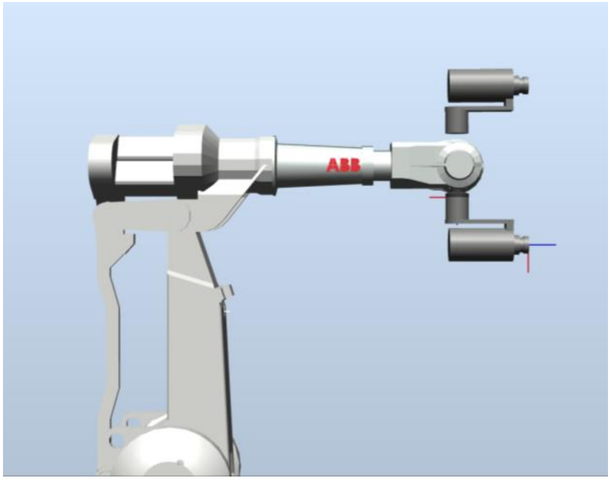

Figure 4.12 Schematic of nozzle mounting optimisation.

In this example, a round-trip trajectory was generated on a plane workpiece. With the spray nozzle kept perpendicular to the substrate, the orientation of the TCP is constant. So fewer joint position changes from axes 4, 5 and 6 are needed to maintain the TCP orientation. The work of defining the TCP position is based on axes 1, 2 and 3. The objective for the new mounting method is to decrease the work load on axes 4, 5 and 6, and transfer it to axes 1, 2 and 3. Thus, the work of nozzle mounting optimisation is to redistribute the joint motion of axes 4, 5 and 6 and find an optimal mounting method based on this basic understanding.

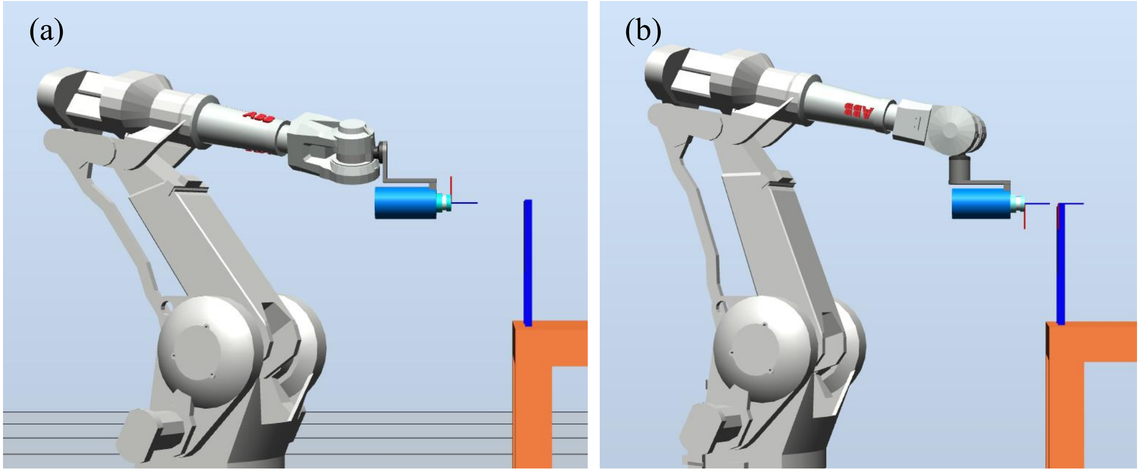

Figure 4.13 Comparison between the original (a) and optimised (b) nozzle mounting method on the robot.

In order to optimise the mounting method according to the basic understanding mentioned above, the nozzle mounting method can be done by depressing the joint motions of axes 4, 5 and 6. An effective method is to adjust the robot posture by rotating axis 5. As shown in Figure 4.12, while executing the round-trip trajectory, the reorientation of the TCP is performed by small adjustments of axis 6 instead of the combination of axes 4, 5 and 6. In this way there are two choices: the nozzle mounted on the upper position or on the lower position (as shown in Figure 4.12). By taking into account the work condition limits such as the cable and powder feed system, an optimised mounting method where axis 6 towards the ground is chosen, as shown in the Figure 4.13 (b). With this optimised mounting method, the initial orientation of the nozzle is normal to the substrate, which means that fewer movements for axes 4, 5 and 6 are needed. Only axes 5 and 6 need to rotate when the first path on the substrate is finished. However, with the original mounting method as shown in Figure 4.13(a), in order to maintain the spray angle, axes 4, 5 and 6 have to rotate along the spray trajectory. The simulation with the software RobotStudio™ is used to verify this conjecture. Under the same conditions and spraying parameters, the spraying process will be simulated with the optimised mounting method. In the next section, kinematic analysis data obtained from the simulation is used to compare the optimised mounting with the original one.

4.2.3.1 TCP speed comparison

As shown in Figure 4.14, the TCP speed is stably maintained at the predefined 1000 mm/s for both paths. A fluctuation is found in the middle, which is the over-length area between two successive paths. Similar to the TCP speed for the original mounting method in Figure 4.7, the effective TCP speeds within the substrate area related to the Y-direction are illustrated in Figure 4.15. As shown in Figure 4.15, the TCP speed is stably maintained as 1000 mm/s within the substrate area. The average value of 999.0 mm/s shows that it is able to guarantee the coating quality by a constant nozzle speed. According to the statistics data shown in Figure 4.8 and Figure 4.15, by applying the optimised nozzle mounting method, the average error and standard deviation of the effective nozzle speed decreased from 207.5 mm/s and 227.2 mm/s to 1.4 mm/s and 2.27 mm/s, respectively, which presented a stabilised robot performance and effective nozzle speed. Compared with the original mounting method, it can be seen that the optimised mounting method can bring a better coating quality by improving and stabilising the robot performance.

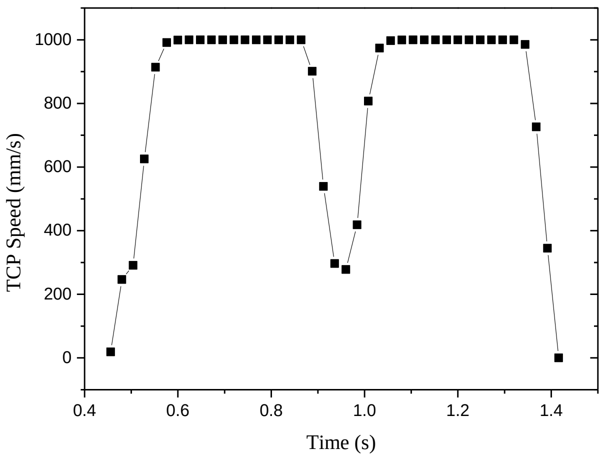

Figure 4.14 The TCP speed variation obtained with the optimised mounting method.

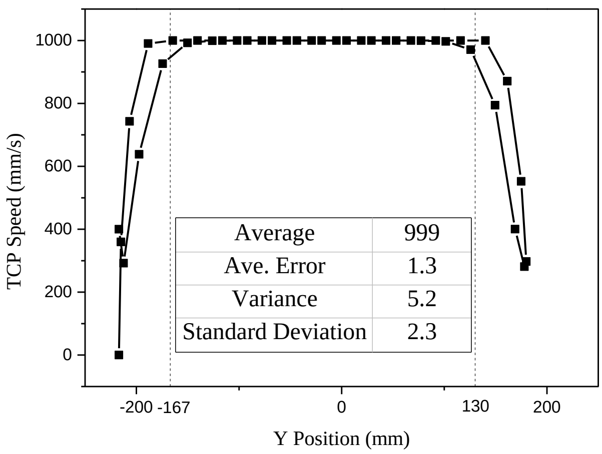

Figure 4.15 The effective TCP speed variation within substrate area which Y-axis obtained with the optimised mounting method.

4.2.3.2 Joint motion comparison

As mentioned above, the fluctuation of TCP speed around the predefined value is due to the bad performance of each individual axis of the robot. Reaching the limit of kinematic parameters of an axis is the reason that the robot cannot perform as it is programmed in the trajectory.

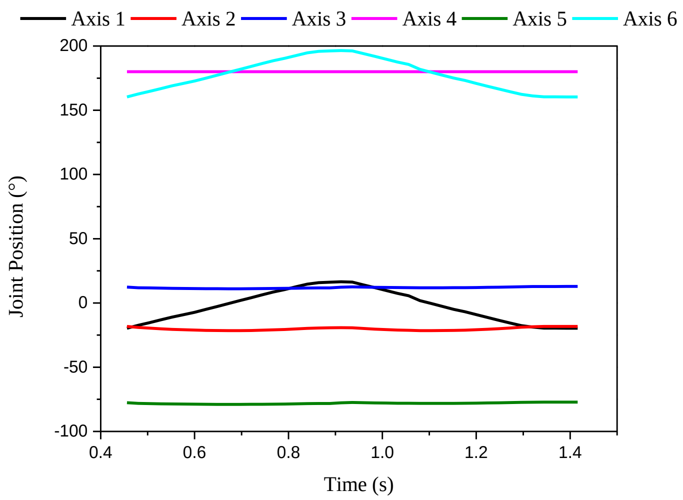

Figure 4.16 The joint position variation of each axis obtained with the optimised mounting method.

In Figure 4.16, the joint positions of axes 1, 2, 3 and axes 4, 5, 6 are presented. It was found that the joint position curves of axes 2, 3, 4, and 5 are nearly horizontally straight, which means less variation and more stable motion for these 4 axes. As for axes 1 and 6, both curves are relatively linear within their joint position limits. It can be seen that the joint motions of axes 4, 5 and 6 are largely decreased, and redistributed to axes 1 and 6. The axis motion of axis 1 is mainly used to reach the predefined TCP position, and axis 6 is for the predefined TCP orientation. The smooth joint position variations of all six axes enable the stable robot performance. Furthermore, the joint speed variation is shown in Figure 4.17, where the curves of axis 1 and axis 6 are identical and overlap each other, as well as axes 3 and 5. It can be seen that apart from axes 1 and 6, joint speed for the other four axes are maintained between -25 °/s and 25 °/s, where the joint speed of axis 4 is zero throughout the process. Apparently, by taking into account the variation of joint position and speed, the more stable and smooth motions are obtained for axes 2, 3, 4 and 5. As for axes 1 and 6, larger amplitudes of 100 °/s and 150 °/s are found for joint speed variation but within their limits of 350 °/s and 450 °/s, respectively.

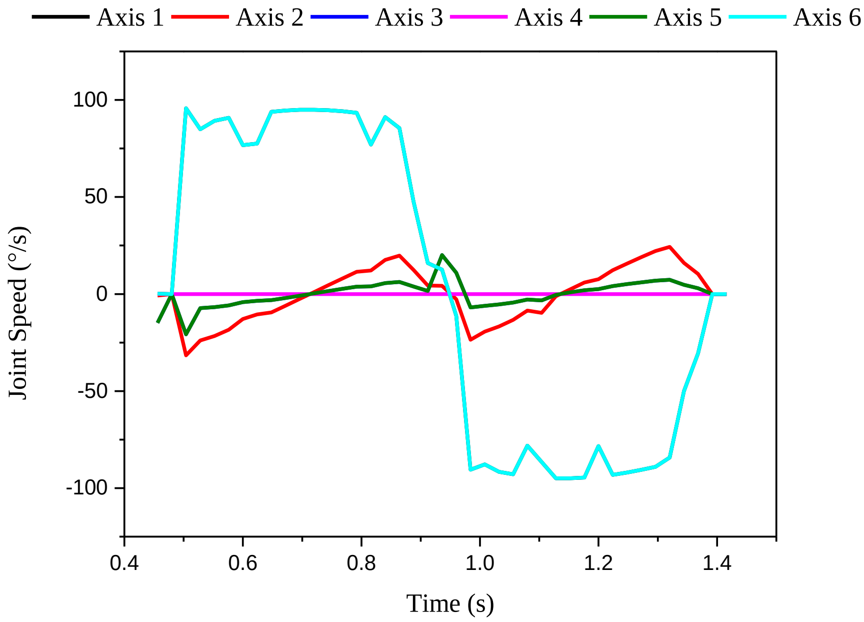

Figure 4.17 Joint speed variation of each obtained with the optimised mounting method, where axes 1 and 6, and axes 3 and 5 are identical and overlap each other.

Table 4.2 Standard deviation of effective joint speed for each axis in different paths and mounting methods.

		Axis 1	Axis 2	Axis 3	Axis 4	Axis 5	Axis 6
Path 1	Original Mounting	42.8	13.7	5.9	151.7	53.6	147.5
	Optimised Mounting	22.8	9.5	3.1	0.0	3.1	22.8
Path 2	Original Mounting	33.4	14.2	6.1	146.6	50.9	143.7
	Optimised Mounting	27.7	10.5	3.3	0.0	3.3	27.7

Compared with the joint speed by original mounting method, it is shown that more regular and stable joint speed variation is obtained for axes 1 and 6. In general, the constant TCP speed variation is based on the stabilised joint motion including the axis position and speed. Meanwhile, the joint speed variation within the substrate area for each path in the round-trip trajectory is evaluated as a standard deviation in order to see its fluctuation. As shown in Table 4.2, a more stable performance of joint motion is found for all six axes in both paths. Especially for axes 4 and 6, the standard deviation is decreased from 151.7 and 147.5 to 0 and 22.8, respectively, and the rapid fluctuations as shown in Figure 4.10 are depressed within its maximum speed limits by applying the optimised mounting method. For the rest of the axes, a stable joint speed variation is also obtained in both paths of the round-trip trajectory.

However, it is not convenient to use six values of individual axes to represent robot movement for one trajectory. In this case the average can be used to give an overall parameter. Nevertheless, the maximum performance of joints should be taken into account in the kinematic analysis. An arithmetic mean cannot describe the relative importance of each quantity on the average, so a weighted mean should be used instead. An evaluation parameter can be calculated by weighing the mean of joint speed by the maximum performance of each joint. The same value of joint speed is more important for an axis that has lower performance, and less important for an axis that has higher performance. Therefore, the weight is inversely proportional to the performance of the joint.

Table 4.3 Weights of axes by evaluating the maximum joint speed.

Axis	1	2	3	4	5	6
Weight	0.24	0.24	0.24	0.1	0.1	0.08

$$w_i = \frac{1}{p_i}(i = 1 \ldots N) \qquad \text{Eq. 4-1}$$

Where p_i is maximum axis speed of axis. Generally, the weights are normalised so that they sum up to 1. A factor is needed to normalise the sum of weight, which is decided by

$$f = \frac{1}{\sum_{i=1}^{N} w_i}(i = 1 \ldots N) \qquad \text{Eq. 4-2}$$

The weight can be rewritten

$$w_i = \frac{f}{p_i} = \frac{1}{\sum_{i=1}^{N} w_i \cdot p_i}(i = 1 \ldots N) \qquad \text{Eq. 4-3}$$

For such normalised weights, the weighted mean is simply

$$\bar{x} = \sum_{i=1}^{N} w_i x_i \qquad \text{Eq. 4-4}$$

Where

$$\sum_{i=1}^{N} w_i = 1 \quad \text{Eq. 4-5}$$

Table 4.4 Overall parameters of standard deviation of effective joint speed for different mounting methods.

Trajectory	Mounting Method	Overall Parameter (°/s)	Improvement (%)
Path 1	Original	47.31	77.55
	Optimised	10.62	
Path 2	Original	44.11	71.68
	Optimised	12.49	

By applying the weights of each axis in Table 4.3 and the standard deviation of joint speed of each axis in Table 4.2, the comparison of overall parameters between different mounting methods is listed in Table 4.4. It shows that by applying the optimised mounting, the overall parameter is decreased from 47.31 °/s to 10.62 °/s for Path 1 and from 44.11 °/s to 12.49 °/s for Path 2, respectively. The results show that the optimised mounting method has a much lower overall parameter than the original mounting method (77.55% less for Path 1 and 71.68% for Path 2), which means that the stability of the joint motion is notably improved. As a result, by redistribution of axis motion and optimisation of spray nozzle mounting, the improvement of robot performance and TCP speed stability were achieved based on stable joint motion.

Meanwhile, the total energy consumption of the robot was also compared between the original and optimised mounting method, which is shown in Figure 4.14. The total energy consumption of the robot is the sum of the instantaneous power for each joint and estimated power of the controller cabinet, which was obtained by the signal collection function in RobtoStudio™ during the process simulation. It can be seen that the energy consumption decreased from 403.2 J to 159.5 J (60.44% less) by using the optimised mounting method. By taking into account the joint position and speed variation, it was found that a stable and smooth joint motion brings a lighter load for the servomotor. However, a rapidly changing joint speed variation, as shown in Figure 4.10, requires a series of accelerations and decelerations for servomotors, which brings more energy consumption to achieve these complex and irregular joint motions. Additionally, the process simulation shows that the process duration decreased from 1.224 s to 0.96 s by applying the optimised nozzle mounting method, which was due to the stabilisation of the nozzle speed within the substrate area and robot performance. Less fluctuation of the TCP speed and joint motion can efficiently reduce the trajectory process duration. In order to evaluate the energy consumption of the whole spray process on the entire workpiece with two different nozzle mounting methods, the complete robot trajectory was simulated. It was found that the energy consumption difference in the single round-trip trajectory case was largely magnified in the whole spray process. The total energy consumption of the whole spray process was depressed from 2720.0 J to 1748.2 J by applying the optimised the nozzle mounting method. It can be seen that in the case of a larger and more complex trajectory, the energy savings will be more obvious. Thus, it can be concluded that by optimising the nozzle mounting method, both the robot energy consumption and process duration are largely economised, which can also contribute to the saving of feedstock and thermal spray system energy consumption such as heating system and driving gas.

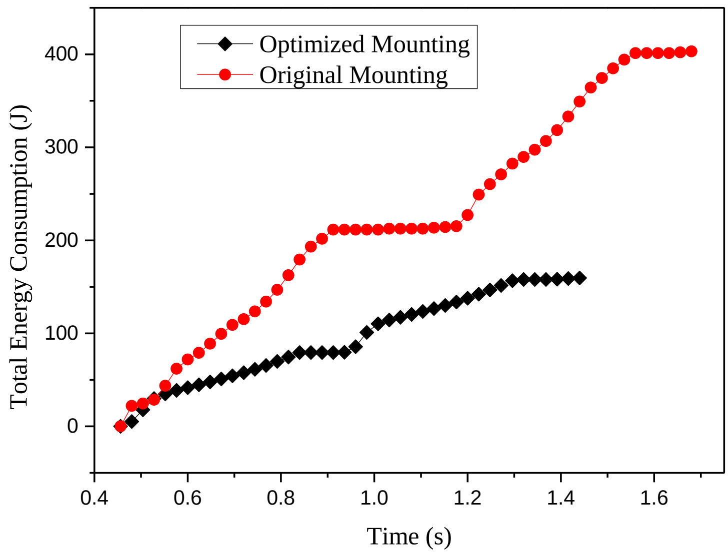

Figure 4.18 Comparison of robot total energy consumption between original (black line) and optimised (red line) nozzle mounting methods.

4.2.4 Discussion

The robot performance and kinematic analysis of the single round-trip trajectory on a plane workpiece were performed. The kinematic analysis results show that the optimised nozzle mounting method can largely improve the stability of the TCP speed, as well as the joint motion of each axis. In order to further evaluate the effects of the optimised mounting method in other thermal spray cases other than the plane workpiece studied above, process simulation and kinematic analysis were carried out on another workpiece with a curved surface. As shown in Figure 4.19, a round-trip trajectory is generated on the free-form workpiece, where the spray angle of each target point is kept at 90° so that the nozzle is always perpendicular to the workpiece. The other operating parameters are the same as the planar workpiece case.

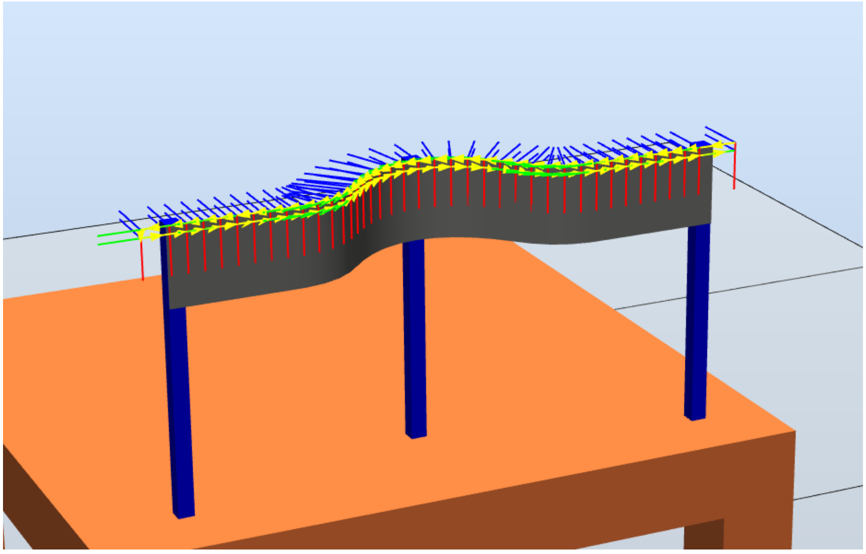

Figure 4.19 Round-trip trajectory and its target points on a free-form workpiece.

The results show that the average TCP speed was significantly improved from 502.8 mm/s to 879.8 mm/s by applying the optimised nozzle mounting method. While evaluating the joint motion of each axis, it was found that the workload was largely transferred from axes 4 and 5 to the other axis with the optimised mounting method. Due to the necessity to adapt the curvature change of the workpiece surface, large joint motion of axis 6 cannot be avoided. With the original mounting method, axes 4, 5 and 6 are all involved to adapt the TCP orientation at each target point, which caused great amount of joint motion. By evaluating the overall parameter that describes the joint motion in Equation (1), it was found that the value decreased from 36.720 °/s to 28.856 °/s. As a result, according to the overall parameter and the average TCP speed, the robot performance largely improved by reasonable distribution of the axis joint based on optimised nozzle mounting. Meanwhile, the total energy consumption of the process was depressed from 451.587 J to 286.474 J by applying the optimised mounting method, which demonstrated that the joint motion optimisation can contribute a lot to the energy saving. In summary, it can be seen that in the case of free-form workpiece, the application of optimised nozzle mounting method can also contribute to the improvement of robot performance in terms of average TCP speed and joint motion of axes.

4.3 Workpiece placement optimisation

As mentioned in previous sections, there are several methods for the purposes of kinematic optimisation, varying from the kinematic parameters optimisation, torch setup optimisation to target position optimisation. It can be seen that the torch setup optimisation can solve the problem of speed fluctuation in thermal spray. But if the torch and its assembly cannot be changed, it is necessary to look for other solutions. In this section, kinematic analysis will be made in order to find an optimised placement of the workpiece on the worktable.

4.3.1 Simulation model

The common case presented at the beginning of this part will be used as a simulation example to demonstrate the kinematic optimisation of workpiece placement (Figure 4.3). For the study purpose, a simple round-trip pass was created on the workpiece and simulated in RobotStudio™. The length of scanning was 400 mm, the predefined TCP speed was 500 mm/s. The real TCP speed was then recorded by the analyser module of RobotStudio™. Figure 4.4 shows the TCP speed in the simulation. There is a fluctuation in the TCP speed around the predefined value of 500 mm/s, where the speed varied from 485.3 mm/s to 515.4 mm/s. As is known, the deposit properties such as coating structure and surface profile (e.g. coating thickness, coating roughness) are highly influenced by the scanning speed. For a better coating quality, the scanning speed of the torch should be constant. Therefore, it is necessary to optimise the trajectory based on simulation results and kinematic analysis during the process of off-line programming stage.

To find out the best placement of the workpiece, the robot trajectory on the different positions of the worktable should be investigated. In this case, the worktable is 910 mm in length, 910 mm in width and symmetrical to the X-axis of the robot. Also, the spray gun is fixed in the middle of the end-effector. Consequently, the movements on two sides of the worktable are mirror-symmetrical and the kinematic studies need only be carried out on half of the worktable. For example, there are two mirror points on the worktable P1 (850, 200, 900) and P2 (850, -200, 900), six joint values of these points are J1 (23.36, -28.48, 25.23, 45.38, -33.86, -40.08) and J2 (-23.36, -28.48, 25.23, -45.38, -33.86, 40.08). It can be seen that the values of joint1, joint4 and joint6 are opposite on these two mirrored points.

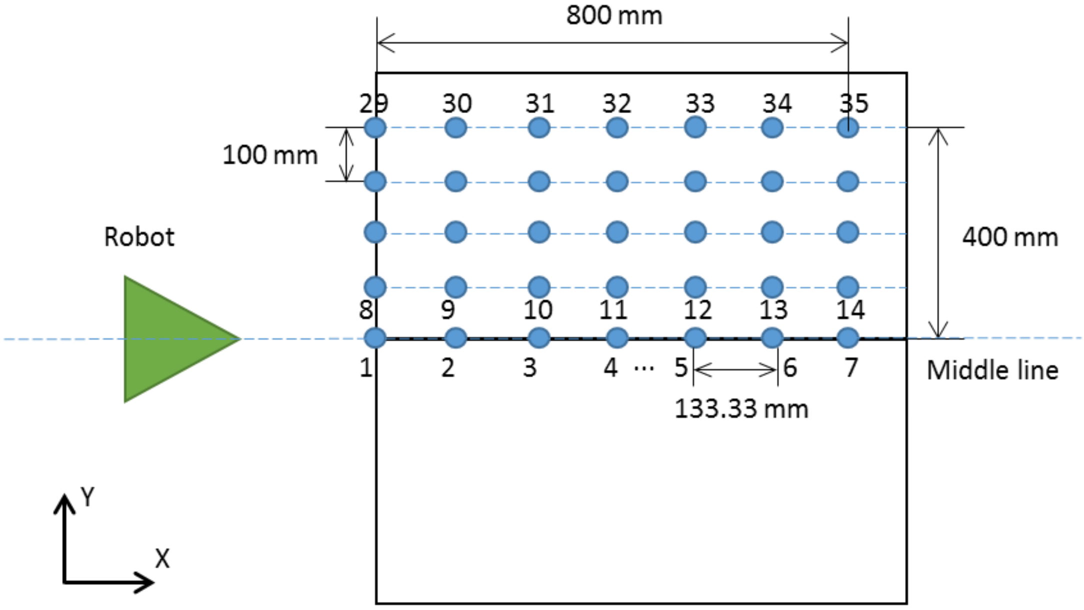

Figure 4.20 Positions chosen for kinematic analysis.

In order to find the laws of robot kinematics regarding the workpiece's position, a series of positions on the worktable were chosen. The zone to be evaluated was defined in a rectangle of 400 mm by 800 mm. Seven equidistant points were arranged along the X-axis and five equidistant points were arranged along the Y-axis from the middle line of the worktable. Figure 4.20 shows the grid and all 35 points on one half of the worktable. The interval between the horizontal points (along the X-axis) was 133.33 mm; for the vertical points, it was 100 mm. After choosing these positions to test, the workpiece was then placed on these positions in order to simulate the robot trajectory and record the joint positions during the movement.

4.3.2 Joint position and joint speed

Based on the robot kinematic theory, the action of the robot is a combination of six individual axes; any complex action such as moving the torch from one point to another can be decomposed in a series of axis motions [24]. Figure 4.21 shows six joint profiles versus time recorded during the movement simulation on position1 of the worktable. It can be observed that axes 1, 4 and 6 have large actions when the robot performs this trajectory. For example, axis 4 changed from +45.2° to -45.1° in 0.838 s and axis 6 varies from -39.9° to +39.5° in the same period.

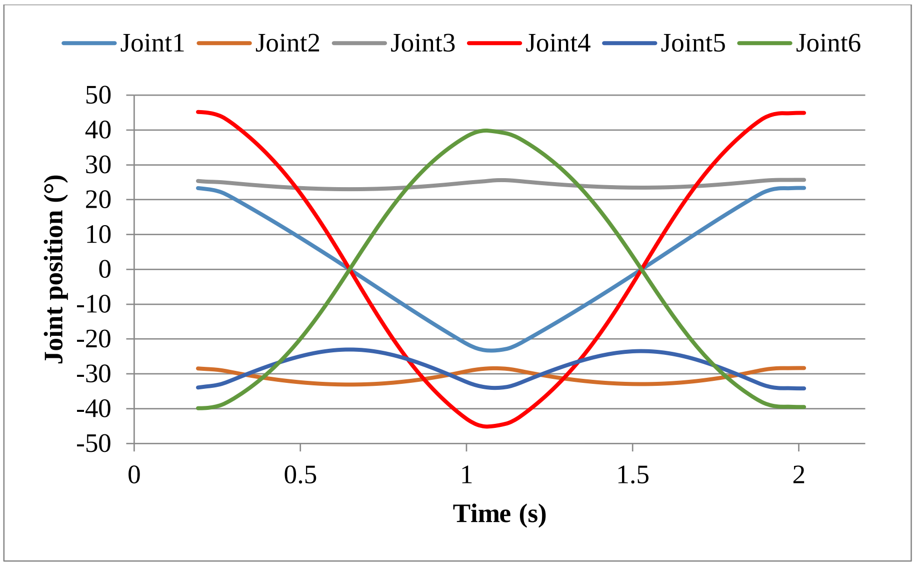

Figure 4.21 Record of joint position.

The robot manipulator consists of a series of links connected by revolute joints. With the direct kinematics, the position and orientation of the end effector can be calculated as a function of the joint variables [25]. Therefore, the instantaneous joint values decide the position and orientation of the TCP, but cannot describe the characteristics of the movement. However, the joint speed represents the variation of the joint position in a certain period, which permits the description of movement for each axis. A high joint speed signifies that the joint performs a relatively large rotation in a given amount of time, while a slow-moving joint performs a relatively small amount of rotation in the same amount of time. In mathematical terms, the angular speed s is defined as the magnitude of the angular speed ω. In this way the joint speeds of each axis were calculated. Generally, we can find the maximum angular speed and working range of each axis from the product specification of the robot. Compared with the robot performance, the joint position and joint speed in the recorded movement are all under limit values. Consequently, the spray trajectory can be performed with a little fluctuation on the TCP speed.

4.3.3 Variance of joint speed

In the robot controller, a motion such as a linear movement between two points is decomposed into a time history of position, speed and acceleration for each joint. For example, the linear movement from P1 to P2 is firstly interpolated by several intermediary points. Inverse kinematics is then performed to determine the joint angles that provide the position of the TCP on those intermediary points. The speed profiles by time for each joint are planned and then interpreted into the control commands, which will be sent to servomotors. Thus, a robot trajectory is generated.

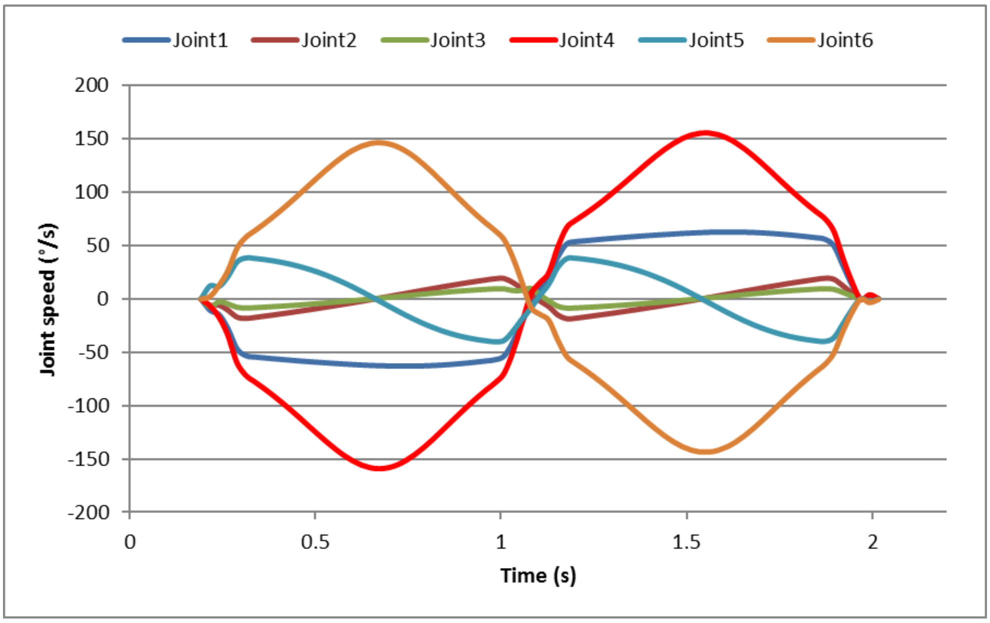

Figure 4.22 Joint speed curves on position1

For the robot system, servomotors consume energy to overcome their inertia and mechanical friction to realise the predefined trajectory. Therefore, a steadier speed profile means more simple motion commands and less energy consumption. A moving object at uniform speed is easier to control than a moving object at variable speed when travelling the same distance. Regarding energy, the acceleration and deceleration of a moving object will lead to additional energy consumption and mechanical wear [4, 26]. As a result, the speed variation can be used as an evaluation parameter to represent the simplicity of the movement for an axis. Less variation signifies that the joint motion is more constant and more uniform so that the controller can respect the speed profile more easily, which leads to less energy consumption.

In statistics and probability theory, the variance is a measure of how far a set of numbers is spread out, and the standard deviation shows how much variation or dispersion exists from the average. Therefore, the standard deviation of joint speed was selected to evaluate the simplicity of the movement for an axis. The standard deviation of joint speed for each axis was calculated and is listed in Table 4.5. It can be seen that axes 4 and 6 have a higher standard deviation of joint speed, which is confirmed by the curves of joint speed in Figure 4.22.

In this case, the overall parameter presented in the previous section is used to evaluate the robot kinematics. The weighted overall parameter for evaluating the movement of joints on position1 was 38.37 °/s.

Table 4.5 Standard deviation of joint speed (position 1).

Axis	1	2	3	4	5	6
Stand deviation of joint speed (°/s)	53.75	11.63	5.80	108.64	26.60	97.01

4.3.4 Analysis Results

To explore the regular pattern of robot kinematics as a function of the position of the workpiece on the worktable, the analysis methods mentioned above were used to evaluate the robot kinematics on all 35 positions of the worktable. A single value, the so-called weighted mean of the standard deviation of joint speed, was used as the overall parameter (OP) of kinematics in this investigation. The workpiece was placed on all the test positions to simulate the trajectory, and the corresponding OPs were calculated. Table 4.6 lists the OPs for all test positions of the worktable. In order to study the trends of the kinematics, these data were plotted in a graph. The data that have the same value of the Y-axis were drawn as a curve; so, all the data were plotted in five curves of different values of the Y-axis (see Figure 4.23). It can be noted that all the curves have the same tendency—the OP is higher when the workpiece is close to the robot. As the distance from the robot (value of X-axis) increases, the OP decreases. When the distance to the robot exceeds a certain value (approximately 667 mm in this case) the OP will increase slightly. When comparing the five curves in the graph, it can be observed that the OPs of two curves (Y=0 mm and Y=100 mm) have the highest value when the workpiece is placed on the nearest location to the robot (X=0 mm). This situation continues until X approaches 466 mm because the robot trajectory passes through the middle line of the worktable, which is also the symmetry axis of the robot. When the robot crosses the symmetry axis (which is also called singularity position), the movements of axes 4 and axis 6 are in a state of mutual coupling compensation that increases the standard deviation of the joint speed.

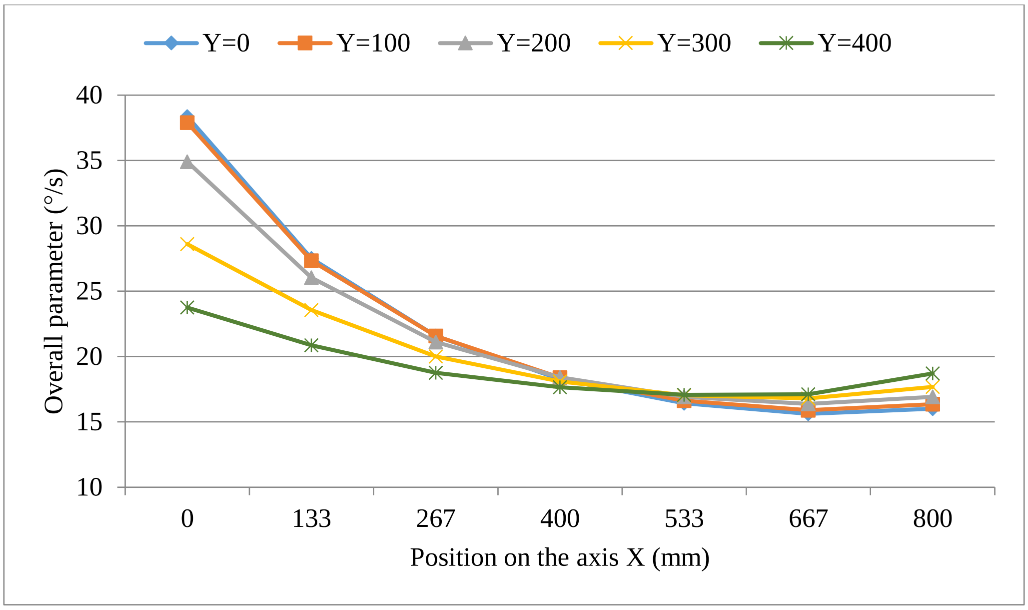

Figure 4.23 Overall parameters of test points on the worktable.

Table 4.6 Overall parameters of kinematics on the test points.

X (mm) Y (mm)	0	133	267	400	533	667	800
0	38.37	27.51	21.59	18.27	16.42	15.62	16.01
100	37.89	27.32	21.58	18.40	16.63	15.90	16.36
200	34.90	26.04	21.10	18.40	16.92	16.38	16.92
300	28.60	23.57	20.01	18.10	17.04	16.80	17.68
400	23.75	20.87	18.75	17.65	17.07	17.12	18.70

In fact, when the position along the X-axis exceeds approximately 400 mm, there are no obvious differences between the five positions along the Y-axis. These positions can be considered as acceptable. To prevent the robot working at the limit of its working envelope, the positions in the middle of the worktable should be chosen to be as far as possible. When comparing all the curves in Figure 4.23, the curve where Y=0 has a lower OP than the others when the value along the X-axis exceeds about 466 mm. Thus, this curve was chosen to find the lowest OP versus the value of X.

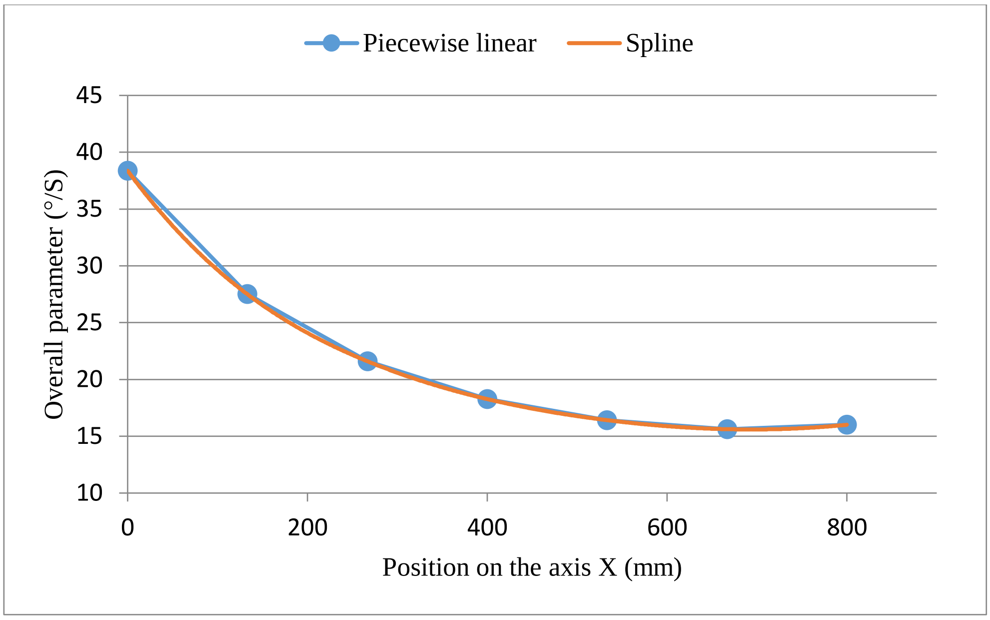

Figure 4.24 Curve interpolation.

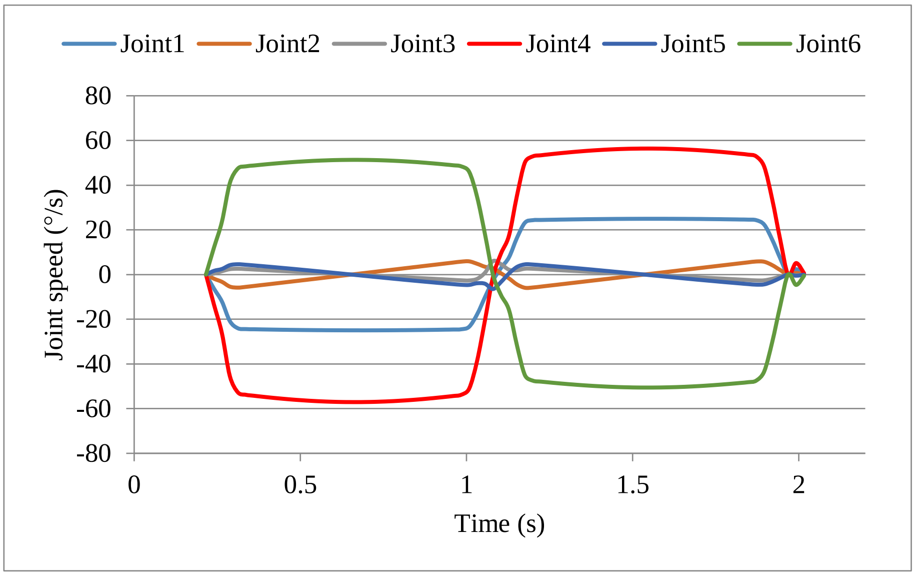

Figure 4.25 Joint speed of joints on the position Y=694 mm.

In order to verify the correctness of this result, a simulation where the workpiece was placed at 694 mm from the edge of the worktable was carried out. Six joint profiles were recorded and analysed with the above method (see Figure 4.25). The real OP was 15.67 °/s, and the relative error corresponding to the predictive value was only 0.51%. The TCP speed during the spray process was verified as well. Figure 4.26 shows the TCP speed on this optimised position in the simulation. It can be noted that the scanning speed is more constant than the speed on the original position (see Figure 4.4). The scanning speed on the best position varies from 498.2 mm/s to 501.5 mm/s, whereas the speed on the original position fluctuated from 485.3mm/s to 515.4 mm/s. There is an astounding 89% increase of speed uniformity in this case. Consequently, this method was confirmed to find the best placement of the workpiece in a limited work space.

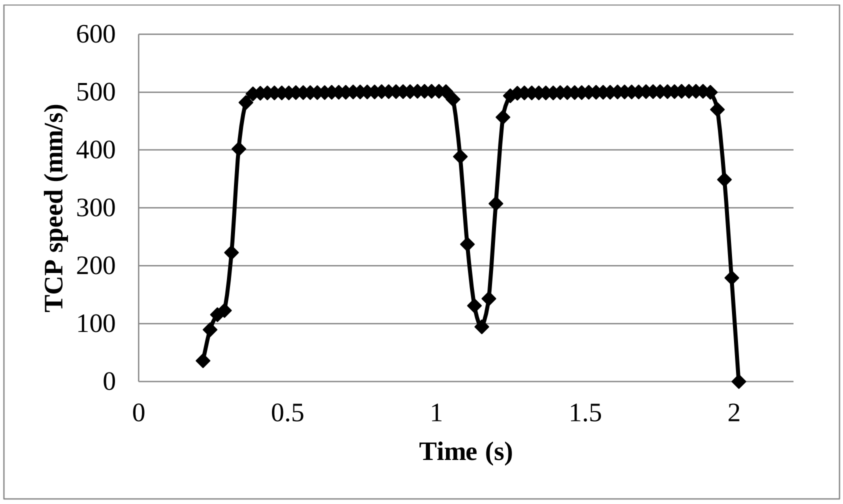

Figure 4.26 Optimised TCP speed.

4.4 Conclusion

With the rapid development of industrial manufacturing and processing technology in different fields, more and more requirements are put forward for the application of industrial robots. Thus, the procedure of robot application in industry has become a hot research topic, which includes the trajectory planning, robot programming, process simulation, kinematic analysis and optimisation, coordinates calibration, programme synchronisation and execution tests. Among these possibilities for robot application, the aspects of trajectory generation and kinematic optimisation can directly improve robot performance.

Firstly, based on practical experience, kinematic analysis was used to investigate the optimised mounting method of spray nozzle on the robot. A rectangle workpiece is used to investigate robot motion in the thermal spraying process. The kinematic parameters such as TCP speed, joint position and the speed of each axis are used to evaluate the robot performance. The statistic processing method such as average value, maximum error, variance and standard deviation are chosen to evaluate the kinematic parameters. The kinematics analysis shows that with the original mounting method, a large fluctuation of TCP speed happens due to the instability of joint motions including its position and speed. This study proposes an optimised mounting method from the point of view of the thermal spraying theory and robot kinematics, in order to reasonably redistribute the workload among all six axes. The results show that the optimised mounting method can obtain a stable TCP speed variation at the predefined value.

The analysis in terms of joint motion shows that constant and stable joint motion leads to less friction and workload on the servomotor of each axis, which leads to a better robot performance. Meanwhile, the energy consumption comparison shows that by reasonably redistributing joint motion, much less energy is consumed, including by each joint servomotor and controller cabinet. The process duration is also reduced by optimising the nozzle mounting method, which can contribute to the thermal spray energy consumption saving including by the driving gas and heat system. As a result, this proposed analysis method and optimised mounting method can be used for the optimisation of robot performance and its trajectory in the field of thermal spraying with offline programming.

Secondly, the kinematic analyses of the robot were also used to investigate the relationships between the placement of workpiece and the movement of robot on this position. In this approach the weighted mean of the standard deviation of joint speed was selected as an overall parameter (OP) to measure the complexity of a robot trajectory. By using the spline interpolation on the recorded data, the best placement of workpiece on the limited zone of the worktable was finally decided. The result was then checked and confirmed by the trajectory simulation on this position, so this approach was proved to be feasible and applicable for the optimisation of robot trajectory in the stage of off-line programming for thermal spraying applications.

References

1. S. Deng, H. Li, H. Liao, C. Coddet, and C. Zeng, New Functions of Thermal Spray Toolkit A Software Developed for Off-line and Rapid Robot Programming. *International Thermal Spray Conference*. 2006 (Seattle, USA). 2006. p 1437-1442.
2. D. Fang, S. Deng, H. Liao, and C. Coddet, The Improvements of Thermal Spray Toolkit, Extended Software for Robotic Off-Line Programming. *International Thermal Spray Conference.* 2010 (Singapore). 2010. p 522-526.
3. F.J. Abu-Dakka, F. Rubio, F. Valero, and V. Mata, Evolutionary indirect approach to solving trajectory planning problem for industrial robots operating in workspaces with obstacles. *European Journal of Mechanics-A/Solids*, 2013. **42**, p 210-218.
4. R. Saravanan, S. Ramabalan, and C. Balamurugan, Evolutionary multi-criteria trajectory modeling of industrial robots in the presence of obstacles. *Eng Appl Artif Intel*, 2009. **22**(2), p 329-342.
5. T. Chettibi, H. Lehtihet, M. Haddad, and S. Hanchi, Minimum cost trajectory planning for industrial robots. *European Journal of Mechanics-A/Solids*, 2004. **23**(4), p 703-715.
6. S.F. Saramago and M. Ceccarelli, Effect of basic numerical parameters on a path planning of robots taking into account actuating energy. *Mech Mach Theory*, 2004. **39**(3), p 247-260.
7. S. Deng, Z. Cai, D. Fang, H. Liao, and G. Montavon, Application of robot offline programming in thermal spraying. *Surf Coat Technol*, 2012. **206**(19-20), p 3875-3882.
8. T. Vivekanandhan, A. Kashani, and R. Echempati, Computer-aided Torch Trajectory Generation for Automated Coating of Parts with Complex Surfaces. *J Therm Spray Technol*, 1994. **3**(2), p 208-215.
9. Z. Cai, S. Deng, H. Liao, C. Zeng, and G. Montavon, The Effect of Spray Distance and Scanning Step on the Coating Thickness Uniformity in Cold Spray Process. *J Therm Spray Technol*, 2014. **23**(3), p 354-362.
10. A. Hansbo and P. Nylén, Models for the simulation of spray deposition and robot motion optimization in thermal spraying of rotating objects. *Surf Coat Technol*, 1999. **122**(2–3), p 191-201.
11. S. Leigh and C. Berndt, Evaluation of off-angle thermal spray. *Surf Coat Technol*, 1997. **89**(3), p 213-224.
12. A. Kout and H. Müller, Parameter optimization for spray coating. *Adv Eng Softw*, 2009.

40(10), p 1078-1086.

13. O. Stier, Fundamental Cost Analysis of Cold Spray. *J Therm Spray Technol*, 2014. **23**(1-2), p 131-139.
14. W. Wong, E. Irissou, A. Ryabinin, J.-G. Legoux, and S. Yue, Influence of Helium and Nitrogen Gases on the Properties of Cold Gas Dynamic Sprayed Pure Titanium Coatings. *J Therm Spray Technol*, 2011. **20**(1-2), p 213-226.
15. M. Fasching, F. Prinz, and L. Weiss, Planning robotic trajectories for thermal spray shape deposition. *J Therm Spray Technol*, 1993. **2**(1), p 45-57.
16. S. Deng, H. Liang, Z. Cai, H. Liao, and G. Montavon, Kinematic Optimization of Robot Trajectories for Thermal Spray Coating Application. *J Therm Spray Technol*, 2014, p 1-8.
17. S. Deng, D. Fang, Z. Cai, H. Liao, and G. Montavon, Application of External Axis in Robot-Assisted Thermal Spraying. *J Therm Spray Technol*, 2012. **21**(6), p 1203-1215.
18. N. Cinca, A. List, F. Gärtner, J.M. Guilemany, and T. Klassen, Influence of spraying parameters on cold gas spraying of iron aluminide intermetallics. *Surf Coat Technol*, 2015. **268**, p 99-107.
19. M. Fukumoto, H. Wada, K. Tanabe, M. Yamada, E. Yamaguchi, A. Niwa, M. Sugimoto, and M. Izawa, Effect of substrate temperature on deposition behavior of copper particles on substrate surfaces in the cold spray process. *J Therm Spray Technol*, 2007. **16**(5-6), p 643-650.
20. J.-G. Legoux, E. Irissou, and C. Moreau, Effect of substrate temperature on the formation mechanism of cold-sprayed aluminum, zinc and tin coatings. *J Therm Spray Technol*, 2007. **16**(5-6), p 619-626.
21. S. Rech, A. Trentin, S. Vezzù, J.-G. Legoux, E. Irissou, and M. Guagliano, Influence of pre-heated Al 6061 substrate temperature on the residual stresses of multipass Al coatings deposited by cold spray. *J Therm Spray Technol*, 2011. **20**(1-2), p 243-251.
22. D. Fang, S. Deng, H. Liao, and C. Coddet. Automatic generation of robot trajectory for free-form surfaces in thermal spraying. *Thermal Spray 2011: Proceedings of the International Thermal Spray Conference*. 2011 (Hamburg, Germany). 2011. p 1110-1114.
23. S. Dong, B. Song, H. Liao, and C. Coddet, Deposition of NiCrBSi coatings by atmospheric plasma spraying and dry-ice blasting: Microstructure and wear resistance. *Surf Coat Technol*, 2015. **268**, p 36-45.
24. L.-W. Tsai, The mechanics of serial and parallel manipulators. *New York, NY: J Wiley*

and Sons, ISBN 0-471-32593-7, 1999.

25. A.P. Pashkevich, A.B. Dolgui, and K.I. Semkin, Kinematic aspects of a robot-positioner system in an arc welding application. *Control Engineering Practice*, 2003. **11**(6), p 633-647.

26. X.F. Zha, Optimal pose trajectory planning for robot manipulators. *Mech Mach Theory*, 2002. **37**(10), p 1063-1086.

Chapter 5

Conclusion and prospects

5.1 Conclusion

After more than 10 years of research, a mature and complete off-line programming assistant system has been developed for the thermal spray process in the laboratory LERMPS of UTBM. According to the work by Deng, Fang and Cai, functions such as trajectory generation, coating thickness simulation and real-time trajectory monitoring have already been realised. Based on previous work, this thesis aims to further discuss the application of off-line programming in the thermal spray process.

Generally, the application of off-line programming technology in the thermal spray process consists of several steps from the generation to the optimisation of trajectory. First of all, the robot trajectory is generated off-line according to the substrate sharp and spray strategy. Secondly, the generated trajectory is simulated by the virtual robot system in RobotStudio™. Thus, it is able to simulate the coating thickness according to the robot kinematic data and the generated trajectory. At the same time, the robot kinematic optimisation can be carried out by performing the kinematic analysis. Based on the aspects mentioned above, theoretical, numerical and experimental work were made in this thesis to further study the application of the off-line programming method in the thermal spray process. The details of the conclusion are listed as below.

1. Trajectory generation

The trajectory generation through the off-line programming method was presented. Firstly, the TST is embedded as a ribbon in the RobotStudio™, which gives a unified user interface as same as other default functionalities. Meanwhile, a few improvements have been made. The meander trajectory for defect repair or workpiece pre-heating was also developed, which can save powder consumption by avoiding excess deposition outside the strict area. Furthermore, in order to maintain a constant scan step, an improvement in the trajectory generation algorithm for the curved substrate surface was developed. In the optimised algorithm, the direction of the orthogonal surface corresponds to the substrate curvature.

Secondly, a novel Archimedean spiral trajectory was developed for damage component recovery applications by the cold spray system. Combined with the scaling method, the spiral trajectory was generated based on the defect area contour, which can decrease material waste outside the recovery area. Furthermore, the nozzle speed was adapted according to the crater depth, which enables the progressive change of coating thickness based on the variation of crater depth. The experiment of an Al5056 coating depositing on a manually manufactured workpiece with a crater defect was carried out to validate the effects of spiral trajectory with an adapted nozzle speed. The experimental results showed that cold sprayed Al5056 coating had fully filled the crater area on the substrate in accordance with its contour. No excessive deposition was found outside the defect contour. The coating surface profile obtained by Profilometer measurements showed that a flat coating surface was achieved by adapted nozzle speed. Compared with the round-trip trajectory, the Archimedean spiral trajectory can significantly save process duration as well as the consumption of powder and spray system energy, which leads to the increase in spray efficiency.

Both cross-section morphology obtained from different areas show an Al5056 coating with high density and low porosity. By evaluating the bonding strength at different spray angles, it was found that the spray angle has little effect on Al5056 coating. It can be concluded that the proposed spiral trajectory is an efficient way for the application of damage component recovery and additive manufacturing with cold spray technology. With the scaling method, an Archimedean spiral trajectory can be further applied to the repair of defects with other irregular shapes.

2. Coating thickness simulation

A numerical model of a single coating profile based on standard experimental results was established, which included the effects of spray angle, nozzle traverse speed as well as scanning step. According to the experimental studies of cold sprayed Al5056 coating by single nozzle path, the numerical model was well validated. Afterwards, a coating thickness model was developed based on the single coating profile model, which enables the thickness distribution on an entire substrate surface. It includes the effects of kinematic parameters such as spray angle, nozzle traverse speed, scanning step and so on. Based on the model above, the coating thickness simulation module was developed and integrated into the add-in software TST as a part of ProfileKit. Two functions are included in ProfileKit: simulation of coating profile in 2D and coating thickness distribution in 3D. ProfileKit 2D, by altering the operating parameters, is able to simulate the coating profile and optimise the operating parameters. In the ProfileKit 3D, the coating thickness distribution can be simulated based on the nozzle trajectory on the substrate surface and robot kinematics data by process simulation in RobotStudio™. The functionality of ProfileKit 2D and 3D were validated respectively by the trapezoid cold sprayed coating with a changing scanning step. It can be concluded that with ProfileKit 2D and 3D, coating thickness can be simulated and predicted, which also provides evidence to optimise the operating parameters, nozzle trajectory and spray strategy.

3. Trajectory optimisation

Considering the increasing requirement for robot performance and coating quality, the trajectory generation, kinematic analysis and trajectory optimisation are becoming hot topics in this field of industry. As mentioned previously, a solution for trajectory generation dedicated to workpieces with different geometries has been developed. Although trajectory generation takes into account of the operating parameters and spray strategy, robot performance still seems to be limited in some cases, which will directly affect the coating quality. Therefore, in this part, kinematic optimisation is introduced for the robot's application in the thermal spraying process. An investigation into the robot kinematics is proposed to find the rules of motion in an application case. The results demonstrate the motion behaviour of each axis in the robot, which identifies the motion problems in the trajectory. This approach optimises the robot trajectory in a limited working envelope. Therefore, different approaches of kinematic optimisation were introduced to improve the robot performance and coating quality. They took into account of the torch setup and workpiece placement on the worktable. As a powerful tool provided by the off-line programming software, the kinematic analysis is used to evaluate the robot performance, which includes the motion of each axis, the TCP speed, cycle time, etc.

5.2 Prospects

In this work, an Archimedean spiral trajectory is proposed for the purpose of damage repair by cold spray technology. Due to the unique advantages of cold spray, the application in additive manufacturing and damage repair is attracting more and more attention. Firstly, optimisation of the current spiral trajectory should be made to obtain a more uniform coating thickness distribution, which can largely decrease the post-machinery work. Secondly, more effort should be made to optimise the robot trajectory for damage repair accounting for the influences of robot kinematics on coating quality. The effects of robot kinematics and robot trajectory on the as-repaired coating quality under different power-substrate combination are also worth considering. Lastly, a robot trajectory specially designed for the repair of defect with complex contour can be expected.

The ProfileKit in 3D is proposed in this work for the purpose of coating thickness distribution in 3D based on kinematic data. However, some improvements can still be made to optimise the functionality of software as well as its stability. Firstly, the algorithm of the simulation model should be extended to complex a workpiece with a curved surface, which is limited to a planar workpiece in the current version. Secondly, the code in the programme as well as the algorithm should be further optimised to improve its robustness and simplification. Finally, finite element analysis focusing on thermal and mechanical evolution based on the coating transient build-up process can be expected. By taking into account the transient coating build-up process via the current coating thickness model, a more realistic thermo-mechanical model can be developed and dedicated to the study of coating quality.

As for the kinematic optimization of nozzle mounting method in thermal spray, more efforts should be made to study the optimization effects in different spray conditions, such as the geometry of workpiece, the nozzle type, the operating parameters and so on. Meanwhile, the experimental study should be made to study the influence of mounting method optimization on the coating quality such as porosity, thickness, microstructure, bonding strength and so on.

Chapter 6

Annexes

Annex 1 List of publications and conferences

Publications:

- **Chaoyue Chen**, Hanlin Liao, Ghislain Montavon, and Sihao Deng, Nozzle Mounting Method Optimization Based on Robot Kinematic Analysis, *Journal of Thermal Spray Technology*, 25 (2016), 1138-48.
- **Chaoyue Chen**, Yingchun Xie, Shuo Yin, Marie-Pierre Planche, Sihao Deng, Rocco Lupoi, and Hanlin Liao, Evaluation of the Interfacial Bonding between Particles and Substrate in Angular Cold Spray, *Materials Letters*, 173 (2016), 76-79.
- **Chaoyue Chen**, Yingchun Xie, Christophe. Verdy, Hanlin Liao, Sihao Deng, Modelling of cold spray coating profile and its application in offline programming software, *Surface and Coatings Technology*, (2016), Accepted.
- **Chaoyue Chen**, Sébastien GOJON, Yingchun Xie, Yin Shuo, Sihao Deng, Christophe Verdy, Hanlin Liao, A novel spiral trajectory for damage component recovery with cold spray, *Surface and Coatings Technology*, (2016), Accepted.
- **Chaoyue Chen**, Yingchun Xie, Marie-Pierre Planche, Sihao Deng, Hanlin Liao, Investigation of particle/substrate bonding between copper powder and different substrates in cold spray, *Journal of Materials Science*, in revision.
- Sihao Deng and **Chaoyue CHEN**, Generation of Robot Trajectory for Thermal Spray in Robot Kinematics and Motion Planning, W. Adams, Editor. 2015, Nova Science Publisher. p. 103-142.
- Sihao Deng and **Chaoyue CHEN**, Kinematic Analysis of Robot Trajectory for Thermal Spray, in Robot Kinematics and Motion Planning, W. Adams, Editor. 2015, Nova Science Publisher. p. 143-180.
- Yingchun Xie, **Chaoyue Chen (Equal contribution)**, Marie-Pierre Planche, Sihao Deng, Hanlin Liao, Effect of spray angle on Ni particle deposition behavior in cold spray, *Journal of Materials Science and Technology*, in revision.
- Nan Kang, Pierre Coddet, **Chaoyue Chen**, Yan Wang, Hanlin Liao, and Christian Coddet, Microstructure and Wear Behavior of in-Situ Hypereutectic Al–High Si Alloys Produced by Selective Laser Melting, *Materials & Design*, 99 (2016), 120-26.
- Yingchun Xie, Shuo Yin, **Chaoyue Chen**, Marie-Pierre Planche, Hanlin Liao, and Rocco Lupoi, New Insights into the Coating/Substrate Interfacial Bonding Mechanism in Cold Spray, *Scripta Materialia*, 125 (2016), 1-4.

Conferences:

- **Chaoyue Chen**, Sihao Deng, Hanlin Liao, and Ghislain Montavon, 'Robot Kinematic Analysis for Torch Setup Optimization in Thermal Spraying', Oral presentation in Thermal Spray 2015: Proceedings of the International Thermal Spray Conference (Long Beach, California, USA: ASM International, 2015), pp. 647 - 53 (7).
- **Chaoyue Chen**, Sébastien GOJON, Sihao DENG, Christophe VERDY, Hanlin LIAO, ‘A novel approach of trajectory generation for damage components recovery by cold spray’. Oral presentation in Processing of the 7th RIPT (Limoges, France 2015).
- **Chaoyue Chen**, Yingchun XIE, Christophe Verdy, Sihao Deng, and Hanlin Liao, 'Modelling of Cold Spray Coating Profile and Its Application in Offline Programming Software', Oral presentation in Thermal Spray 2016: Proceedings of the International Thermal Spray Conference (Shanghai, China: 2016).

Annex 2 Signal analyzer by API in RobotStudio™

In order to realize the communication between the virtual robot controller and the signal recorder, a data recorder sink class should be created. It will get notified when signals subscribed by the data recorder is updated. The details of the class declaration are listed as below.

1. Firstly, a class named DataRecorderTextSink is declared based on the class template DataRecorderSinkBase. It should be noted that in this exemplary program, only the important instructions are listed in this annex.

```
public class DataRecorderTextSink : DataRecorderSinkBase, IDisposable
```

After the declaration of the class, variables can be created for the manipulation of the collected signal values.

```
protected override void OnData(double time, DataRecorderSignal signal, object value)
    Logger.AddMessage(new LogMessage("Data Recorder: " + signal.DisplayPath.ToString()
+ ", value: " + Convert.ToDouble(value).ToString()));
protected override void OnStart()
    Logger.AddMessage(new LogMessage("Simulation starts!"));
protected override void OnStop(double duration)
    Logger.AddMessage(new LogMessage("Simulation stops!"));
```

In the class DataRecorderTextSink, the methods like “OnStart”, “OnData” and “OnStop” are created to realize the functions that can be used as the collection and the processing of signals. The “OnStart”, “OnData” and “OnStop” are the main methods used for the collected signal and other related instructions. The methods “OnStart” and “OnStop” are triggered at the beginning and at the end of simulation process. The manipulation and process of signal data can be inserted into these methods, as well as the notification information of the simulation. the method “OnData” can be used as signal data process during the simulation. For example, the functions like the classification of signal among different types, the extraction of signal value and time, as well as the storage of signal information can be realized in this method. In the exemplary program shown above, the instructions written in each method are used for the notification of simulation status and the display of signal value.

2. Secondly, the class DataRecorderTextSink can be used to record signal during simulation. For example, as the button of simulation is clicked, the data recorder will be triggered with the simulation. The sentences about signal recorder should be added in the main program. As the program is shown below, a receiver sink of signal data is created. Multiple sinkIDs can be created if several apps are talking to the same controller. In this case, the sink named DataRecorderTextSink is declared which can be found below.

```
DataRecorderTextSink myDatarec = new DataRecorderTextSink ("myAppsUniqueIdentifier");
```

3. Then, it is able to add the desired signal to the sink. You use the API instruction which is "GetMotionSignal" to read the signal from the active controller. In the exemplary code below, the TCP speed of the default mechanism from the first controller is used as the target signal. Several declarations can be made if more than one signals are desired to be recorded, such as the TCP positions and the joint positions of different axes.

```
DataRecorderSignal
signal1=(Station.ActiveStation.BuiltInDataRecorderSignals.ControllerSignals.GetMotionSig
nal(Station.ActiveStation.Irc5Controllers[0].SystemId, "ROB_1",
BuiltInDataRecorderMotionSignal.TCPSpeedInCurrentWorkObject));

signal1.Name = "TCP";
```

4. After the declaration and definition of the signal variable, it is then added to the sink waiting to be activated during simulation.

```
myDatarec.Signals.Add(signal1);

Simulator.DataRecorder.Sinks.Add(myDatarec);
```

```
myDatarec.Enabled = true;
```

Annex 3 Presentation of coating thickness on workpiece

In this thesis, the coating thickness distribution is simulated based on the kinematic data of the robot. The kinematics data is obtained through the virtual robot system simulation according to the robot trajectory generated on the substrate surface. Thus, in order to present the result of coating thickness simulation directly on the substrate surface in RobotStudio™, a graphic development method should be proposed in the C# development environment and in RobotStudio™. Meanwhile, this method should be simple to load and robust enough.

According to the API function in RobotStudio™, while rendering the face of an object, it is achieved by the definition of its material. The material of the face is defined according to the texture details. A texture represents a texture image that can be applied to surfaces in the 3D view, which is usually defined by a Bitmap. Thus, by which consists of the pixel data for a graphics image and its attributes. A Bitmap is an object used to work with images defined by pixel data. Thus, it is able to define the color of the pixel with the format of RGB according to the coating thickness value at the coordinate of this pixel. Then the texture and the material of the face at the object can be defined by the Bitmap. An exemplary program is given as below.

Firstly, workpiece surface is divided into a mesh grid with the dimension of length*width. The color value of RGB format at each coordinate is defined according to the coating thickness value at this node and the minimum and the maximum value of the overall coating thickness on substrate surface. Afterwards, the generated Bitmap is assigned to the texture variable of the face.

```
figure = new Bitmap(length, width);
Color ColorRGB;
for (int i = 0; i < length; i++)
{
   for (int j = 0; j < width; j++)
   {
         ColorRGB = AddinFunction.ColorMapDistribution(min, max, Thickness[i, j]);
         figure.SetPixel(i, j, ColorRGB);
```

```
    }
}
Texture FaceText = new Texture(figure);
Material FaceMat = new Material(FaceText);
PickedFace.SetMaterial(FaceMat);
```

SPIM

■ École doctorale SPIM - Université de Technologie Belfort-Montbéliard
F - 90010 Belfort Cedex ■ tél. +33 (0)3 84 58 31 39
■ ed-spim@univ-fcomte.fr ■ www.ed-spim.univ-fcomte.fr

utbm
université de technologie
Belfort-Montbéliard